

PUSAT PENGURUSAN PENYELIDIKAN (RMC)

BORANG PENGESAHAN LAPORAN AKHIR PENYELIDIKAN

TAJUK PROJEK : **DEVELOPMENT OF FIBRE METAL LAMINATE MATERIALS FOR
AUTOMOTIVE APPLICATION**

Saya : DR. MOHD RUZAIMI BIN MAT REJAB

(HURUF BESAR)

Mengaku membenarkan **Laporan Akhir Penyelidikan** ini disimpan di Perpustakaan Universiti Malaysia Pahang dengan syarat-syarat kegunaan seperti berikut :

Laporan Akhir Penyelidikan ini adalah hakmilik Universiti Malaysia Pahang

Perpustakaan Universiti Malaysia Pahang dibenarkan membuat salinan untuk tujuan rujukan sahaja.

Perpustakaan dibenarkan membuat penjualan salinan Laporan Akhir Penyelidikan ini bagi kategori **TIDAK TERHAD**.

* Sila tandakan (/)

SULIT (Mengandungi maklumat yang berdarjah keselamatan atau Kepentingan Malaysia seperti yang termaktub di dalam AKTA RAHSIA RASMI 1972).

TERHAD (Mengandungi maklumat **TERHAD** yang telah ditentukan oleh Organisasi/badan di mana penyelidikan dijalankan).

 /

**TIDAK
TERHAD**

Tandatangan & Cop Ketua Penyelidik

.....

Tarikh :

CATATAN : ** Jika Laporan Akhir Penyelidikan ini SULIT atau TERHAD, sila lampirkan surat daripada pihak berkuasa/ organisasi berkenaan dengan menyatakan sekali sebab*

**DEVELOPMENT OF FIBRE METAL LAMINATE MATERIALS
FOR AUTOMOTIVE APPLICATION**



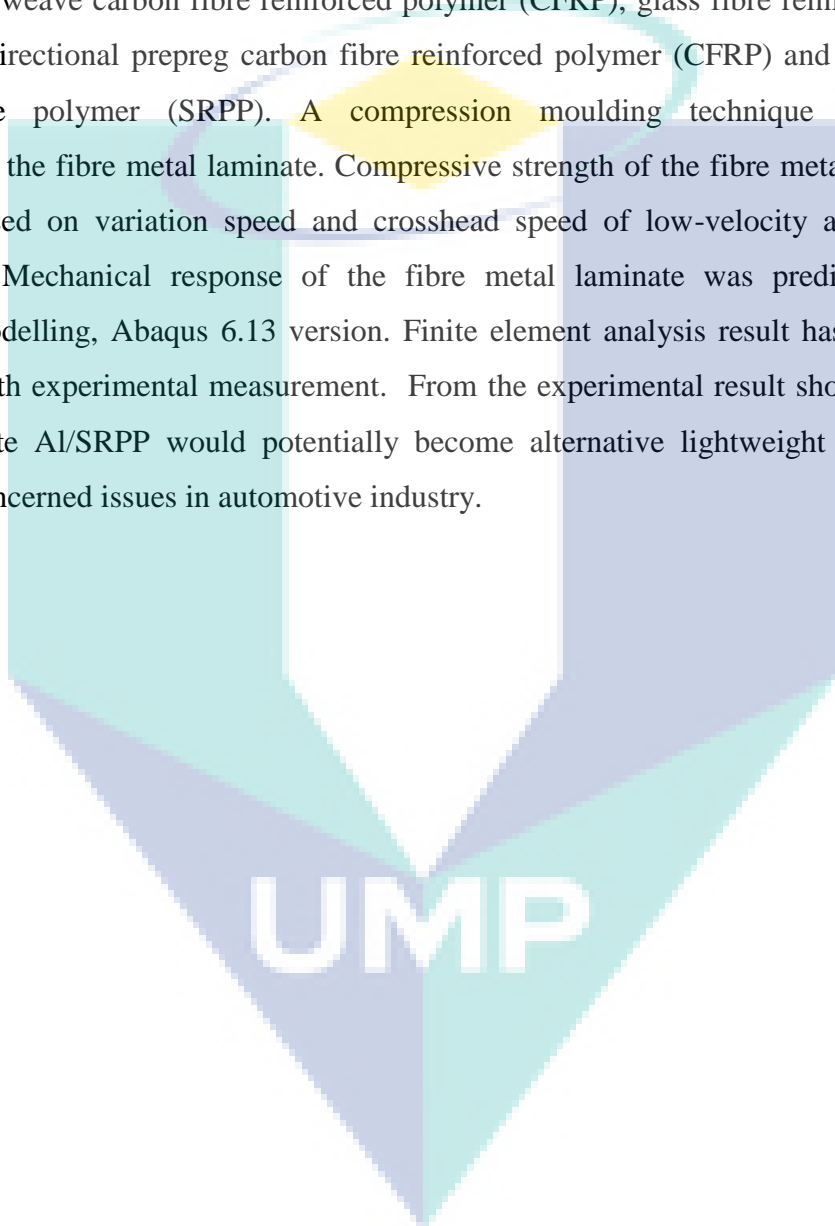
ABSTRAK

Penggunaan laminat logam gentian telah ditemui khusus dalam industri aeroangkasa. Pembangunan bahan baru dalam industri automotif telah mula mengurangkan kesan kemalangan kereta dan penggunaan bahan api. Laminat logam gentian direka dengan menggunakan bahan-bahan komposit yang berbeza seperti polimer bertetulang gentian karbon serat poliester (CFRP), polimer bertetulang gentian kaca (GFRP), polimer bertetulang gentian karbon (CFRP) dan polimer polipropilena yang diperkuat sendiri (SRPP). Teknik pengacuan mampatan digunakan untuk menghasilkan laminat logam gentian. Kekuatan mampatan lamina logam gentian diukur berdasarkan variasi kelajuan dan kelajuan rendah dan kuasi-statik masing-masing. Hubungkait mekanikal laminat logam gentian telah diramalkan dengan menggunakan pemodelan berangka, versi Abaqus 6.13. Hasil analisa elemen telah menunjukkan persetujuan yang baik dengan pengukuran daripada eksperimen. Dari hasil eksperimen menunjukkan bahawa, laminat gentian Al / SRPP berpotensi menjadi bahan ringan alternatif untuk mengurangkan isu-isu kebimbangan dalam industri automotif.



ABSTRACT

Application of fibre metal laminate have found specifically in aerospace industries. Development new material in automotive industry has begun to reduce car crash impact and fuel consumption. Fibre metal laminate was fabricated by using different composite materials such as plain weave carbon fibre reinforced polymer (CFRP), glass fibre reinforced polymer (GFRP), unidirectional prepreg carbon fibre reinforced polymer (CFRP) and self-reinforced polypropylene polymer (SRPP). A compression moulding technique was used to manufactured the fibre metal laminate. Compressive strength of the fibre metal laminate was measured based on variation speed and crosshead speed of low-velocity and quasi-static respectively. Mechanical response of the fibre metal laminate was predicted by using numerical modelling, Abaqus 6.13 version. Finite element analysis result has showed good agreement with experimental measurement. From the experimental result showed that, fibre metal laminate Al/SRPP would potentially become alternative lightweight material as to reduce the concerned issues in automotive industry.

The logo for UMP (Universiti Malaysia Perlis) is a large, stylized shield shape. It is divided into four quadrants by a white 'V' shape pointing downwards. The top-left and bottom-right quadrants are light blue, while the top-right and bottom-left quadrants are light purple. The letters 'UMP' are written in white, bold, sans-serif font across the center of the shield.

UMP

TABLE OF CONTENTS

DECLARATION

TITLE PAGE

ABSTRAK 3

ABSTRACT 4

TABLE OF CONTENTS 5

LIST OF SYMBOLS 6

LIST OF ABBREVIATIONS 9

CHAPTER 1 INTRODUCTION 11

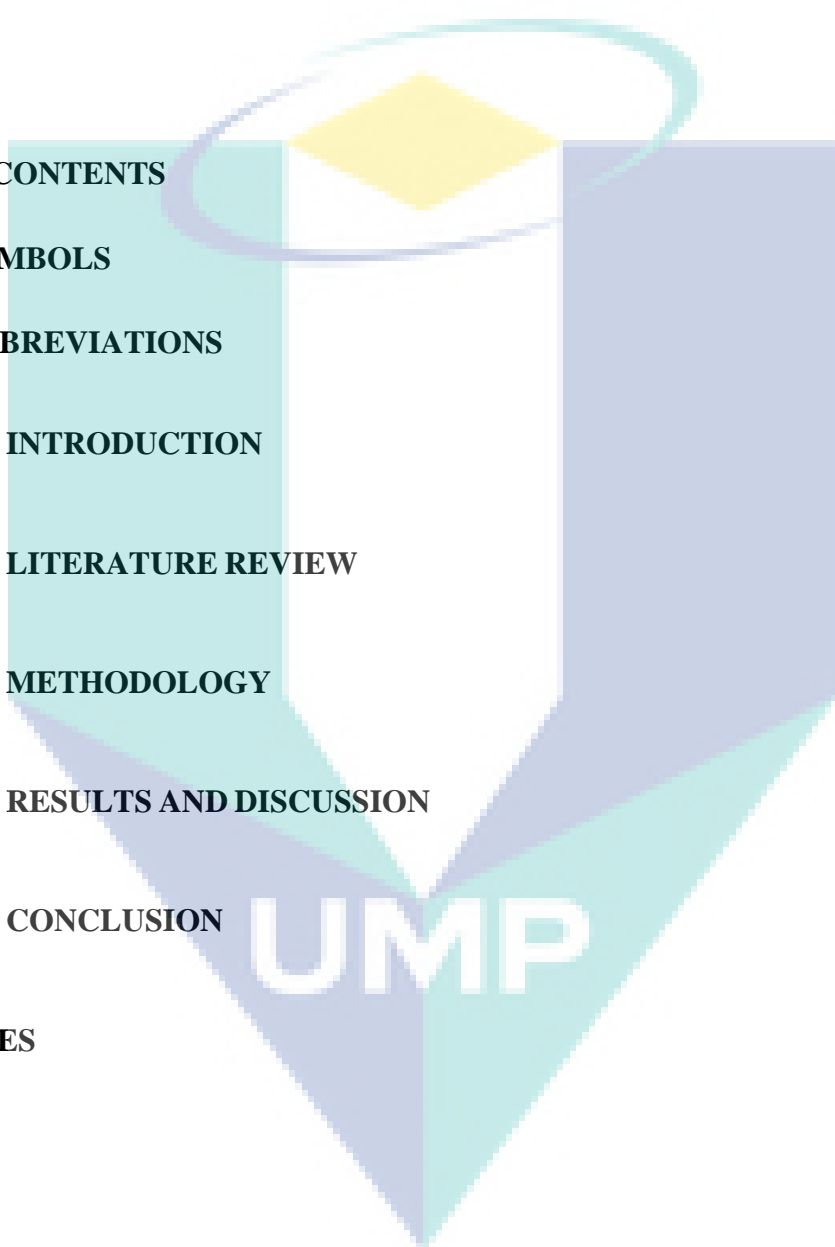
CHAPTER 2 LITERATURE REVIEW 17

CHAPTER 3 METHODOLOGY 40

CHAPTER 4 RESULTS AND DISCUSSION 63

CHAPTER 5 CONCLUSION 97

REFERENCES 100



LIST OF SYMBOLS

$^{\circ}C$	Degree Celsius
σ	Stress
T, T_a, T_f	The actual temperature
n	Constant of plastic behaviour
C	Sensitivity to strain rate
$\dot{\epsilon}_0$	Reference strain rate
ϵ_p	Plastic strain
$\dot{\epsilon}_p$	Plastic strain rate
E	Modulus elasticity
ν	Poisson's ratio
ρ	Density
A	Yield stress constant
B	Strain hardening constant
m	Thermal softening
ϵ_0	Reference strain rate

K	Melting and transition temperature
$D1, D2, D3, D4, D5$	Fracture strain constant
$\bar{\varepsilon}^{pl}$	Equivalent of the plastic
$\dot{\bar{\varepsilon}}^{pl}$	Equivalent of a plastic strain rate
σ^0	Static yield stress
$\bar{\sigma}$	Yield stress at non zero-zero strain rate
$R(\dot{\bar{\varepsilon}}^{pl})$	Ratio of yield stress at non zero-zero strain rate
ω	Damage parameter
$\Delta\varepsilon^{pl}$	Increment of the plastic equation
σ_m	Mean stress
\hat{T}	Non-dimensionless temperature
F_f^t	Breakage of fibre from the tension
F_f^c	Buckle of fibre from the compression
F_m^t	Crack of matrix from the tension
F_m^c	Crush of matrix from the compression
$\sigma_{11}, \sigma_{22}, \sigma_{12}$	Applied stresses
α	Coefficient of shear stress

δ_{eq}^f

Equivalent of a displacement in a FE when a stress reached to zero in stress-displacement

δ_{eq}^0

Equivalent of a displacement when the damage initiated

δ_{eq}

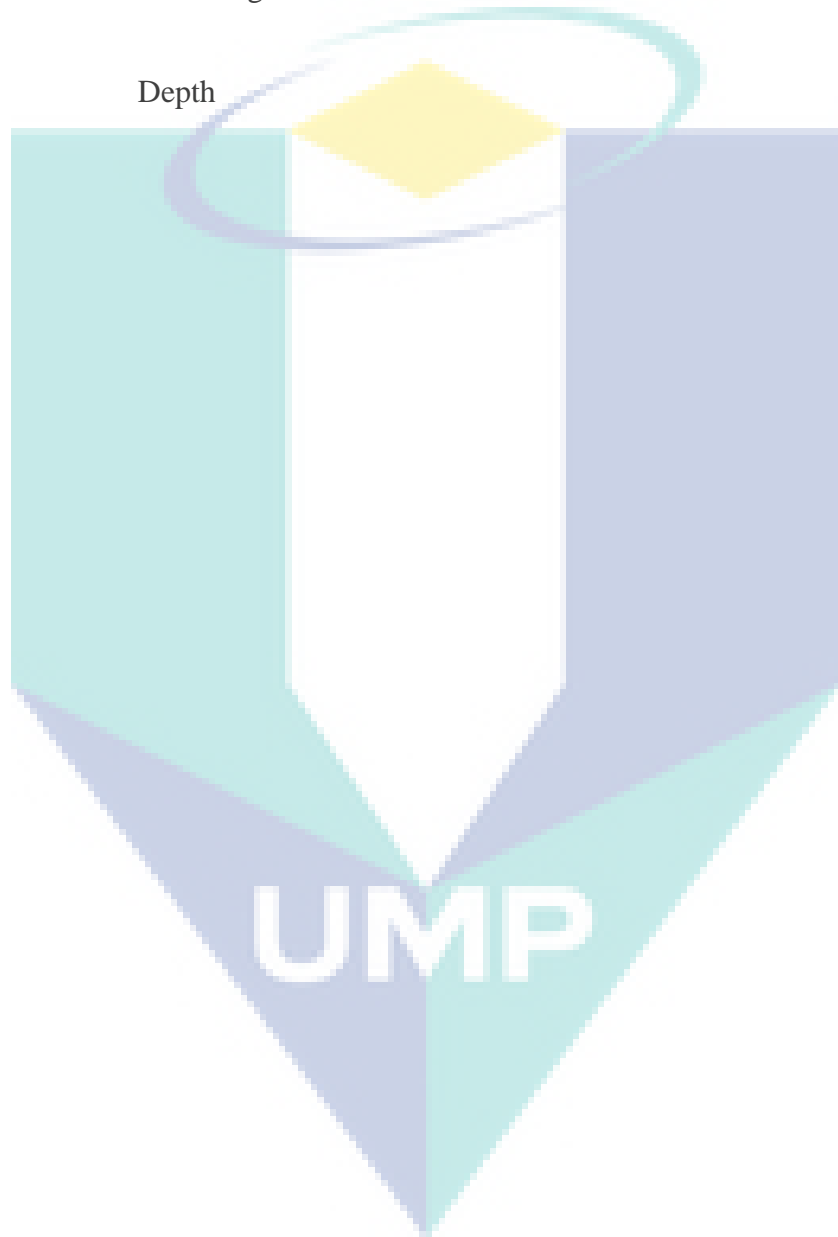
Equivalent of a displacement in FE

%

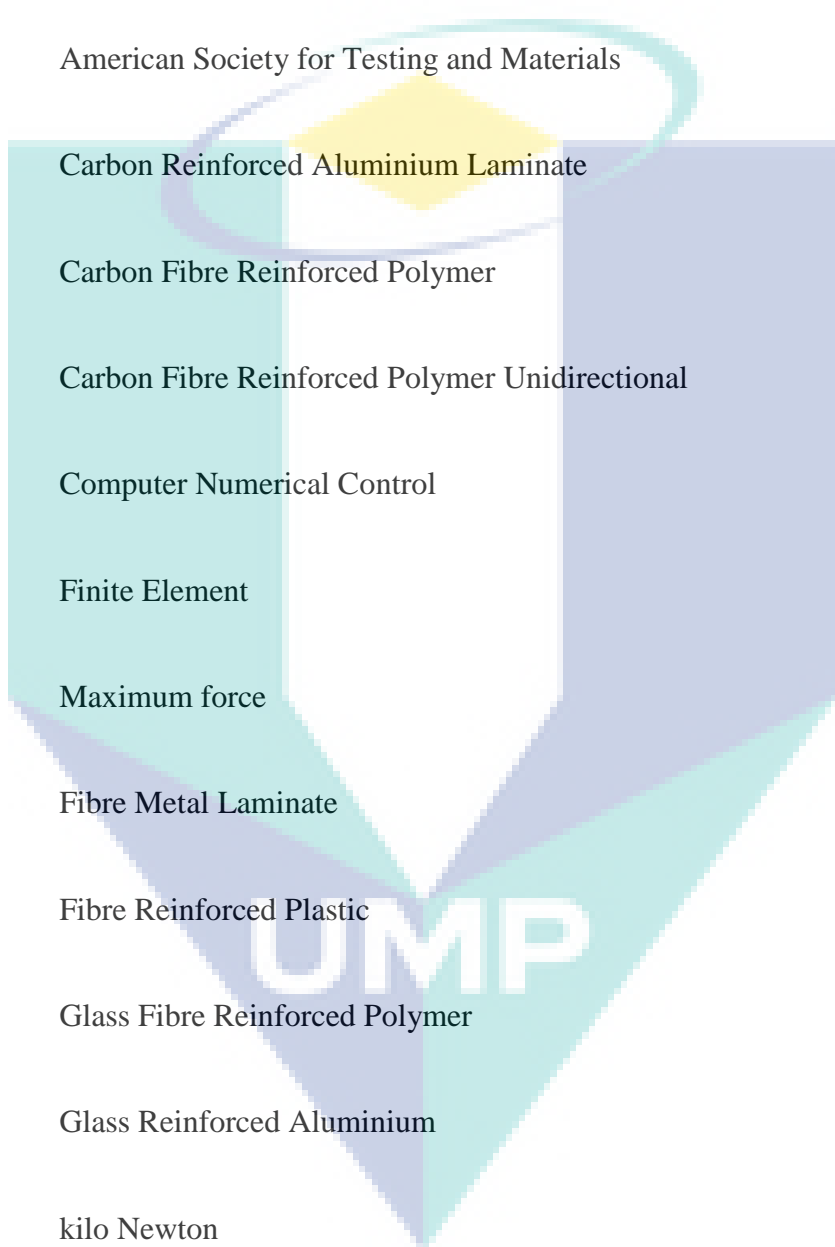
Percentage

d

Depth

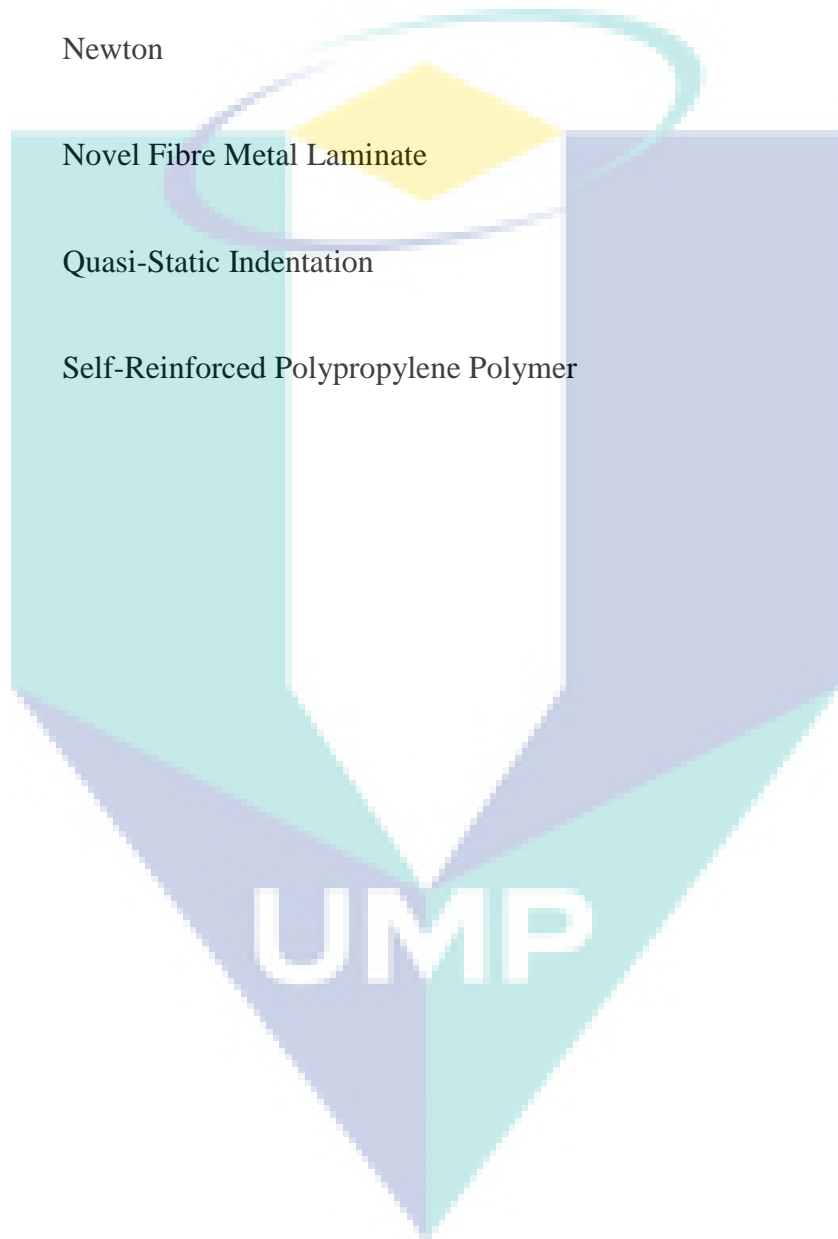


LIST OF ABBREVIATIONS



3D	Three dimensions
Al	Aluminium
ARALL	Aramid Reinforced Aluminium
ASTM	American Society for Testing and Materials
CARALL	Carbon Reinforced Aluminium Laminate
CFRP	Carbon Fibre Reinforced Polymer
CFRP UD	Carbon Fibre Reinforced Polymer Unidirectional
CNC	Computer Numerical Control
FE	Finite Element
F_{\max}	Maximum force
FML	Fibre Metal Laminate
FRP	Fibre Reinforced Plastic
GFRP	Glass Fibre Reinforced Polymer
GLARE	Glass Reinforced Aluminium
kN	kilo Newton
kPa	kilo Pascal

LVI	Low-Velocity Impact
M5	Metric thread with screw diameter 5 mm
MPa	Mega Pascal
MQL	Minimum Quantity Lubricant
N	Newton
NFML	Novel Fibre Metal Laminate
QSI	Quasi-Static Indentation
SRPP	Self-Reinforced Polypropylene Polymer



CHAPTER 1

INTRODUCTION

1.1 Introductory

As the automotive industry is in a steady development, the demand of improving the properties for available material has increased. Based on research conducted, composite material can lead to the material improvement in a car such as the mechanical properties by new generations. The composite of the materials have their own unique mechanical properties, which are have high specific strength and stiffness, high damping ratio, and low coefficient of thermal expansion. The applications of the composite materials are widely used in many industries such as the interior parts of automobiles, aerospace, naval and constructions industries (Rejab & Cantwell, 2013).

1.2 Fibre Reinforced Polymer (FRP) Composite

A composite material is made from at least two chemically distinct materials, with a distinct interface separating the constituents. The combinations of two distinct interfaces are usually to design and form the composite material properties. Generally, the composite material consists of a *matrix* and a *reinforcement*. The structure of the composite should be as light as possible, has high strength and stiffness and has some tolerance on damage (Bieniaś, Jakubczak, Surowska, & Dragan, 2015). The efficiency of a structure is based on the material and the geometry structure. These are important requirements for the optimum design.

The fibre reinforced polymer (FRP) composite materials are highly recommended by the designers because of high performance in the structural components. In the automotive industry, the composite materials are found to reduce weight of the components and provide savings in oil consumption. Fibre glass was applied to the Corvette body. Fatigue life of

Corvette with glass/epoxy composite leaf springs is five times higher than the steel leaf springs. It provides smoother ride and safety to a driver. The advantages of the composite materials are high modulus elasticity, low density, long life cycle and able to withstand high load.

The fibre reinforced composite materials consist of high strength and modulus fibres which are surrounded by matrix or polymer. The fibre and matrix has different properties of physical and chemical. The combination of fibre and matrix at microscopic level is not soluble to each other. Generally, the fibres main function is load-carrying and the matrix acts as stress transferor between the fibres, to avoid the fibres from the adverse environment and surface protector from the mechanical damages.

The polymer composites are widely used in the industries more than fifty years. The composite materials replaced the high-density materials as to reduce weight of a component. Besides that, the composite materials also have a good stability in dimension, better in a corrosion resistance and flexible for development of a design (Abdullah, Prawoto, & Cantwell, 2015). However, the bonding strength of the fibres and matrix remain as an issue for a composite material. This factor affected by the thermoplastic polymers such as polypropylene, polyethylene, polyvinylchloride, polystyrene and polyamide.

The adhesion between fibre and polymer will determine the effectiveness of the reinforcement. The adhesion layer is confined to third phase region, which is located between of fibre and matrix. Besides that, the third phase is also known as an interphase for the stress-transfer. The mechanical strength of the adhesive bond affected as the molecular diffused across the interface. The strength of polar interaction in chemical bond will affect the cross-linkage process that may denote the strength of an adhesion bond. There are many types of treatment to improve the adhesion strength. In the compatibility procedures, the improvement can be made by modifying the alkaline treatment, acetylation and copolymerisation of the graft.

In Figures 1.1, 1.2 and 1.3 showed the improvement of composite material and aluminium application in a car structure. In year 1995, iron and steel are mostly used in car manufacturing to make car chassis which about 57.90%. Starting in year 2000, aluminium and composite materials started increase in car manufacturing to reduce weight especially in supercar production. Composite materials are polymer matrix reinforced with continuous

composite fibres. They have high stiffness and strength, lightweight and good damping properties. The use of carbon fibre and glass fibre reinforced polymer could reduce weight up to from 40-65% and 20-35%. In the other hand, the lightweight properties of composite materials could help automotive industry reduce fuel consumption and provide safety to users (Santhanakrishnan Balakrishnan & Seidlitz, 2018).

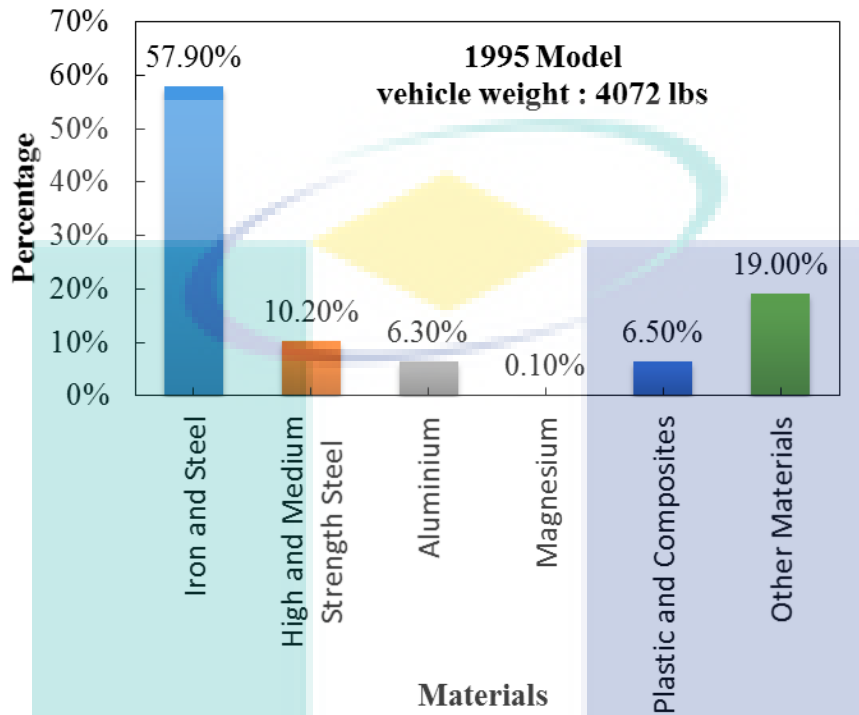


Figure 1.1 The percentage of materials usage in automotive application in year 1995
Source: Desnoo (2015)

UMP

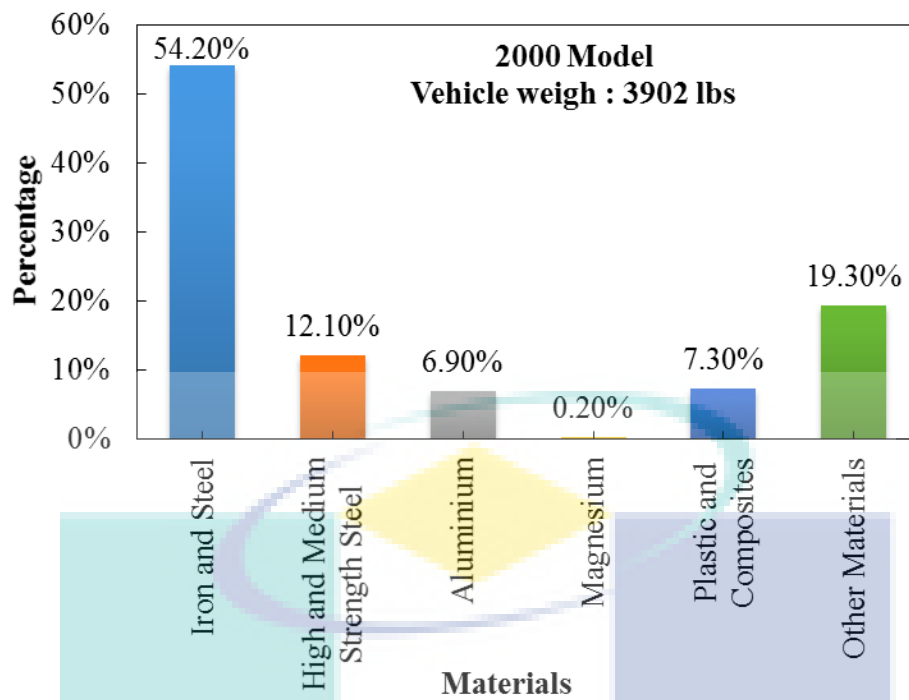


Figure 1.2 The percentage of materials usage in automotive application in year 2000

Source Desnoo (2015)

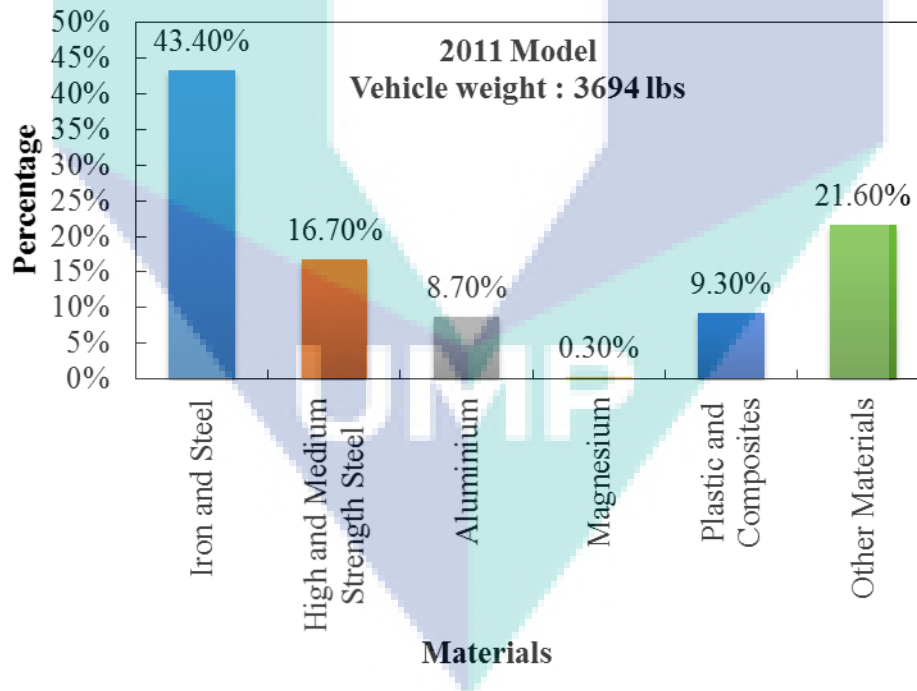


Figure 1.3 The percentage of materials usage in automotive application in 2011

Source : Desnoo (2015)

1.3 Problem Statement

The reduction of fuel consumption and safety improvement of vehicles are important aspects in the transportation sector. The lightweight structure materials offer damage tolerance based on demands (Múgica, Aretxabaleta, Ulacia, & Aurrekoetxea, 2014). The structural weight of materials has effect on a vehicle performance, a transport capacity and the fuel consumption. A structural weight is an important issue because vehicle efficiency could be improved by decreasing the weight of the vehicle's structures, thus, the need to consider the materials that have high specific strength.

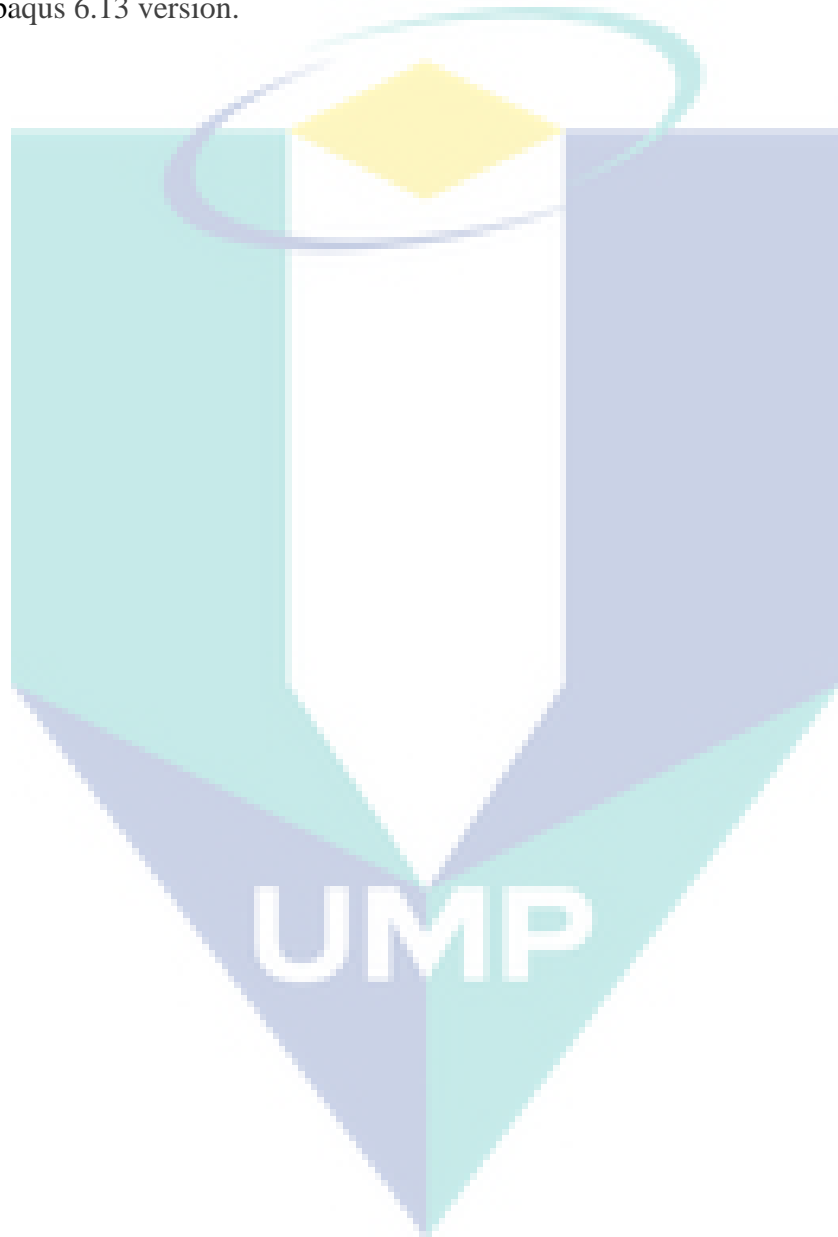
1.4 Objectives

- (i) To compare behaviour of fibre metal laminate materials for automotive applications subjected to static and dynamic impacts.
- (ii) To model the structural behaviour, then predict the failure pattern and mechanism of fibre metal laminate structures for quasi-static indentation and low-velocity impact.
- (iii) To investigate the correlation between two types of behaviours under quasi-static indentation and low-velocity impact tests.

1.5 Scopes of Research

- (i) Type of aluminium alloy sheet metal used; 2024-0.
- (ii) The thickness of these sheet metals is 0.80 mm. The sheet metals are used as the top and bottom skin of the fibre metal laminates specimens.
- (iii) Sand grinding method was used as surface treatment to rough the sheet metal surface.
- (iv) There are four types of materials that were used in this research:
 - a) A roll of plain weave carbon fibre reinforced polymer (CFRP), type 3K.
 - b) A roll of plain weave glass fibre reinforced polymer (GFRP)
 - c) The plies of self-reinforced polypropylene polymer (SRPP)
 - d) A roll of unidirectional prepreg carbon fibre.
- (v) The compression moulding technique used to fabricate fibre metal laminate and the configuration type of the fibre metal laminate is 2/1.

- (vi) The design of the experiment for the fibre metal laminate specimens is Al/CFRP/Al, Al/SRPP/Al, Al/UD-CFRP/Al and Al/GFRP/Al.
- (vii) The film of polypropylene (PP) was used to bond SRPP with the sheet metals.
- (viii) The mechanical performance of the specimens was evaluated by using a Drop Tower Impact Tester CEAST 9350 and Universal Testing machine Instron 3369 for the low-velocity impact and quasi-static tests, respectively.
- (ix) The finite element analysis data was validated with experimental data by using Abaqus 6.13 version.



CHAPTER 2

LITERATURE REVIEW

2.1 Introduction

Fibre metal laminate started to be studied by two countries; Great Britain and U.S. they studied about combination between metal and composite material. Delft University, Netherland developed first fibre metal laminate ARALL (Aramid Reinforced Aluminium Laminates). AKZO is a large Dutch company who manufactured aramid fibre while ALCOA produce thin sheets. 3M is one of company made good adhesive and also manufacture prepreg. In 1982/83 and 1987, ALCOA commercialised four grades of ARALL; ARALL 1 ARALL 2, ARALL 3 and ARALL 4. Another type of laminate has been developed, CARALL (Carbon Fibre Reinforced Aluminium Laminate). Then in 1990 another type of fibre metal laminate has been developed; Glare (Glass Reinforced Aluminium) (D. Liu, Tang, & Cong, 2012).

2.2 Fibre Metal Laminate

Fibre metal laminate (FML) comprises combination of metal and composite materials layers (Dadej, Surowska, & Bieniaś, 2018; Jones, 2017; Li et al., 2018; Majerski, Surowska, & Bienias, 2018). It was designed for a lightweight structure application such as an airplane. The crack growth on FML which contained fibre glass was investigated and found that there was excellent fatigue and damage tolerance behaviour on the specimen due to the crack opening on the layer of metal (Zhang, Wang, Rans, & Benedictus, 2016).

The fibre metal laminates are new development of the composite materials for the aerospace industry. The good combination between thin sheet metal and composite material will result in the fatigue and impact properties (Y. Hu et al., 2015). The FML can be applied

in many applications because it is able to withstand from the impact and the dynamics of loading. The fibre metal laminate was applied at the fuselage and lower wing of airplane. The FML is characterised by parameters. However, the results will be similar even the sets of design are different. For example, variety of lay-up still has fatigue characteristic (Şen, Alderliesten, & Benedictus, 2015a).

The fibre metal laminates are developed in the airplane industry because of the lightweight materials and high tolerance in the damage characteristics. The effects of using the fibre metal laminate reduces cost especially in the fabrication process and develop safety to the users. Prior to developing the advance material onto the airplane, the maintenance cost was very high and the consideration to reduce weight of the airplane was still needed. The aluminium alloys and fibre reinforced composite were good choices as to reduce cost of the structure and increase damage tolerance to the airplane. Both materials also have disadvantages such as aluminium alloys has poor fatigue strength and carbon fibre has low residual strength. Since the 1980s, the FML was widely used because the materials were highly damage tolerant reduce weight (Vogelesang & Vlot, 2000). The strength of the FML was due to high ductility of the metal alloys.

The GLARE was developed as second generation of the FML and was applied to fuselages and wing of airplane. The GLARE has excellent fatigue strength and high resistance to the impact (Huaguan et al., 2016). The fibre metal laminate is type of a hybrid material that consist of metal and composite materials mostly applied to many applications because the laminate could withstand with the dynamic-loading and impact for long term. The high loading from the impact involve debonding, delamination, fibre fracture and plasticity behaviour of the metal (Pärnänen, Kanerva, Sarlin, & Saarela, 2015).

The manufacturing and assembling process of hybrid structures are quite challenging because those require machining procedure such as drilling operation for riveting. The machining process became difficult when the mechanical and thermal properties of the metal and composite material are different (Giasin, Ayvar-Soberanis, & Hodzic, 2016). The FML has low density, high stiffness, high resistance to the corrosion and low cost and is popular in the aeronautic industry. The FML has particular characteristic and different failure behaviour due to the combination of the metal and composite materials (Simas Filho et al., 2016). The fibre metal laminate has simple metallic structure such as high impact resistance, corrosion and fire (Abdullah et al., 2015). A design of the fibre metal laminate to improve fatigue and

damage tolerance was presented. The lay-up configuration was based on the type and amount of the fibre used (Şen, Alderliesten, & Benedictus, 2015b). Nowadays, the lightweight structure of the composite material is widely used in the engineering field such as in load-bearing application. The workers said that many plies of composite materials often fail when a load is impacted on it (Abdullah & Cantwell, 2006). There are many types of fibre metal laminate for examples; ARALL, CARALL AND Glare.

2.2.1 Aramid Reinforced Aluminium Laminate (ARALL)

The ARALL laminate material was introduced since 1980 started to develop at the area that sensitive to fatigue (Aboudi & Paley, 1992; Hai, Rongzhen, Chunhu, & Hongyun, 1996; Schijve, 1990). The ARALL is unidirectional fibre and suitable to be applied at the structure of wings and application in fuselage skin was prohibited (Asundi & Choi, 1997). ARALL offers many benefits for instances high strength and excellent in fatigue properties (Bucci, Mueller, Vogelesang, & Gunnink, 1989; Marissen, 1984). Different types of ARALL laminates consisted with different configuration lay-up and types of sheet metal used. For examples ARALL 2 consisted with three layers of aluminium 2024-T3 and bonded to two layers of unidirectional prepreg aramid fibre by using 3M AF-163-2U epoxy adhesive. While, ARALL 3 consisted with aluminium alloy 7475-T76 and unidirectional prepreg aramid fibre (Sun, Dicken, & Wu, 1993).

The material was focused on wing structure. A lot of test on critical detail of the wing were done by Fokker through an inspection procedure (Vermeeren, 2003). Durability was considered in economic life and damage tolerance in airframe serviceability. Durability related to behaviour of fatigue and crack initiation. Fatigue cracking was found which due to degradation of aluminium structures. Besides that, the cracking could also affect from environmental effects. Crack initiation usually happened at outer layer of aluminium. From the tensile test has shown that ARALL hardly to degrade after fatigue loading and even in aggressive environment. From these test, ARALL durability was not influenced by a decisive factor such as crack initiation (Gunnink, 1988; Ritchie, Yu, & Bucci, 1989).

2.2.2 Carbon Fibre Reinforced Aluminium Laminate (CARALL)

CARALL laminates was investigated by the Delft University (E. C. Botelho, Pardini, & Rezende, 2007; Rao, Perumalla Janaki, Vardhan, & Chandramouli, 2016; Yu, Wu, Ma, &

Xiong, 2015). Fibre failure has been found in CARALL during flight simulation (Dhaliwal & Newaz, 2017). CARALL was tested at high elevated stress level and resulted in poor performance of fatigue (Lin & Kao, 1995; Lin, Kao, & Jen, 1994; Xue, Wang, Takao, & Matsubara, 2011). Failure strain of carbon fibre was noted as 0.5-2.0% and became disadvantage. CARALL laminates was sensitive to notch behaviour compare to monolithic aluminium alloy. Besides that, the sensitivity also due to galvanic corrosion between carbon fibre and aluminium alloy (Sinmazçelik, Avcu, Bora, & Çoban, 2011; Zamani Zakaria, Shelesh-nezhad, Navid Chakherlou, & Olad, 2017).

2.2.3 Glass Laminate Aluminium Reinforced Epoxy (GLARE)

In 1990, ARALL was attempted to improve the laminate by adopting high strength of glass fibre aramid fibre which called as GLARE. Then, it was developed successfully (Asundi & Choi, 1997). In 1991, GLARE started to be commercialised by AKZO and ALCOA (Edson Cocchieri Botelho, Silva, Pardini, & Rezende, 2006). GLARE became a structural material in aircraft. Meanwhile, the GLARE mostly apply at the fuselage (Vogelesang & Vlot, 2000). The laminate successfully applied in Airbus A380 airplane (Beumler, Pellenkoft, Tillich, Wohlers, & Smart, 2006; Vogelesang & Vlot, 2000)

2.3 Preparation of Fibre Metal Laminate

The FML design requirements can be done by changing the sequence of stacking, number metal, sheet metal thickness and ply of fibre orientation. The performance for each ply of fibre is different. A good selection lay-up is important for determining the performance of the FML whether it suitable with design requirements. In a manufacturing of the FML, a manufacturer will limit the choice of fibre orientation from 0° , $\pm 45^\circ$, 90° and they would fix a thickness of sheet metal (Şen et al., 2015a).

The types of laminates used were the glass FML, carbon FML and stainless steel sheet. A nitric acid was used for etching process on a surface of stainless steel and it affected on the result of bonding toughness. The adhesive film FM 300NK and FM 300-2K were used for the carbon fibre FML and glass fibre FML. The laminates were cured in an autoclave (Pärnänen et al., 2015). The ARALL and GLARE were cured at 120°C by using an autoclave (Asundi & Choi, 1997). The GLARE specimens were prepared by using a vacuum bagging method then cured inside the autoclave. The metal layer and composite material layer were assembled at a degree of 120°C with a pressure of six bar.

The specimen cut by using a water-jet cutter to reduce stress during cutting the laminate (Abouhamzeh, Sinke, & Benedictus, 2015). The laminate could be prepared by the different metal thickness, and number of ply (Şen et al., 2015b). The polypropylene-based of fibre metal laminate was layered with two types of the aluminium; 2024-T3 and 2024-O.

The adhesive film, polypropylene film, bonded the interlayer of the aluminium sheet and polypropylene fibre, the aluminium surface was cleaned from the dirt or dust by using the acetone solution. The laminates were pressed and heated to 165° at rate of 10°C/min and 5°C/min before the laminates being were cooled. Once the temperature decreased to 60°C, the panel could be removed from the mould (Abdullah & Cantwell, 2006).

The degradation on a mechanical strength would reduce service life of the material. The investigation on the effect of post-cure temperature and phases of reinforcement was studied. The damaged laminate was repaired by adhesive bonded method. The quasi-static indentation was applied on the laminate and evaluation based on the phase changes in propagation of damage, energy absorbed and residual deflection. The laminates were exposed to ambient temperature of post-cure, 30, 50, 70, and 90°C. The damaged specimen of glass/epoxy was repaired by chopping the short fibres and exposed to the post-cure temperature, 50°C. The result showed that it was the most favourable behaviour. The damaged specimen that was repaired by using chopped fibre absorbed large amount of indentation energy and high ultimate deflection. The specimen that repaired with particulate fibres delayed and reduced a progression of the fracture but was not effective with the tensile stress (Jefferson Andrew, Arumugam, & Santulli, 2016).

2.4 Failure Factors on Fibre Metal Laminate

The failure of the FML will cause delamination, debonding and fibre breaking to the composite materials. The other failure factor is at the preparation stage. The hand lay-up process require high skill of a labour to handle it.

The impact responses on the different steel surface treatment are caused by the deflection profile of post-impact and damage of the ultrasonic inspection. During impact, the dissipation of the energy and plastic deformation of the FML are depended by metal surface treatment.

The major failure in a glass fibre metal laminate is due to high shear crack at centre of composite layer. The debonding between the non-impacted steel and adhesive layers were extended and the composite material damaged was closed to the impact point. The modes of damages are very important to be analysed. The debonding would occur after the specimen reached at the maximum deflection (Pärnänen et al., 2015).

The adhesive layer applied in a reasonable amount as to improve the strength, fatigue and properties of the interlaminar (Huaguan et al., 2016). Besides that, the adhesive layer used and sprayed on metal surface because it determines a bonding strength between sheet metal and prepregs layers. Then it would affect to the performance of the whole laminates (Huaguan et al., 2016).

A cryogenic liquid nitrogen cooling was applied at a minimum quantity to the GLARE in the drilling process. The GLARE surface was investigated based on the cutting force, surface roughness, condition of the tools and machining process. The MQL reduced the cutting forces during drilling. The result of MQL was similar to the flood lubricant condition, which improved surface roughness. The cryogenic coolant has many advantages such as environment friendly, clean and safer. Besides that, the coolant contributed in tool life when the high temperature generated was reduced from the continuous machining operation (Giasin et al., 2016).

The GLARE, better known as a damage tolerance than the ARALL. The laminate was applied in two directions and suitable to the area that caused by the biaxial stresses. The crack growth in thin sheet material because the laminate was affected by a plane-stress.

The curing process of FML referred to the thermosetting system, which consisted of a heating temperature to cure, curing temperature isothermally and cool down temperature. The

fatigue life of an aluminium sheet and a composite material can be also influenced by the residual stress and distortion in thermo elastic or non-thermo elastic mechanisms. During the curing process, the polymerisation occurred and caused a residual stress on the matrix. The contraction or shrinkage occurred while cooling down the composite materials and produced stiffness throughout the process. The residual stresses developed from a thermal contraction inside the laminate and a cross linkage of the polymerisation (Abouhamzeh et al., 2015).

As the metal thickness increased, the number of life fatigue crack propagation became decreased. It because of the metal volume fraction increased and fibre volume fraction decreased. These were caused by the thickness of the metal layer. The GLARE 2A, GLARE 4A and GLARE 4B were used in this research. A GLARE 2A consisted with two plies of 0° contributed to fibre bridging. A GLARE 4A consisted additional of a 90° fibre orientation and it was not showed any improvement in a property of the residual stress. A GLARE 4B with a single layer of 0° fibre has worsen behaviour of residual strength (Şen et al., 2015b).

Internal degradation happened due to plastic deformation of the fibre metal laminates. Besides that, the delamination of the laminates occur because of the hybrid laminate that absorbed energy and the cracks number increased. The surface contact between an impactor and the laminate produced contact force that was causing the high transverse shearing stress and the cracks occurred. The failure on the material is caused by decreasing of the structural stiffness. Higher impact energy was resulted in degradation of laminate structure. Deformation on the FML increased as the impact energy increased. The impact at first mode caused a crack on the matrix and degradation between the fibre and matrix. The matrix became brittle and resisted to crack formation. The bending cracks happened due to the normal stress that acted on the surface of the FML and through a maximum bending of stress. The bending stress initiated delamination at lower layer. The mechanical properties of FML reduced once a delamination occurred. The delamination happened at a high resin content and distributed shear stress at the area that surrounded the impactor (Bieniaś et al., 2015).

At the first generation of thermosetting-based on fibre metal laminate was suffered in a limitation numbers in the processing cycles, interlaminar toughness and difficulties in the repairs. The sandwich structure of the FML which based on the aluminium 2024-T3 was offered a superior failure resistance than the FML based on the aluminium 2024-O (Abdullah & Cantwell, 2006).

A high dynamic loading of the laser peen produced the bending deformation. The laser induced a pressure with a wavelength 532 nm to the different fibre orientation until the bending deformed. The delamination of the FMLs occurred because of the bending deformation (Y. Hu et al., 2015).

A study on the damaged composite materials have been proven due to low-velocity impact and caused cracking on matrix. The damage cross section decreased as angle fibre orientation increased. Angle fibre has an important role in mechanical properties of the composite materials. The damage area would effect on strength of the specimen (Kumar, Prasad, Ravishankar, Sateesh, & Ravi, 2015).

2.5 Evaluation on Fibre Metal Laminate Performance

The procedure of the genetic algorithm was developed to find an optimum number of the lay-up, which required to determine the fatigue life. The prediction of the crack initiation on the metal depended on an S-N curve. The selection of the curve could be done by two methods. In the Method 1, the amplitude of stress was corrected to read fatigue life. Meanwhile, the Method 2 was an interpolation at between of the S-N curve (Şen et al., 2015a).

The evaluation on the fatigue test was done at Delft University. Two types of GLARE were used; cross-plyed GLARE 3 and unidirectional fibre GLARE 2 and the other materials such as an ARALL 2 and a monolithic 2024-T3. From the observation, the cracks growth of GLARE is at rate 10-100 times slower than the monolithic aluminium and it showed that the GLARE was higher compared to the other materials. The deformation effect of the impact, it was gave an advantage to the FML because this would increase the ability detection and inspect quality (Vogeleisang & Vlot, 2000).

Two different tests on fibre metal laminate were evaluated under the effect of the pin and bypass loading. The results showed that there was an extension of delamination between the metal and fibre interface and there was a crack growth. The crack growth of the pin without bypass decreased as the crack length increased. Meanwhile, the crack growth of pin and bypass loading became stable after reaching the crack length, 10mm (Frizzell, McCarthy, & McCarthy, 2008). The repairs on a Boeing 747 were found that 57.6% is from the fatigue

cracks, 29.4% by corrosion and 13.0% affected from impact damage (Vogelgesang & Vlot, 2000). The crack growth caused by the pin loading. The crack growth resulted in a shape delamination (Zhang et al., 2016).

The fatigue crack growth of FML was tested by using a Digital Image Correction. The DIC was used to detect the delamination at the interface between the metal and fibre layer. Besides that, the DIC also used to detect the distribution of the strain on a specimen surface. The deformed specimen picture took by the DIC camera and the evolution of delamination obtained. The crack length read from the high-resolution camera picture. Seven points polynomial method used to obtain the crack growth rate which is based on the life cycle and crack length (Zhang et al., 2016).

2.6 Energy Absorption of Impact Response

The vehicles components were designed by using a good quality of the fibre reinforced polymer matrix composites and to be applied in automotive industry especially in light vehicles. Braided composites tubes were considered as energy absorber, which has potential in reducing cost of manufacturing. The characteristics of tubes were influenced by a few factors such as parameters, geometry and condition of loading. The circular tube has a higher Specific Energy Absorption than square and rectangular tube. This was caused by a thickness of the wall tube and energy absorption. The failure behaviour characterised by a global buckling, wall folding and crushing at ends (McGregor, Vaziri, Poursartip, & Xiao, 2016).

The composite materials were recommended in designing of helicopter in order to improve performance of the structure and reduce weight of the structure. The composite materials have good performance of *SEA* and widely used for designing lightweight structures. The energy absorption was influenced by the hybrid system of two or more materials, orientation of fibre, layup technique, properties of fibre and matrix and geometry of structure.

A specimen with E-glass and basalt fibre has lower in *SEA*. Amount of energy absorption could be optimised by using a suitable hybrid ratio. The energy absorption improved by following a sequence of the fibre orientation (D. Hu, Zhang, Ma, & Song, 2016).

2.7 Numerical Analysis

The alternative way to predict experimental result is by using numerical analysis. Study of numerical analysis on fibre metal laminate is crucial to identify the impact behaviour of it. The process of simulation could be done by adding the properties material used such as the Young's modulus, Poisson's ratio, density of the materials, elasticity and plasticity. The simulation process required reasonable numbers of structural tests for a validation process. Moriniere studied on combination of two theories; failure criteria and plasticity as to simulate the degradation behaviour of plate and study the behaviour of nonlinear numerical model.

The damage of an impact was controlled by degradation of the stiffness and fracture was due to energy releases which aimed to delamination growth. The simulation of deformation process of 3D FE model involved sensitivity of strain-rate and large changes in transverse compression. The damaged of composite plies cannot be used directly in Abaqus (Morinière, Alderliesten, & Benedictus, 2014). In Abaqus simulation, the composite material was extruded in shell element so that the stresses and strain through the composite thickness neglected. The failure criteria in Abaqus applied to an unidirectional composite material (Fan, Guan, & Cantwell, 2011). The result was predicted successfully by identifying a feature of the key in tracers. The damage behaviour was modelled by using a Hashin's failure criterion.

The FE results were higher than the experimental result (Fan et al., 2011). The finite element method used as effective way to examine the complex structures through a detail information of the loading. Besides that, the finite element method also used to validate experimental results and study failure behaviour of FML models. For example, Hashin's

failure criterion was used to analyse damaged composite model. The simulation of composite models were influenced by the various factors such as, plies in the FML structures, boundary condition, density of mesh (number of nodes). A numerical analysis provided valuable information for experimental results (Frizzell, McCarthy, & McCarthy, 2011). The finite element analysis is a flexible method to study mechanical behaviour of fibre metal laminate.

The behaviour of FML structures is based on a configuration of layup, acted load and boundary condition application. The FML model simulated through detail information in distribution of stress and damage tolerance on the structure. The finite element analysis provided accurate result and reasonable. The finite element, FE models was simulated under a comprehensive stress and caused the delamination, which would develop to a failure of the FML structures.

The composite structure was exhibited in plasticity and analysed failures through the material behaviour. Isotropic elasticity and plasticity hardening in Abaqus modelled the metal layer of FML and their mechanical behaviours of the damage effects were proposed. The plasticity behaviour of the composite structure was described through the shear and transverse stress as to predict the failure of damages (Chen, Morozov, & Shankar, 2014). In the Abaqus simulation, the Johnson Cook Dynamic Damage was model applied to the aluminium and the equation expressed as in Eq (2.1) (Santiago, Cantwell, Jones, & Alves, 2018):

$$\sigma = \left[A + B(\varepsilon_p)^n \right] \left[1 + C \ln \left(\frac{\dot{\varepsilon}_p}{\dot{\varepsilon}_0} \right) \right] \left[1 - \left(\frac{T - T_a}{T_f - T_a} \right)^m \right] \quad 2.1$$

A is an elastic limit B , n is expressed for a characteristic constants of the plastic behaviour, C is a sensitivity to the strain rate, $\dot{\varepsilon}_0$ is the reference strain rate while ε_p and $\dot{\varepsilon}_p$ are respectively the plastic strain and the plastic strain rate and T, T_a, T_f are respectively the actual temperature. The example of the actual temperature is room temperature and melting temperature in an absolute scale. Lastly, m is a temperature dependency of a material constant. The constants A , B and n are obtained and calibrated through a series of tensile tests supported by numerical models.

The alternative way to predict experimental result is by using numerical analysis. Study of numerical analysis on fibre metal laminate was become crucial as to know the

impact and behaviour of it. The process of simulation could be done by adding the properties material used such as the Young's modulus, Poisson's ratio, density of the materials and others. The simulation process required reasonable numbers of structural tests for a validation process. Previous studies combined two theories of failure criteria and plasticity as to simulate the degradation behaviour of plate and study the behaviour of nonlinear numerical model. The damage of an impact was controlled by degradation of the stiffness and fracture was because of energy releases, which aimed to delamination growth. The simulation of deformation process of 3D FE model involved sensitivity of strain-rate and large changes in transverse compression. The damaged of composite plies cannot be used directly in Abaqus (Morinière et al., 2014).

The Abaqus/Explicit was used to develop a numerical simulation of the FML under the low velocity impact. The FML consisted with two different of constituent materials; 2024-0 and unidirectional prepreg carbon fibre. The failure of the FML depended on the ductility of the materials.

2.7.1 Modelling of the Aluminium 2024-0 by using Isotropic

The aluminium alloy 2024-0 was modelled by using an isotropic elastoplasticity to predict elastic and plastic behaviour as either a rate-dependent or rate dependent model and it has a simple form. In Table 2.1 showed properties of aluminium 2024-0 under isotropic hardening as below:

Table 2.1 Properties of aluminium 2024-0

Symbol	Value	Property
ρ	2780 kg/m ³	Density
E	70.6 GPa	Young's modulus
ν	0.3	Poisson's ratio

Source: Rejab & Cantwell (2013)

2.7.1.1 Elasticity

A model of isotropic linear elasticity was generated for the elastic respond for a material in a numerical analysis. The material that performed the linear elastic behaviour, the total stress defined through this an equation (Nowak, 2018):

$$\sigma = D^{el} \varepsilon^{el} \tag{2.2}$$

Where σ the total stress, D^{el} is the fourth order of an elasticity tensor and ε^{el} is the total elastic strain. From the Equation (2.1) the stress-strain relationship of isotropic linear elasticity strain.

$$\begin{bmatrix} \sigma_{11} \\ \sigma_{22} \\ \sigma_{33} \\ \sigma_{12} \\ \sigma_{13} \\ \sigma_{23} \end{bmatrix} = \frac{E}{(1+\nu)(1-2\nu)} \begin{bmatrix} 1-\nu & \nu & \nu & 0 & 0 & 0 \\ \nu & 1-\nu & \nu & 0 & 0 & 0 \\ \nu & \nu & 1-\nu & 0 & 0 & 0 \\ 0 & 0 & 0 & \frac{(1-2\nu)}{2} & 0 & 0 \\ 0 & 0 & 0 & 0 & \frac{(1-2\nu)}{2} & 0 \\ 0 & 0 & 0 & 0 & 0 & \frac{(1-2\nu)}{2} \end{bmatrix} \begin{bmatrix} \varepsilon_{11} \\ \varepsilon_{22} \\ \varepsilon_{33} \\ \varepsilon_{12} \\ \varepsilon_{13} \\ \varepsilon_{23} \end{bmatrix} \tag{2.3}$$

The symbol of E is a Young's modulus and ν is a Poisson's ration. These are defined in the equation above. The inverse relationship is defined as an equation below:

$$\begin{bmatrix} \varepsilon_{11} \\ \varepsilon_{22} \\ \varepsilon_{33} \\ \gamma_{12} \\ \gamma_{13} \\ \gamma_{23} \end{bmatrix} = \begin{bmatrix} \frac{1}{E} & \frac{-\nu}{E} & \frac{-\nu}{E} & 0 & 0 & 0 \\ \frac{-\nu}{E} & \frac{1}{E} & \frac{-\nu}{E} & 0 & 0 & 0 \\ \frac{-\nu}{E} & \frac{-\nu}{E} & \frac{1}{E} & 0 & 0 & 0 \\ 0 & 0 & 0 & \frac{1}{G} & 0 & 0 \\ 0 & 0 & 0 & 0 & \frac{1}{G} & 0 \\ 0 & 0 & 0 & 0 & 0 & \frac{1}{G} \end{bmatrix} \begin{bmatrix} \sigma_{11} \\ \sigma_{22} \\ \sigma_{33} \\ \sigma_{12} \\ \sigma_{13} \\ \sigma_{23} \end{bmatrix} \quad 2.4$$

$$G = \frac{E}{2(1+\nu)} \quad 2.5$$

G is a shear modulus. The elastic material in the properties of aluminium 2024-0 was used in the numerical modelling. The properties were taken from experimental results. The value of Young's modulus, $E = 70.6$ GPa and the Poisson's ratio is $\nu = 0.3$ (Duarte, Díaz Sáez, & Silvestre, 2017).

2.7.1.2 Yielding

An isotropic yielding is applied to a von Mises yield surface. The surface is assumed that yielding of a metal is independent where experimental works confirmed the observation. The metal was applied under a positive pressure stress. When the metal applied in that kind of situation which high-pressure stress, it may be inaccurate because voids can nucleate and grow in the metal (Nowak, 2018).

2.7.1.3 Plasticity

Beyond the yield point is a permanent deformation or called as the plastic behaviour of the aluminium. The plastic behaviour is defined in an isotropic hardening. To describe the isotropic hardening, the yield stress, σ^0 , which given in a plastic strain tabular function. The interpolation of the yield stress at any plastic strain rate can be done from the table of data. The data will remain constant when it reached to the last value that has been given in the Table 2.2 (Rejab & Cantwell, 2013).

Table 2.2 Yield stress (MPa) and Plastic strain value for aluminium 2024-0

Yield stress (MPa)	Plastic strain
70.5	0
103.7	0.01
132.5	0.0198
151.7	0.0296
164.7	0.0392
175.2	0.0489
198.8	0.09531
210.9	0.1398
221.8	0.1823
223.9	0.1851

Source: Rejab & Cantwell (2013)

For rate-dependent of material the relationship of the equivalent plastic strain rate, $\dot{\bar{\epsilon}}^{pl}$ followed by the uniaxial flow rate definition as:

$$\dot{\bar{\epsilon}}^{pl} = \varphi(q, \bar{\epsilon}^{pl}, \theta_r) \tag{2.6}$$

φ known as a function, q is the von Mises equivalent stress, $\bar{\varepsilon}^{pl}$ is an equivalent of the plastic strain and θ_r is the temperature.

2.7.1.4 Failure Criteria

The development of damage and failure of ductile material are used in Abaqus/Explicit to model the damage behaviour of the aluminium. *SHEAR FAILURE and *TENSILE FAILURE or a combination of both are two material failure models will offer in the Abaqus to account the damage and failure in a ductile metal. To calculate the failure, shear and tensile failure models can use an equivalent of the plastic strain and hydrostatic cut-off stress respectively. If the failed meshes removed from the meshes it may for both failure models (Duarte et al., 2017).

2.7.1.5 Damage for Ductile Materials

There is two mechanisms for the ductile metals will be used in this study; ductile damage and shear damage models. The ductile fracture or ductile damage is an initial criterion for predicting the onset damage which due to nucleation, growth and the voids. This model will active when the following condition is satisfied:

$$\omega_D = \int \frac{d\bar{\varepsilon}^{pl}}{\bar{\varepsilon}_D^{pl}(\eta, \bar{\mathbb{E}}^{pl})} = 1 \quad 2.7$$

ω_D is a state variable that increases monotonically with plastic deformation. The model is assumed that the equivalent plastic strain at the onset of damage, $\bar{\varepsilon}_D^{pl}$ is a function of triaxiality, $\eta = -p/q$, and the equivalent of plastic strain, $\bar{\mathbb{E}}^{pl}$. Note that p is the pressure stress and q is the Mises equivalent stress.

The shear damage model is a fracture, which comprises to shear band localisation in the ductile metals. The model will be activated when the following condition is satisfied.

$$\omega_s = \int \frac{d\bar{\varepsilon}^{pl}}{\bar{\varepsilon}_s^{pl}(\theta_s, \bar{\mathbb{E}}^{pl})} = 1 \quad 2.8$$

ω_s is a state variable that increases monotonically with plastic deformation and is relative to the incremental change in equivalent plastic strain, $\bar{\varepsilon}^{pl}$. The model is assumed that

the equivalent plastic strain at the onset of damage, $\bar{\epsilon}_s^{pl}$ is a function of the shear stress ratio, $\theta_s = (q + k_s p) / \tau_{\max}$ and the equivalent plastic strain rate, $\dot{\epsilon}^{pl}$. Note that τ_{\max} is the maximum shear stress k_s is a material parameter ($k_s = 0.3$ for the aluminium alloy) (G. Liu, Li, Msekh, & Zuo, 2016).

2.7.2 Modelling of Composite by Hashin Damage Criterion

The Hashin damage criterion based on works of Hashin and Rotem and Hashin (Hashin, 1980; Hashin & Rotem, 1973). This criterion is unlike other criteria like Tsai-Hill and Tsai-Wu (Tsai, 1965; Tsai & Wu, 1971). Those criteria purposed an equation to predict damage initiation. The Hashin's damage presents for failure modes with four corresponding indexes (a) breakage of fibre from the tension (F_f^t), (b) buckle of fibre from the compression (F_f^c), (c) crack of matrix from the tension (F_m^t) and (d) crush of matrix from the compression (F_m^c). There are four equation that applied to those failure modes respectively (Duarte et al., 2017)

$$\left(F_f^t\right) = \left(\frac{\sigma_{11}}{S_{t1}}\right)^2 + \alpha \left(\frac{\sigma_{12}}{S_{12}}\right)^2 \leq 1.0 \quad \text{and } \sigma_{11} \geq 0 \quad 2.9$$

$$\left(F_f^c\right) = \left(\frac{\sigma_{11}}{S_{c1}}\right)^2 \leq 1.0 \quad \text{and } \sigma_{11} < 0 \quad 2.10$$

$$\left(F_m^t\right) = \left(\frac{\sigma_{22}}{2S_{s23}}\right)^2 + \alpha \left(\frac{\sigma_{c2}}{2S_{s23}}\right)^2 \leq 1.0 \quad \text{and } \sigma_{22} \geq 0 \quad 2.11$$

$$\left(F_m^c\right) = \left(\frac{\sigma_{22}}{2S_{s23}}\right)^2 + \left[\left(\frac{S_{c2}}{2S_{s23}}\right)^2 - 1\right] \frac{\sigma_{22}}{S_{c2}} + \left(\frac{\sigma_{12}}{S_{12}}\right)^2 \leq 1.0 \quad \text{and } \sigma_{22} < 0 \quad 2.12$$

σ_{11} , σ_{22} and σ_{12} are applied stresses while α is a coefficient of the shear stress σ_{12} which contributed in fibre breakage by a tension criterion. In the Abaqus, the criterion of Hashin could be implemented in a conjunction with a damage evolution law. The law based on a specification of four fracture energy values G_f . The values corresponded to the material

degradation in each mode. The values constituent in an implementation of the Hashin-based and analysed with the damage evolution in the Abaqus. The damage variable for fibres d_f , matrix d_m and shear d_s were assessed by the expression as follows (Duarte et al., 2017):

$$d = \frac{\delta_{eq}^f (\delta_{eq} - \delta_{eq}^0)}{\delta_{eq} (\delta_{eq}^f - \delta_{eq}^0)} \quad 2.13$$

δ_{eq}^f is an equivalent of a displacement in a FE when the stress reached to zero in a stress-displacement while δ_{eq}^0 is an equivalent of a displacement when the damage initiated. δ_{eq} is an equivalent of a displacement in FE for the given applied strain (Duarte et al., 2017). The model of composite material modelled for damage initiation. There are four mechanisms of the damage initiation, which named as fibre tension, fibre compression, matrix tension and matrix compression ($F^t_f, F^c_f, F^t_m, F^c_m$). Fibre tension, fibre compression, matrix tension and matrix compression are expressed as below (Duarte et al., 2017):

$$F^t_f = \left(\frac{\tilde{\sigma}_{11}}{X_T} \right)^2 + \alpha \left(\frac{\tilde{\sigma}_{12}}{S_L} \right)^2, \tilde{\sigma}_{11} \geq 0 \quad 2.14$$

$$F^c_f = \left(\frac{\tilde{\sigma}_{11}}{X_C} \right)^2, \tilde{\sigma}_{11} \leq 0 \quad 2.15$$

$$F^t_m = \left(\frac{\tilde{\sigma}_{22}}{Y_T} \right)^2 + \left(\frac{\tilde{\sigma}_{12}}{S_L} \right)^2, \tilde{\sigma}_{11} \geq 0 \quad 2.16$$

$$F^c_m = \left(\frac{\tilde{\sigma}_{22}}{2S_T} \right)^2 + \left[\left(\frac{Y_C}{2S_T} \right)^2 - 1 \right] \frac{\tilde{\sigma}_{22}}{Y_C} + \left(\frac{\tilde{\sigma}_{12}}{S_L} \right)^2 \quad 2.17$$

The variables X_T, X_C are stand for tensile and compressive strength in a longitudinal direction, Y_T, Y_C are tensile and compressive strength in transverse direction, S_L, S_T are shear strengths of longitudinal and transverse. Besides that, this symbol; α is a coefficient of shear stress that specified to the damage initiation for tensile fibre. These criteria could be used in element removal procedure to remove failed elements whether fibre or matrix (Fan et al., 2011).

2.8 Literature Summary

In Chapter 2 presents a review of relevant previous and current research study on fibre metal laminate which subjected to static and dynamic impact loading. The mechanical responses of fibre metal laminate under static and dynamic impact have been reviewed with some relevant examples. The impact responses have been discussed. Finally, procedures for modelling the impact response of fibre metal laminate have been reviewed with some examples of published numerical work. Nowadays, the limited literature is available for aerospace application. A summary of the relevant work is presented in the Table 2.3.

Therefore, the aim of this research work to assess behaviour of fibre metal laminate materials for automotive applications which subjected to static and dynamic impacts, to model the structural behaviour, then predict the failure pattern and mechanism of fibre metal laminate structures for quasi-static indentation and low-velocity impact and to investigate the correlation between two types of behaviours under quasi-static indentation and low-velocity impact tests . Quasi-static indentation and low-velocity impact test are carried out for fibre metal laminates under a specific range. A numerical modelling used to predict failure behaviour in quasi-static indentation and low-velocity impact.

Table 2.3 Table of literature review based on fibre metal laminate

Title	Year	Author	Findings
Low-energy impact behaviour and damage characterization of carbon fibre reinforced polymer and aluminium hybrid	2015	Bieniaś, J., P. Jakubczak, B. Surowska and K. Dragan	Delamination can reduce the mechanical properties of FML. Delamination occurred at high resin content and distributed shear stress at area that surrounded the impactor. There was an internal

laminates

degradation because of plastic deformation of fibre metal laminates. Besides that, delamination of laminates occurred because of fibre metal laminate absorbed energy and number of cracks increased.

Lay-up optimisation of fibre metal laminates based on fatigue crack propagation and residual strength

2015

Şen, I., R. C. Alderliesten and R. Benedictus

As metal thickness increased, the number of life fatigue crack propagation decreased. It is due to the increase of metal volume fraction and decrease of fibre volume fraction.

Debonding and impact damage in stainless steel fibre metal laminates prior to metal fracture

2015

Pärnänen, T., M. Kanerva, E. Sarlin and O. Saarela

Nitric acid was used for etching process on surface of stainless steel and it affected on result of bonding toughness.

Effect of adhesive quantity on failure behaviour and mechanical properties of fiber metal laminates based on the aluminium–lithium alloy

2016

Li, H., Y. Hu, X. Fu, X. Zheng, H. Liu and J. Tao

The adhesive layer should be applied in reasonable amount as to improve the strength, fatigue and properties of interlaminar because it will determine bonding strength between metal sheet layer and prepregs layer then it will affect the performance of

Table 2.3 Continued

Title	Year	Author	Findings
Effect of different lay-ups on the microstructure, mechanical properties and neutron transmission of neutron shielding fibre metal laminates	2016	Fu, X., X. Tang, Y. Hu, H. Li and J. Tao	The tensile strength and elastic modulus of laminate increased as the numbers of lay-ups also increased.

Table 2.4 Evidence of important

Previous research			
Author	Lay-up configuration	Method	Result
J.Bienas, P.Jakubczak, B.Surowska and K.Dragon	2/1	Aluminium 2024-T3 Surface treatment by anodizing in chromic acid (CAA) Al/CFRP prepreg Curing in autoclave at 135°C with pressure of vacuum 0.5 and	At energy of 5J, the maximum force acted on the FML was 497 N.

Shengqing Zhu and
Gin Boay Chai

2/1

Aluminium 2024-T3
Surface treatment by
sand grinding method
and used 400 grit size
of sand paper.

At 3.16 m/s, the
maximum force
was **2.48 kN** and
energy used;
12.06 J

Al/GFRP woven
laminate with L-530
epoxy

Curing in autoclave at
120°C under 0.69 Mpa
pressure for 2h 30min.

Table 2.4

Continued

Current research

Lay-up configuration

Method

Result

2/1

Aluminium 2024-T0
Surface treatment by sand
grinding with 100 grit sand
disc.

At energy of 5J, the
maximum force was
1.834 kN.

Al/CFRP UD prepreg

Pressed by a hot press machine and cured at 125°C under 4 bar pressure for 1h.

2/1

Aluminium 2024-T0

At energy of 12.06 J, the maximum force was 3.07 kN

Surface treatment by sand grinding with 100 grit sand disc.

Al/GFRP woven laminated with epoxy DER 331

Cured and pressed by a moderate load at room temperature for 24h.

UMP

CHAPTER 3

METHODOLOGY

3.1 Introduction

The motivation for this research is based on the need for lightweight materials in the automotive industry and the continuous evolution of testing methodologies used to evaluate their dynamic impact performance. This research therefore bridges the assessment of potential lightweight automotive materials with the evaluation of two testing methodologies used in assessing their low-velocity and quasi-static impact tests. The experimental work referred to ASTM D7136. The types of data were collected and recorded for the low-velocity impact tests as force (kN) against velocity (m/s). While for the quasi-static impact test, the data of load (kN) against central deflection (mm) was collected and recorded.

3.1.1 Flowchart

The flowchart of research shown below is a flow of research work which started by reviewing previous articles that related to major study; Fibre Metal Laminate. The research work involved experimental work and finite element modelling. Finite element modelling used to predict the failure behaviour of fibre metal laminate under static and dynamic impact. The experiment results validated with result of finite element analysis. The validation would be repeated if the analysis failed. The analysis would be failed if have problems on mesh geometry and material properties input of the modelling.

3.2 Finite Element Modelling

The analysis of a structure can be conducted by using a finite element method. Furthermore, the current finite element software is capable to simulate nonlinearity material or geometry, contact interaction of a structural with fluids, metal forming, crash simulation and more. The FE modelling is a useful numerical technique to predict the behaviour and performance of the FML. The finite element analysis data of the FML model would be validated with the experimental data as the final task. Assessment of the FML composites as replacement material will be conducted and compared with existing commercial structures and materials available in the market.

3.2.1 The Details of Simulation development by using Abaqus

In this research, a model of FML was built to predict the failure behaviour of the model as to achieve the third objective of this research. The FML was model constructed by using the Abaqus/Explicit. The Abaqus was used to develop a simulation. A few were required to be followed as to fulfil the requirements for getting a result of the simulation.

The first step in building a model of FML is to create the part. The part was constructed by deciding a shape and the dimensions. A FML (aluminium and composite) indenter was sketched as shown in Figures 3.1 and 3.2. The FML model was extruded by two types of extrusions. The materials, aluminium and composite were modelled by using a solid and shell extrusion. The illustration of extrusion could be referred in Figure 3.3. In addition, the composite part was extruded by the shell extrusion because in a material property, the part would be applied with Hashin's damage criteria.

While, the indenter was modelled by using a solid revolution. The degree of the revolution was 360 degree. The illustration of 360 revolution could be referred in Figure 3.4. The FML consisted with three layers, which have same configuration layup to the fabrication which 2/1. The shape of FML was sketched in a circular shape with a diameter 160 mm. Furthermore, the indenter was created by using a combination of line and circle. The diameter of the circle is 12.7 mm and height of the indenter was 70.00 mm. Each part has a reference point as a reference during assembling the parts.

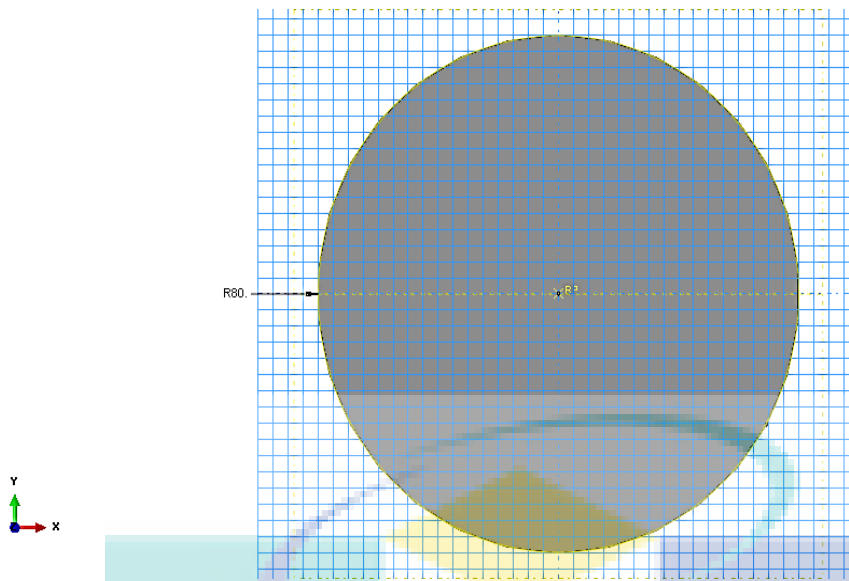


Figure 3.2 Sketch of FML with radius 80 mm and specify a reference point at the centre of the FML model

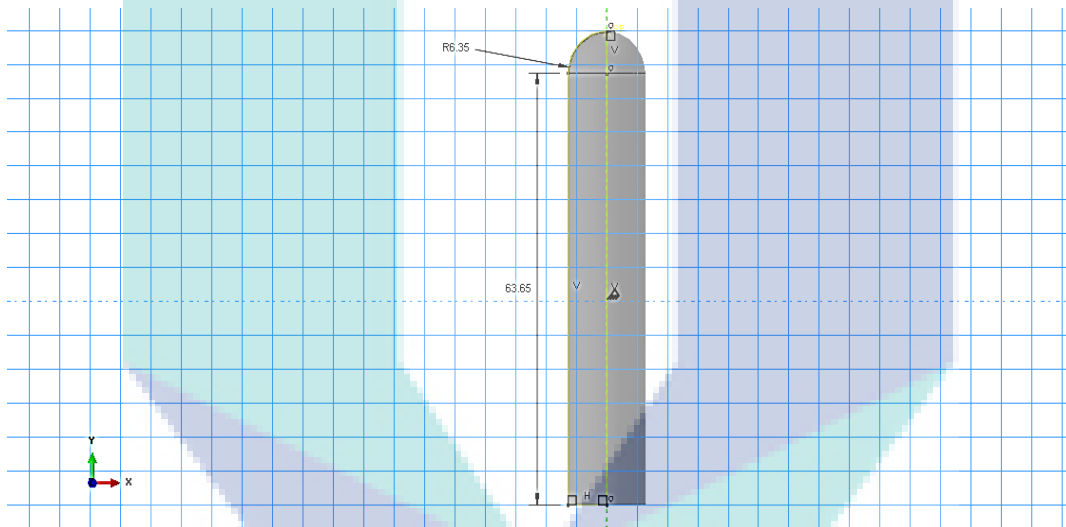


Figure 3.3 Sketch of indenter with specific dimension and define a reference point at the tip of the indenter.

The next step after creating all part for LVI and QSI models is defining material for those parts as in Figures 3.5. The FML was modelled based on two types of materials, aluminium 2024-0 and composite material (whether CFRP, GFRP or SRPP). The Hashin Damage was applied to the composite material. For impact prediction the aluminium 2024-0 was modelled by types of hardening based on Johnson-Cook and Isotropic. The Johnson-Cook was used in failure behaviour prediction for low-velocity impact and the Isotropic was used for quasi-static indentation. Since the purpose of the simulation is to predict the damage

behaviour of the FML, the material setting for the Aluminium needs to have Ductile Damage and Ductile Evolution. The Elasticity and Plasticity of the sheet metal were decided. The Damage Evolution and Damage Stabilisation were already set in Hashin Damage setting.

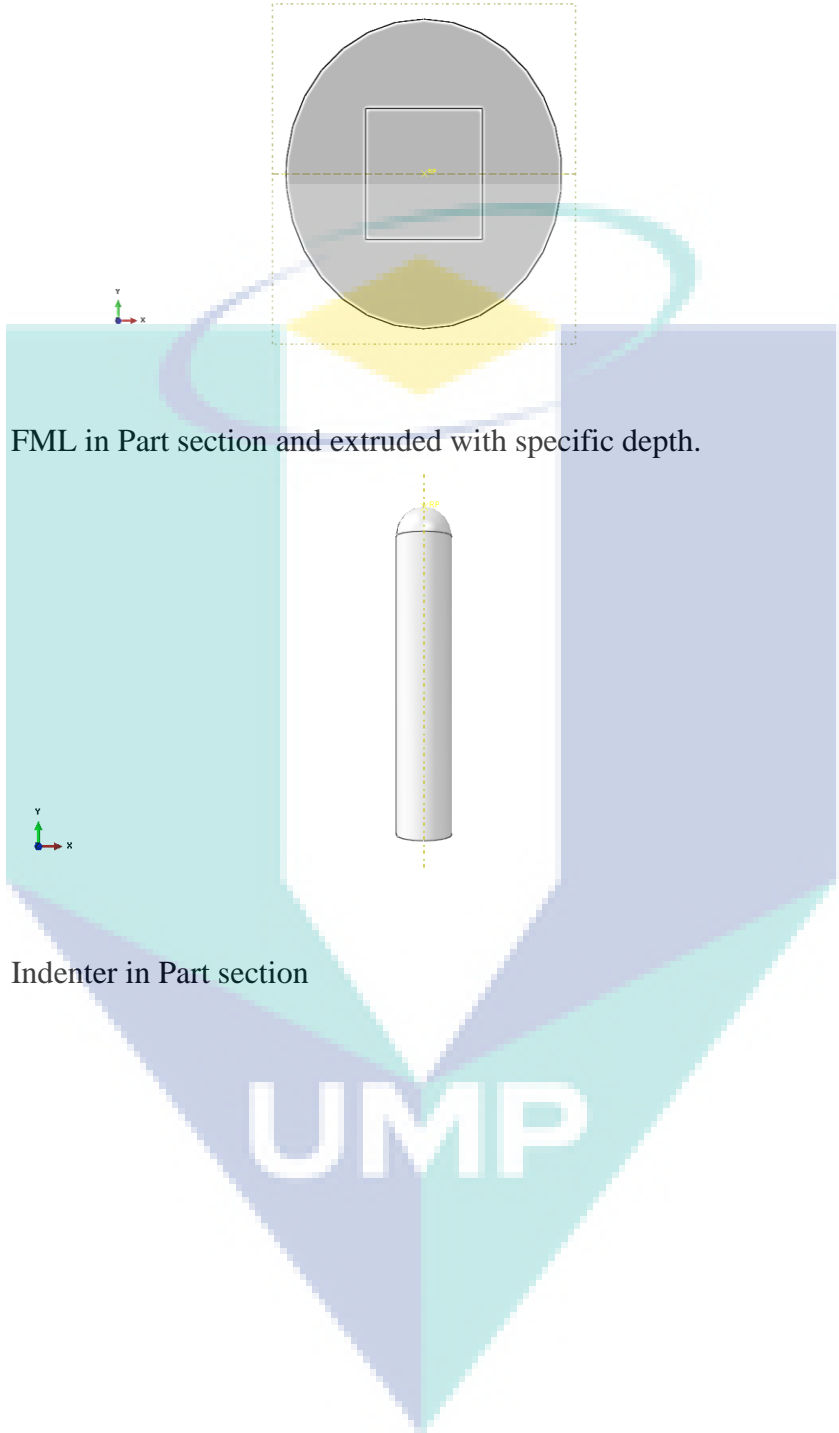


Figure 3.4 FML in Part section and extruded with specific depth.

Figure 3.5 Indenter in Part section

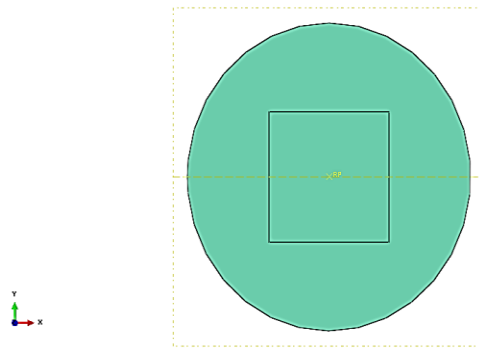


Figure 3.6 FML in Property section

The next step of the task is as shown in Figure 3.6 would be setting the assembly of the FML and indenter. The assembly of FML model, the aluminium and composite was based on a reference point from each part. The parts should be independent so that meshing could be done by part. The indenter should be positioned at the centre and opposite to the FML.

After assembling the materials to the indenter, the next procedure is to create a Step. In LVI model, the Step of analysis was defined as a Dynamic, Explicit and applied to the whole model of the FML as to have a graphic motion of damage behaviour on the FML model. While, in QSI model was defined as a Static, General, which is suited for the quasi-station motion. The model would behave throughout of the chronological timeline when the simulation starts. At the beginning of the simulation, there was no load and movement occurred. The simulation would start right when a load was applied to the FML. To make it simple, the simulation is a process where the model was set how it would behave initially before the simulation and analysed the model movement once the simulation started. An initial step must be conducted before applying a load onto the model. A new step is created by selecting a Step icon on the left side in the Model Tree. It was created by default. For this simulation, the step was mentioned earlier.



Figure 3.7 Indenter and FML in Assembly

A field output from the data that was spatially distributed and generated to the entire model or over a portion. During running the simulation, the field output used to view deformed shape, contour or symbol plots. During analysis, the Abaqus would generate large amount of field output. Then the Abaqus would write the data in a low rate; for example, after every step or at the end of the analysis. In Abaqus, a user could decide the frequency of the outputs in increments or the user could request it after the last increments. The Abaqus would write the selected variable in an output database.

The Abaqus would generate history output from a data at a specific point. In Visualisation module, the history outputs would be displayed in X-Y plots. The output rate depended by the user. The user would decide on how to use the data generated by the analysis.

The interaction on the FML was created and showed in Figure 3.7. Type of the interaction that has been chosen was general contact (explicit). The first interaction was created for a top surface of the FML and the application was for a moment when the indenter touched the top surface. The second interaction was applied to a surface-to-surface contact (aluminium- to-composite). The second type of the interaction and to be applied to the surface-to-surface was a contact type. The mechanical behaviour of the contact applied as; tangential behaviour. Penalty selection in the tangential behaviour used to permit some relative motion on the surface like an elastic slip. When the surface stacked to another surface, the Abaqus would adjust a magnitude of the penalty constraint and apply to the condition. In

this simulation, setting of boundary conditions on the FML were developed as shown in a Figure 3.8.

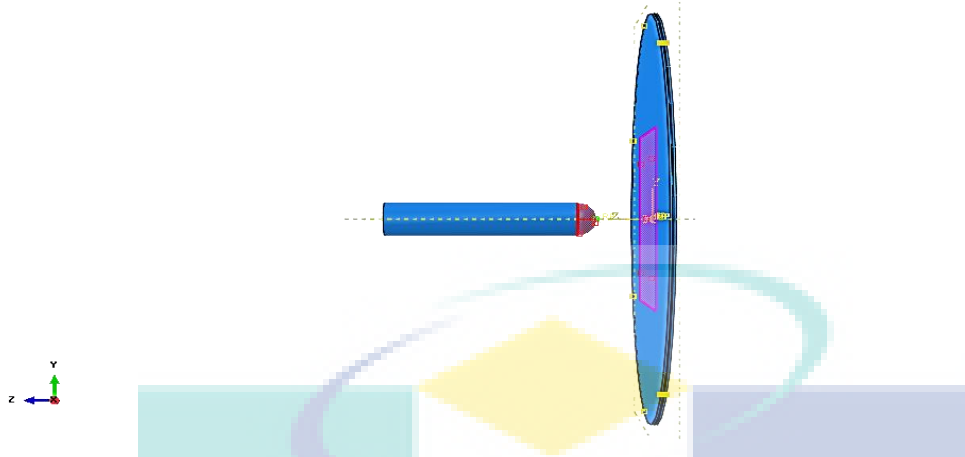


Figure 3.8 Surface interaction between indenter and FML

The boundary condition of the FML was created by clicking the boundary condition icon in the Model Tree. A type of boundary condition, Encaster was applied to the FML. Another boundary condition, Displacement/Rotation was created and applied to the reference point of the indenter. In this simulation, the FML would be hit by the indenter. Therefore, velocity was applied to the indenter by creating a predefined field from the Model Tree. The velocity was applied to the reference point of the indenter. After the boundary conditions have been set up, the process of the simulation was continued by applying to the FML. The type of load that has been applied was a concentrated force.

UMP

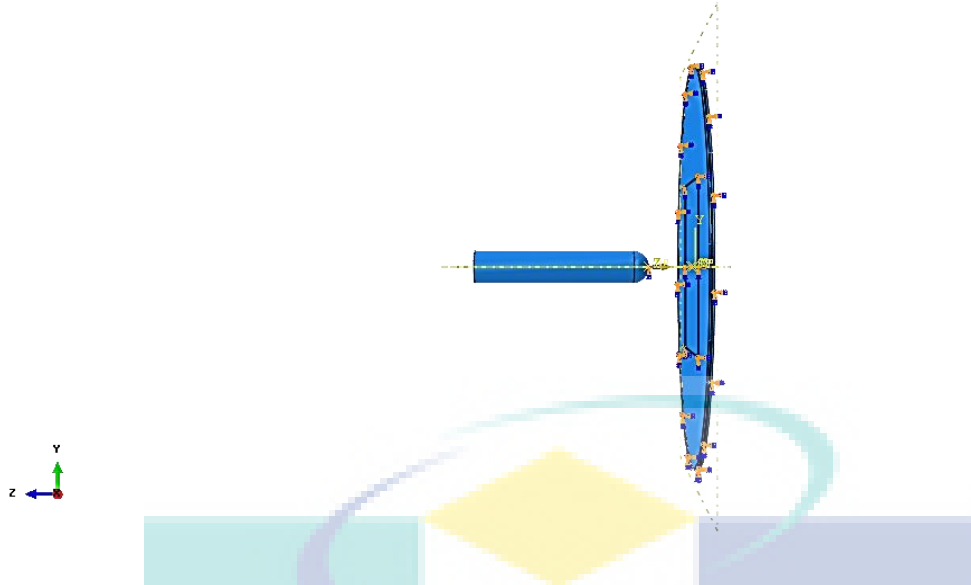


Figure 3.9 Boundary condition location on indenter and FML

The meshing is a stage that almost complete the construction of the simulation. In Figure 3.9, two types of meshing were applied to the Aluminium and Composite; 3D stress and Continuum shell. Then, the mesh element was defined to the both model, the indenter and FML. The size of the mesh element could be decided by changing the size of global seed in the Model Tree. The number of meshing element for the FML was consisted with 536 hexagonal elements of an aluminium plate and 436 hexagonal elements of composite ply; meanwhile, the indenter has 438 hexagonal elements. At the middle area of the FML model, a partition was created and the size of global seeds was smaller than other area and indenter part. The partition was created for fining the mesh size and focusing at particular area of failure.

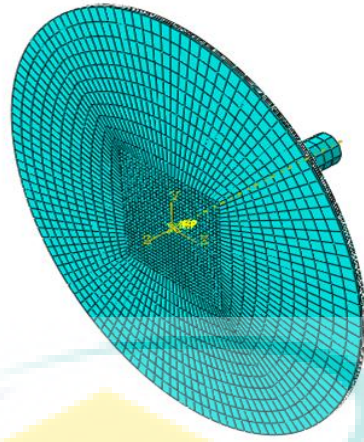


Figure 3.10 Meshing of indenter and FML

3.3 Design of Experiment

In this research certain limitations were implemented. Only four different variations of lightweight materials would be tested. The size of the FML specimen is 150 mm x 150 mm. The configuration of specimens that were fabricated as:

- (i) Al/CFRP/Al
- (ii) Al/SRPP/Al
- (iii) Al/GFRP/Al
- (iv) Al/UD-CFRP/Al

UMP

Table 3.1 Design of experiment for quasi-static indentation and low-velocity impact tests.

Low-velocity impact (m/s)					Quasi-static indentation (mm/min)					
Speed	2.70	3.33	3.90	4.50	Speed	1	5	10	50	100
Al/CFRP					Al/CFRP					
Al/SRPP					Al/GFRP					
Al/GFRP					Al/UDCFRP					
Al/UDCFRP					Al/SRPP					

3.4 Research Procedure

The research procedures comprise of the surface treatment and fabrication process of the fibre metal laminate. Besides that, the research procedures also contain modelling steps of fibre metal laminate as to predict the failure characteristic by applying the low-velocity and quasi-static impact. The impact applied based on velocity.

3.4.1 Metal Sanding on Aluminium Surface

A metal sanding is a surface treatment used to rough the aluminium surface by using a hand grinder. This is an effective and cheaper way for roughing the surface be and ensure the bonding between the composite fibre and metal would strong enough. An aluminium oxide sandpaper is the best material to be used for the metal sanding application.

The sandpaper can be used to many types of materials such as wood and metal. There are many grit sizes for the specific applications. The ranges of sand grits can be achieved for metal finishing. A sandpaper with grit 100 is similar to sand blasting treatment and can be applied to outdoor furniture, car parts and railings. Meanwhile, fine grit can apply to softer materials such as copper. If using aluminium oxide it is similar to 200-grade sandpaper. In addition, the sandpapers can be found in various shapes such as sheets, discs, belts and more. The other purposes of the metal sanding are:

- (i) Advance cleaning process.
- (ii) Removal of old paint, casting material or coatings.

- (iii) Remove stubbornly dirties such as grease, rust, scale or water deposits.
- (iv) Protect metal surface.
- (v) Surface preparation prior to painting, bonding and coating operations.
- (vi) Remove machined profiling such as burr or edge.

3.5 Materials Preparation

In this study, four types of material were used and tested under quasi-static indentation and low-velocity impact tests. These materials bond to the aluminium alloys by using the polypropylene film which acts as the adhesive layer and interlayer between sheet metal and composite fibre. The results of FMLs validated with the finite element analysis. Abaqus 6.13 version. The finite element analysis, Abaqus/Explicit was used and applied as isotropic and damage models to the aluminium 2024-T0.

3.5.1 Aluminium Sheet Metals

In the Fibre Metal Laminate (FML) specimen used aluminium alloy sheet metal then followed by composite materials. The preparation of the specimen used compression moulding method. The aluminium alloy surface roughened by sanding technique. The purpose of sanding is to improve toughness of bonding between the prepreg fibres (carbon fibre) or SRPP with aluminium alloy sheet metal. The type of the aluminium alloy that has been used; 2024-T0. The data sheet of the aluminium alloy could be referred at **APPENDIX D**



Figure 3.11 Aluminium alloy sheet metal

3.5.2 Self-Reinforced Polypropylene Polymer (SRPP)

The self-reinforced polypropylene polymer or known as SRPP commonly used in the automotive application as to replace incompatible of recycled plastic in the industry and reduce weight of the vehicles. The SRPP has been used in manufacturing non-structural of car components. The SRPP is cheap and resistant to corrosion. The material cannot be used at a high temperature. A polypropylene film has been used as an adhesive layer to bond between SRPP and aluminium alloy sheet metal. The SRPP prepared by a manufacturer, Curv. The fibre orientation of the SRPP is weave. The data sheet of self-reinforced polypropylene polymer (SRPP) attached at **APPENDIX E**.



Figure 3.12 Self-reinforced polypropylene polymer (SRPP)

3.5.3 Adhesive Film



Figure 3.13 Polypropylene film

This polypropylene film used as an adhesive layer to bond between sheet metal alloy, aluminium 2024-0 and self-reinforced polypropylene polymer. The adhesive film manufactured by Collano. A specific temperature (165°C) applied to melt the adhesive film. The adhesive film cut with the same size of the specimens. A polypropylene film was used as an adhesive film to attach sheet metal and composite prepreg fibre. The adhesive film known as an interlayer between the layer of sheet metal and prepreg fibre. During hot press process, the temperature should not be higher than the melting point of the adhesive film. The polypropylene film is manufactured by Collano. Data sheet of the adhesive film shown in **APPENDIX F**.

3.5.4 Carbon Fibre Reinforced Polymer (CFRP)

The uses of the carbon fibre prepreg are or sports ware, aviation, renewable energy, bicycle parts, carbon roller, fishing rods/poles and structures. There are two types of carbon fibre used in FML specimens; Al/CFRP/Al such as prepreg and dry fibres. Carbon fibre reinforced polymer manufactured by Za Composite. Fibre orientation of dry fibre is plain weave fibre and type of the fibre is 3K. The fibre should be laminated by using epoxy and cured at room temperature for 24 hours. Data sheet of carbon fibre shown in **APPENDIX G**. The prepreg fibres is unidirectional orientation fibre and cured by hot press process. The prepreg fibre would be pressed under a pressure of 4 bar at 125 °C for one hour.

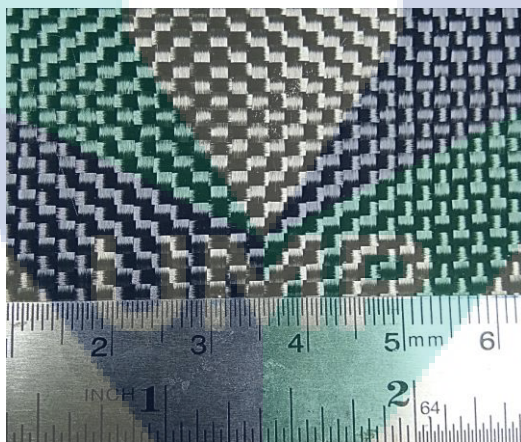


Figure 3.14 Dry plain weave fibre of CFRP



Figure 3.15 Prepreg unidirectional fibre of CFRP

3.5.5 Glass Fibre Reinforce Polymer (GFRP)

The glass fibre used in the fabrication of FML specimen and layup as Al/GFRP/Al. The fibres were laminated with thermoset epoxy and cured in room temperature for 24 hours. The hardener and epoxy was mixed in ratio 2: 1. Both need was prepared at a room temperature so that the mixture did not produce bubbles. The strength of plain weave glass fibre are (Rejab & Cantwell, 2013):

Table 3.2 Table of mechanical properties for plain weave glass fibre

Property	Symbol	Value (MPa)
Transverse tensile strength	(Y_T)	320
Transverse compressive strength	(Y_C)	260
Longitudinal tensile strength	(X_T)	320
Longitudinal compressive strength	(X_C)	260

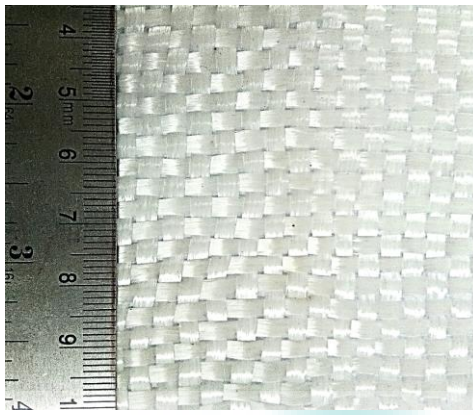


Figure 3.16 Dry plain weave fibre of GFRP

Table 3.3 Summary of material mechanical properties

Aluminium alloy 2024-0		
Yield Tensile strength (MPa)	Young's modulus (GPa)	Ultimate Tensile strength (MPa)
95	73.1	220
Carbon Fibre Reinforced Polymer (CFRP)		
Flexural strength (MPa)	Young's modulus (MPa)	Tensile strength (MPa)
170	3000-4000	68-78
Self-Reinforced Polypropylene Polymer (SRPP)		
Flexural modulus (MPa)	Young's modulus (MPa)	Tensile strength (MPa)
3500	4200	120
Polypropylene (PP) film		
Yield stress (MPa)	Young's modulus (MPa)	Tensile strength (MPa)
4	20	26

3.5.6 Epoxy and Hardener

The type of resin used as a matrix for the plain weave carbon fibre and glass fibre is thermoset epoxy. The thermoset epoxy requires curing when it undergoes a polymerisation process, cross-linking. During the process, a high thermal stability, a good rigidity and hardness and resistance to the creep are required. Besides that, the resin provides heat and chemical resistance and basic flammability. The reinforcement can affect by those and the main effect is on tensile strength and toughness. Normally a hardener used to comprise the resin system for the reinforcement. The thermoset epoxy and hardener is prepared by Salju Bistari Sdn. Bhd. The brand of the epoxy is DER 331 while the brand of the hardener is Joint Mine.



Figure 3.17 Epoxy and hardener

3.6 Specimen Preparation

Fibre metal laminate (FML) consisted of two different layers; sheet metal layer and composite materials layer. The types of composite materials used are carbon fibre reinforced polymer, glass fibre reinforced polymer and natural fibre. The specimens would be fabricated in form of Al/CFRP/Al, Al/SRPP/Al, and Al/GFRP/Al. The dry fibres were laminated by using thermoset resin, epoxy. Thermoset polymer contains of strong covalent bonds and formable at high temperature and pressure because of the bonds are weak. The polymers are

insoluble and infusible after cure because the bonds bonded rigidly. The epoxy mixed with hardener at right amount. The amount ratio is 2:1. The advantages of epoxy are:

- (i) High mechanical strength
- (ii) Good adherence to metal and glasses

The mixing between epoxy and hardener affected on viscosity, impact tolerance and degradation. Besides that, the mixing process creates an exothermic reaction whereby the heat would be released. Although epoxy is expensive than other polymer matrices, it commonly used by many industries because of the advantages. Epoxy is low molecular weight organic liquids, which contained epoxide groups. The other reasons why epoxy popular and still used by industries are:

- (i) High strength
- (ii) Low volatility during cure
- (iii) Low viscosity and flow rates: allow good wetting to fibres and prevent fibres misalignment during processing.
- (iv) Low shrink rates: to reduce the tendency of gaining large shear stresses of bond between epoxy and reinforcement.
- (v) There are more than 20 grades of epoxy to meet specific property and processing requirements.

3.7 Procedures of Fibre Metal Laminate Fabrication

- (i) Aluminium 2024-0 that was roughened and placed as first layer.
- (ii) Polypropylene film put as adhesive interlayer at interface of self-reinforced polypropylene (SRPP) and aluminium 2024-0 sheet.
- (iii) The plain weave carbon fibre and glass fibre were prepared by using epoxy and hardener as showed in Figure 3.17. The specimen cured at a room temperature for 24 hours.

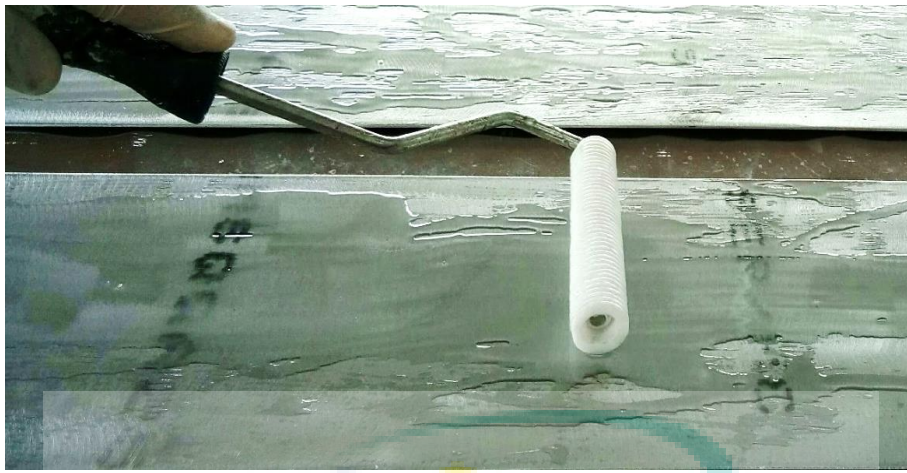


Figure 3.18 The resin applied by using a roller

- (iv) The fibres were stacked by following the orientation of fibre.
- (v) The fibre metal laminate with prepreg fibre (UD-CFRP) was pressed under the pressure 4 bar at temperature 125 °C for 2 hours. While the fibre metal laminate with SRPP was pressed at 165 °C under 30 bar. These fibre metal laminate was pressed by using a hot press machine. In Figure 3.18 showed a hot press machined which used to press and cured specimen Al/UD-CFRP and Al/SRPP.



Figure 3.19 Hot press machine

- (vi) The panel removed from the mould when temperature cools down to 60°C.
- (vii) The mould was coated with Teflon film so that easily to remove the laminate.

- (viii) The roller used to squeeze excess of epoxy on the fibres.
- (ix) All materials for quasi-static indentation test were drilled to make holes as to fix the material position onto the material clamber. The size of the holes were exactly same to the hole size of the material clamber. The materials were drilled by using a milling machine as illustrated in Figure 3.19. The value of 1096 RPM was used in the drilling process. The holes were made by using M6 drill. Before that, a centre drill was used to make as a benchmark for the drilling process.

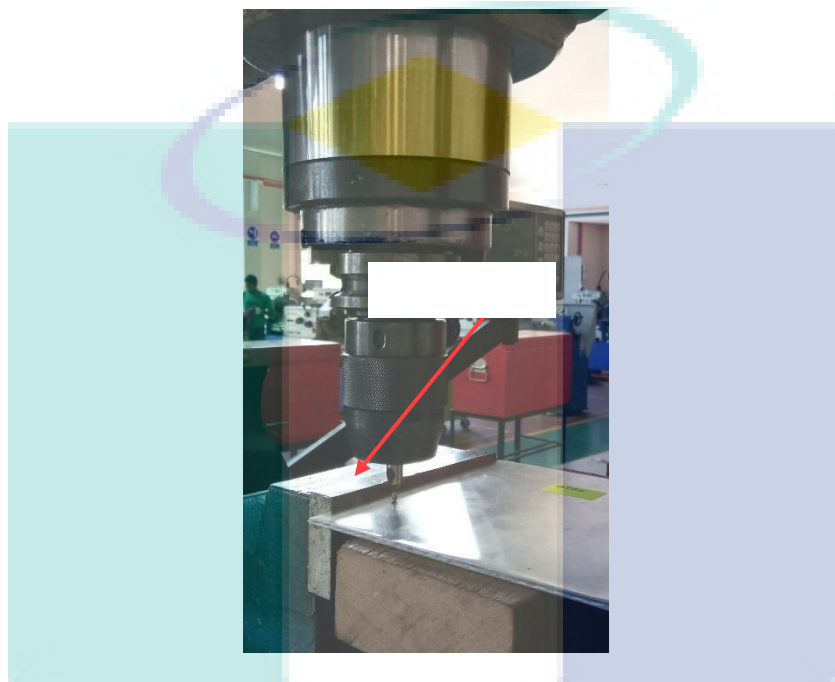


Figure 3.20 Drilling process on FML

3.8 Static and Dynamic Testing Machines

There are two types of machines used for static and dynamic impact testing. The machines are Drop Tower Instron CEAST 9350 and Instron 3369 Universal Testing Machine. The result of force (kN) against displacement (mm) was recorded from the Instron 3369 Universal Testing Machine while the data of force (kN) against displacement (mm) by using the Drop Tower Instron CEAST 9350 machine. Data were collected by five variation of velocity (m/s) and crosshead speed (mm/min).

3.8.1 Drop Tower Instron CEAST 9350 Impact Testing

The fibre metal laminate specimens were tested by using this machine, in Figure 3.20. The testing conducted at Universiti Teknologi Malaysia UTM, Skudai for a low-velocity impact testing. The testing machine is high-energy configuration. The high-energy

configuration increases the energy capacity from 757-1800 J and the velocity from 4.65-24.0 m/s. The anti-rebound system can avoid from hitting the sample for a second time. The pivoting specimen loader test can up to 10 specimens in a rapid sequence within the environmental chamber. The weighing system measures the total weight of falling mass and tub insert. The specimen feeding system performs tests in an automatic cycle within the environmental chamber. The system designed to meet the demand for an automation cycle. The high-volume testing required 60-120 per hour. The environmental chamber can cool down the specimen during testing to -70°C or heat specimen to $+150^{\circ}\text{C}$. Diameter of upper material clamber is 33 mm. Outer diameter of lower material clamber is 160 mm while inner diameter is 127 mm. the material clamber showed in Figure 3.21. The diameter of impactor is 12.7 mm and showed in Figure 3.22.



Figure 3.21 Low-velocity impact test machine (Instron CEAST 9350)



Figure 3.22 Material clamper

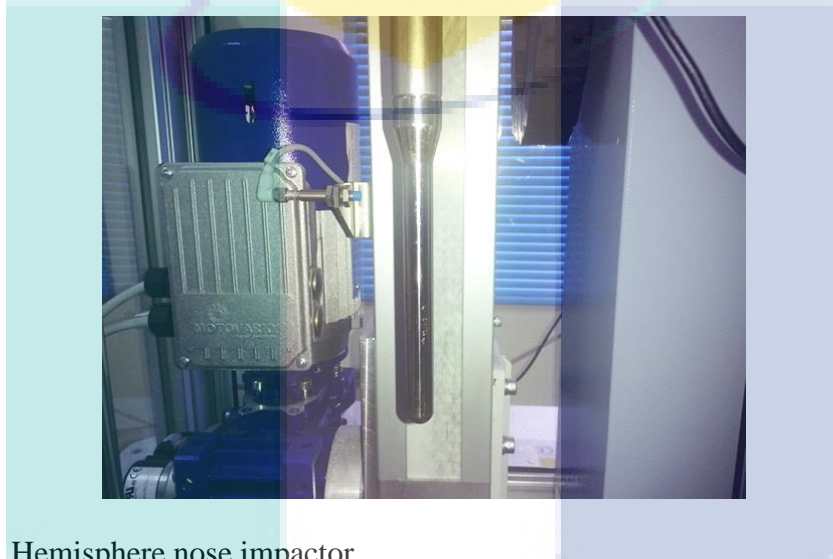


Figure 3.23 Hemisphere nose impactor

3.8.2 Instron 3369 Universal Testing Machine

The Instron Universal Testing Machine will be used in a Quasi-static test. The testing will be handled at Universiti Malaysia Pahang (UMP). The machine installed a few strain gauges that functioned to give outputs such as force, strain displacement and speed. While, the force of the machine is 50 kN. The software of BlueHill Light would use during conducting the experiments. The method of the experiment could be set up by using this software. The compression plate is not suitable to be used for the quasi-static test. The indenter and material clamper have been will be fabricated. The diameter of the indenter is 12.70 mm. The outer diameter and inner diameter of material clamper are 160 mm and 127 mm. The sizes are exactly followed to the low-velocity impact machine. The quasi-static impact test has been done to FML specimens by different crosshead speed rate; 1 mm/min, 5

mm/min, 10 mm/min, 50 mm/min and 100 mm/min. the data were collected and analysed through a graph of load (kN) against displacement (mm).

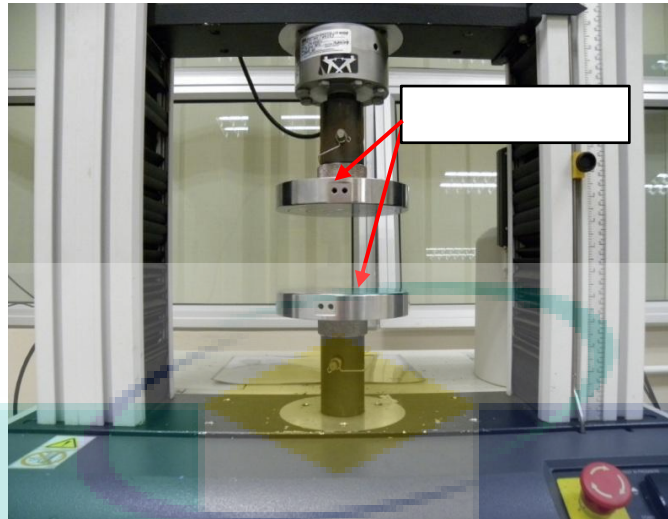


Figure 3.24 Compression test machine (Instron 3369 Universal Testing Machine)

A drilling process drilled the material clamped by using CNC machine. A coolant that has been used during the machining as to reduce the surface roughness and the temperature during the machining process can be lowered. The drill holes were made to clamp the material tightly and make sure the material in the fix position. Besides that, it could also reduce errors during running the impact testing. The position of the material has been tightened by using eight of counter bolts. The size of the counter bolt is M5.

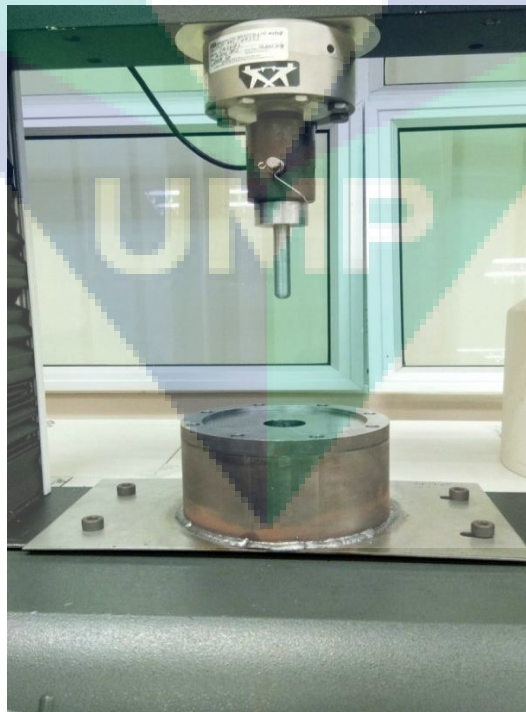
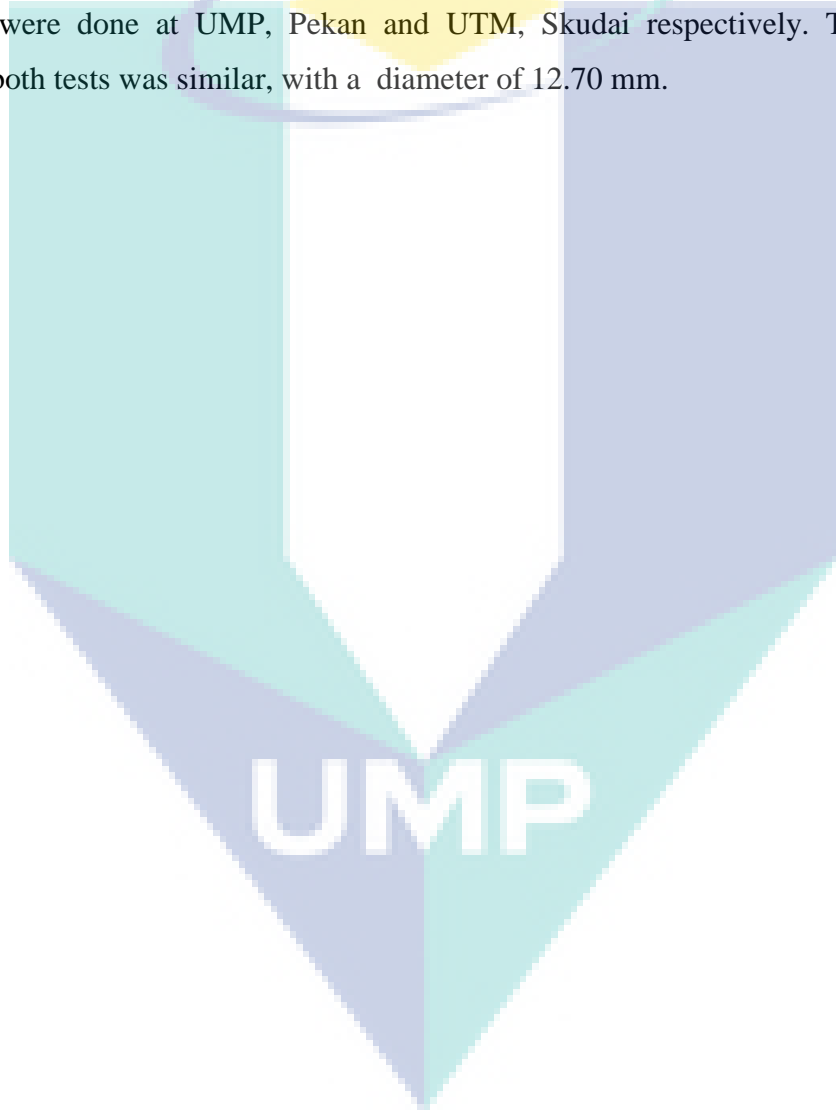


Figure 3.25 The compression plate replaced with an indenter

3.9 Summary

Chapter 3 presented details of the fabrication of the fibre metal laminate, the experimental set up as well as the testing procedure for the quasi-static and dynamic loading. The fibre metal laminates were fabricated by using aluminium alloy 2024-0, plain weave and prepreg CFRP, GFRP and SRPP. These fibre metal laminates were fabricated by using a compression moulding technique. The geometry of the specimens was fixed, 150 mm x 150 mm. The quasi-static indentation and low-velocity impact test were used to investigate the failure behaviour on the fibre metal laminate. The quasi-static indentation and low-velocity impact tests were done at UMP, Pekan and UTM, Skudai respectively. The size of an impactor for both tests was similar, with a diameter of 12.70 mm.



CHAPTER 4

RESULTS AND DISCUSSION

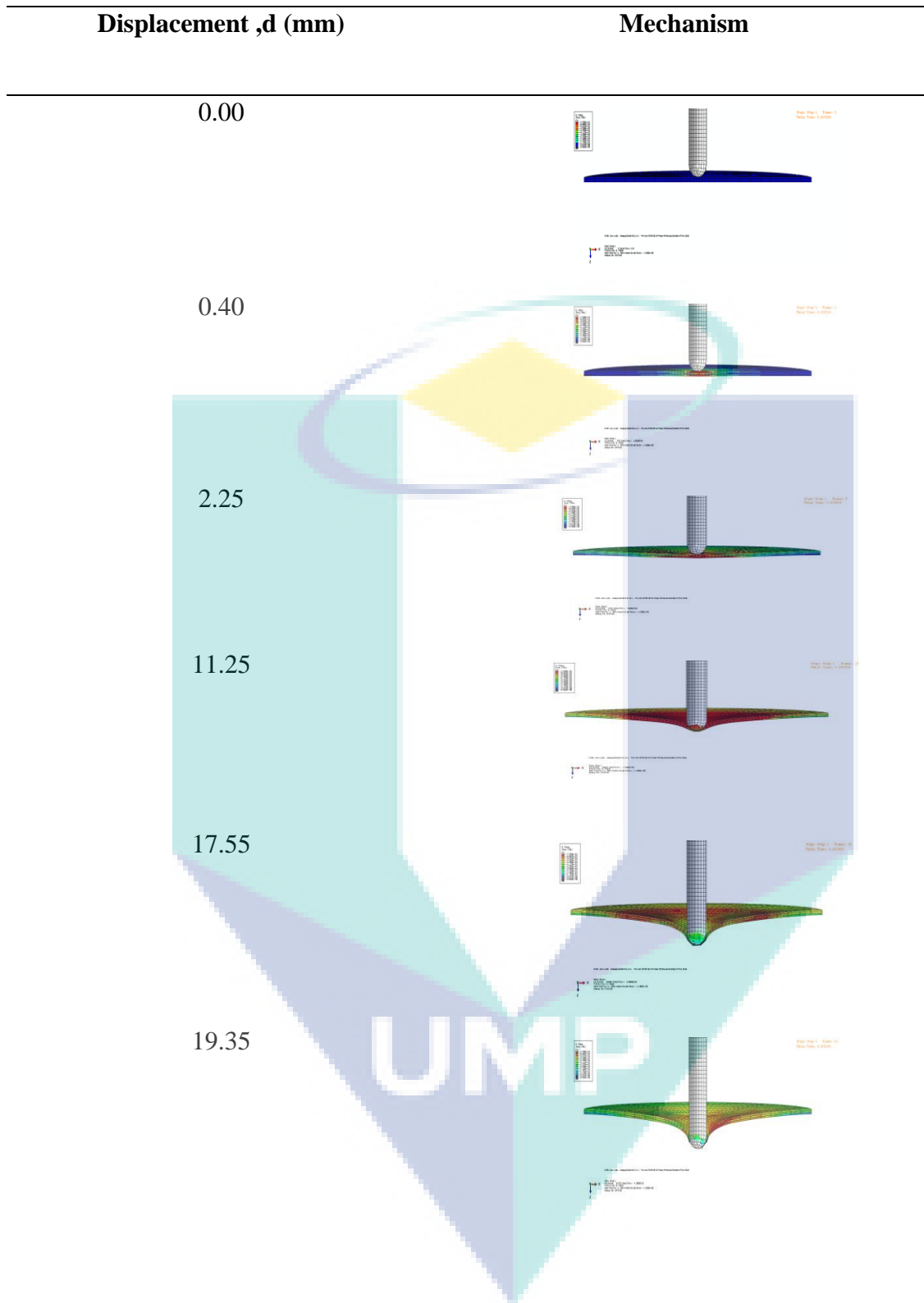
4.1 Introduction

This chapter discusses the results from the experiments conducted. The type of material used were plain weave of carbon fibre-3K and glass fibre, woven fibre of self-reinforced polypropylene polymer and unidirectional prepreg carbon fibre. These materials were tested with two types of impact tests such as low-velocity and quasi-static impact test. Besides that, these materials were using five variations of velocities. The variables of the experiments; velocity, the orientation of the fibre and types of the materials. The geometry of the specimens is fixed. The size of the specimens are 150 mm x 150 mm. The compression moulding technique was used as the manufacturing process.

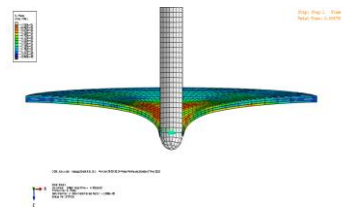
4.2 Prediction of Impact Failure

A failure prediction of fibre metal laminate was made for quasi-static indentation and low-velocity impact. The failure pattern of quasi-static indentation was similar to low-velocity impact failure pattern. The failure mechanisms were captured and recorded based on the displacement as in Table 4.1.

Table 4.1 Prediction of failure for fibre metal laminate



UMP



4.3 Quasi-Static Indentation (QSI) Test

Two types of testing were done; quasi-static indentation test (QSI) and low-velocity impact test (LVI). The QSI test was done by using Instron 3369 series Universal Testing machine, which was held at UMP, Pekan. The QSI specimens were tested based on different crosshead speed. The crosshead speeds that have been decided were 1, 5, 10, 50 and 100 mm/min. The compression plate of the machine was replaced with an indenter. The size of the indenter exactly followed to an indenter size of LVI machine. The result for every specimen was collected and recorded. The graph of load against central deflection was plotted based on the results.

4.3.1 Aluminium/Plain Weave Carbon Fibre Laminate

The damage area of the laminate is depended on a crosshead speed of the quasi-static loading. The crosshead speed and the constituent materials, the 2024-0 aluminium alloy and the carbon fibre reinforced polymer were in the present case. The prior to testing, the type of resin used and metal sanding were investigated. The thermoset epoxy was used as a matrix to laminate the carbon fibre with the aluminium alloy. The sandpaper with grit size 100 was applied on the aluminium alloy as to increase the bonding between the sheet metal and matrix. From the graph, it showed that the trending of failure on the fibre metal laminate increased when the crosshead speed increased from 1 mm/min to 100 mm/min.

The graph in Figure 4.1 shows that the performance of aluminium/carbon fibre with a crosshead speed 1 mm/min has lower load than 5, 10, 50 and 100 mm/min. The depth of the deflection was 21.28 mm and lower than an aluminium/glass with a crosshead speed 10 mm/min, which was 21.70. The thickness of both specimens are 2.22 mm and 2.27 mm. When the crosshead speed was increased, it could reflect the FML degradation. The degradation could be continued with the stages of failure such as delamination, matrix

cracking and fibre breakage. A symptom of cracking at the bottom layer of 2/1 configuration layup could happen because the laminate was hit until the maximum force.

Based on the graph shown the Figure 4.1, the maximum deflection of the aluminium/glass laminate 5 and 10 mm/min decreased when the thickness of laminate was increased. The thickness of 5 and 10 mm/min are 2.16 mm and 2.27 mm. The observation shows that the failure of the laminate based on the stiffness of the laminate. Usually, a thin laminate easily deformed because the aluminium alloy performed the elastic and plastic behaviour. When the kinetic energy of the indenter hit on the laminate, it could be transformed to an internal damage. The failure behaviour of the laminate such as perforation and penetration, which were dependent on a laminate thickness. The laminate that has high stiffness would result in a lower deflection.

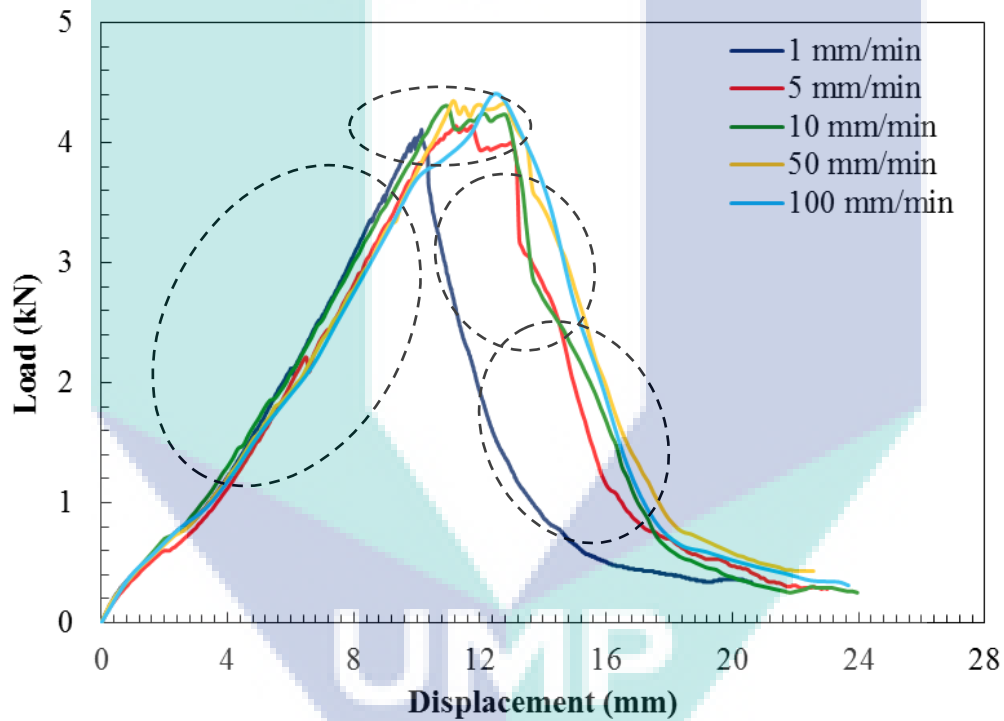


Figure 4.1 Graph of load against central deflection in Aluminium/Carbon Fibre Reinforced Polymer (CFRP) fibre metal laminate

The failure process of the quasi-static indentation on the FML was investigated by examining the front surface and rear surface of the impact-damaged samples. The initial fracture onto the 2/1 FML by 1 mm/min crosshead speed. The experiment was handled by using Instron 3369 Universal Testing Machine. The 1 mm/min impact as shown in Figure 4.2

(a). The damaged cross section has been taken through an indentation stage by the indenter at a top surface of the aluminium alloy. At the first stage, there was a localized crack on the matrix. The failure on the matrix was because of the preparation of layup process. The laminate start to bend because of the maximum load that acted on it and the laminate has a maximum bending. After that, there was a fibre breakage because of the maximum bending of the loading and the stiffness of the fibre. Then, there was an indentation on the bottom ply, aluminium alloy. The perforation on the laminate happened at the third stage of failure. The passage of the indenter through the target and produce a clean hole with a diameter that similar to the indenter. From the graph, the perforation involved a local ductility.

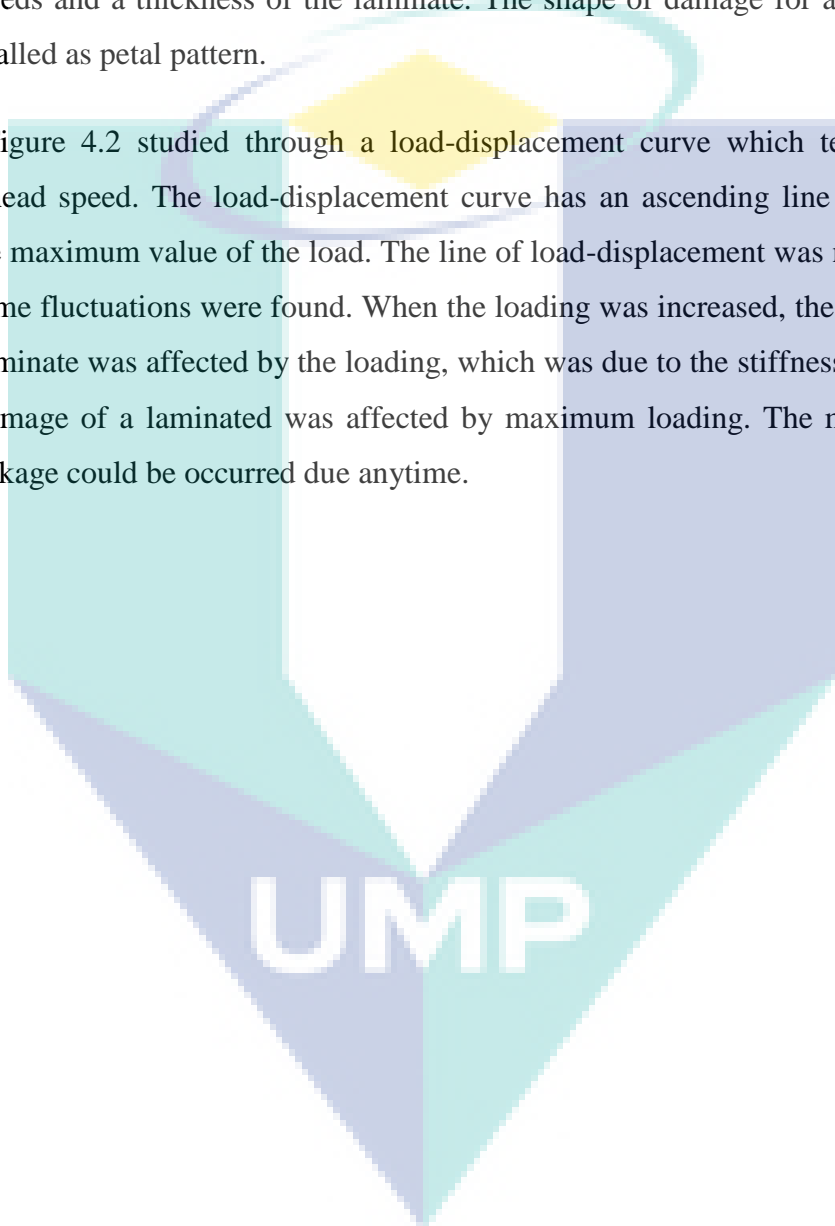
The higher crosshead speed resulted in an increase of composite structure degradation. Besides that, there was a number of transverse cracks which increased the delamination of the laminate especially at the middle area of the specimen (Bienias et al., 2015). The matrix crack also caused delamination of the laminate. When the testing was carried out with the highest crosshead speed of quasi-static loading it resulted in an extensive delamination at the middle part and bottom ply. When the crosshead speed increased, the deformation on the fibre metal laminate occurred at the same time. The matrix of the laminate damaged caused by impact and the connection between matrix-fibre became degradation. The epoxy resin is brittle and has low resistance to the crack propagation. The crack happened at a high transverse shearing stress, which connected with the contact force. The bending crack occurred easily if the volume of the matrix is higher than the volume of the fibre.

In the experimental works, the range of crosshead speed 1-100 mm/min involved delamination layer, failure of the fibre, plastic deformation and cracking of the aluminium layer. Impact crosshead speed increased when energy lost also increased and it defined as $1 - \eta$

(Bienias et al., 2015). The lost energy would constituent the energy which used to rebound the impactor. Besides that, the energy was also used as to overcome the friction from the indenter and during the impact, a sound would be produced. The sound signed for the failure of the fibre and cracking of the aluminium alloy. The deformation behaviours of the top surface is shown in Figure 4.2, respectively. The increasing of impact crosshead speed caused the impact energy localised around the impacted area, which leaded to fracture and penetration of that area for fibre metal laminate panels with plain weave composite fibre.

Based on the Figure 4.2 showed a cross section of indentation damage for the aluminium/carbon fibre laminate, which based on different crosshead speeds of the indentation. The evaluation of a composite structure based on the damage cross section. A delamination between a sheet metal and fibre layer normally found after cracking of the matrix and fibres. The damage cross section on the fibre metal laminates was analysed and followed by increasing the crosshead speed of the indentation. The values of the damage cross section were determined through an experimental. The values were compared based on the crosshead speeds and a thickness of the laminate. The shape of damage for all specimens is same which called as petal pattern.

The Figure 4.2 studied through a load-displacement curve which tested based on impact crosshead speed. The load-displacement curve has an ascending line when the load reached to the maximum value of the load. The line of load-displacement was not smooth and there were some fluctuations were found. When the loading was increased, the material of the fibre metal laminate was affected by the loading, which was due to the stiffness of a structure. The major damage of a laminated was affected by maximum loading. The matrix cracking and fibre breakage could be occurred due anytime.



UMP

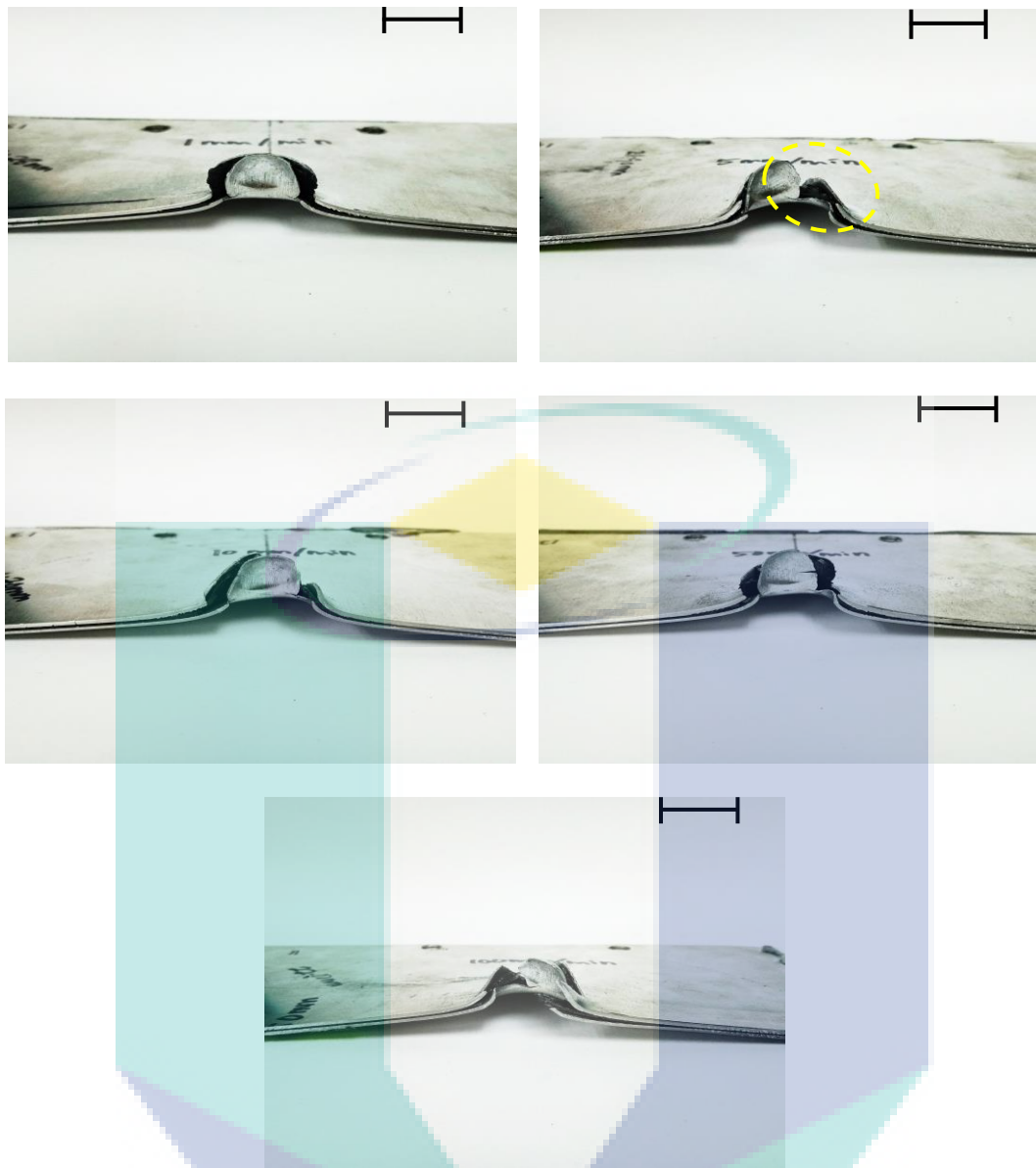


Figure 4.2 Typical damage of fibre metal laminate based on different crosshead speeds (a) 1 mm/min (b) 5 mm/min (c) 10 mm/min (d) 50 mm/min (e) 100 mm/min.

4.3.2 Aluminium/Glass Fibre Laminate

The typical curve of the load against central deflection was based on quasi-static indentation test at various crosshead speed; 1, 5, 10, 50 and 100 mm/min as shown in Figure 4.3. From the graph below, the aluminium/glass fibre laminate was responded to the maximum load yield and traced in the graph. At that point, the matrix started to crack and propagate. The maximum load of an aluminium/GFRP at 5 mm/min was greater than 1 mm/min. The impact loading was continued and resulted in a matrix cracking which was occurring in a stable manner. The aluminium/GFRP was impacted by crosshead speed 5

mm/min in an unstable manner where the cracking rapidly formed. A small residual displacement appeared after unloading. The residual displacement was traced in the load-central deflection curve. In a bi-material system, the residual displacement associated with a residual stress. The crack growth of the FML at 1 mm/min started to initiate at a value of 1.50 kN while at crosshead speed 5 mm/min started to crack at the value of 1.62 kN. The value of crack initiations at 5 mm/min was higher than 1 mm/min before reached to plateau value, 4.55 kN. It was because of the interfacial toughness was increased and associated with the fibre bridging formation the crack propagation. An investigation on the damage indentation of the fibre metal laminate by measuring indentation depth for each specimen.

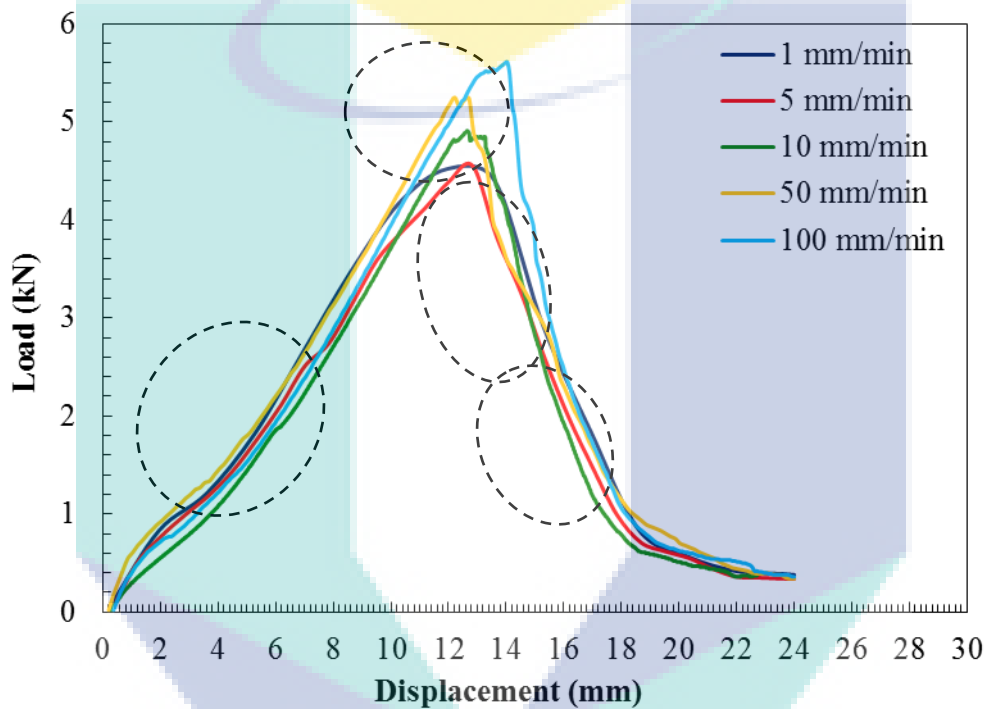


Figure 4.3 Graph of load against central deflection in Aluminium/Glass Fibre Reinforced Polymer (GFRP) fibre metal laminate

The failure area of the fibre metal laminate was depending on the crosshead speed of the quasi-static indentation. The variables of the testing were crosshead speed and type of composite materials used. The constants in the experiment are sheet metal alloy, aluminium alloy 2024-0 and size of the specimen. The size of the fibre metal laminate was 150 mm x 150 mm. The thickness of each specimen was different because of the fabrication technique. The fibre metal laminate was fabricated by using a compression moulding. A thermoset epoxy was used to laminate each ply of the fibre metal laminate. The surface of the sheet metal was

sanded by using a metal sanding technique and a type of sandpaper used was 100 grit. Based on the graph above, Figure 4.3 the length of deflection was measured roughly.

The observation of each specimen was made and found the pattern of the failure became increased when the crosshead speed increased from 1 to 100 mm/min. The performance of aluminium/glass fibre with a crosshead speed 1 mm/min has lower load than 5, 10, 50 and 100 mm/min which has been proven in the Figure 4.3. The depth of indentation was 21.48 mm and lower than an aluminium/glass with a crosshead speed 50 mm/min, which was about 20.70 mm. The thickness of both specimens was 2.35 mm and 2.59 mm. When the crosshead speeds have been increased, it could reflect the FML structure. The structure degradation could continue with the stages of failure behaviour such as matrix cracking, delamination and fibre breakage. A symptom of cracking at the lower ply of 2/1 configuration laminate could happen because the layup was hit until reached to the maximum load. The deflection length of the aluminium/glass laminate 5 and 10 mm/min have been increased. The thickness of both FMLs was 2.50 mm and 2.22 mm. From the observation, it showed that failures happened when the crosshead speed increased, the matrix was easy to crack by the maximum load.

Besides that, the stiffness of the laminate also one of the failure factor. Normally the thinner laminate easily deformed because of the elastic and plastic sheet metal. When the kinetic energy of the indenter was hit on the laminate, it could be transformed to an internal degradation. The failure behaviours like perforation and penetration were depending on a laminate thickness. The laminate that has high stiffness would result in a lower deflection. The process of failure in the quasi-static impact on the fibre metal laminates was investigated by examining the front surface and rear surface of the impact damage samples. There was an initial fracture onto the 2/1 laminate by 1 mm/min.

The quasi-static test was tested by using a testing machine, Instron 3369 series. The damage area of 1 mm/min is as shown Figure 4.4 (a). The area of damage has been taken through the indentation stage by an impactor at a top surface of the sheet metal alloy. At the first stage, there was a crack that localised on the matrix. The failure on the matrix affected by the fabrication technique of laminate process. The started to bend because of maximum loading that acted perpendicularly onto the aluminium alloy surface and the laminate has a maximum bending. The fibre breakage happened at a second stage when the laminate had a

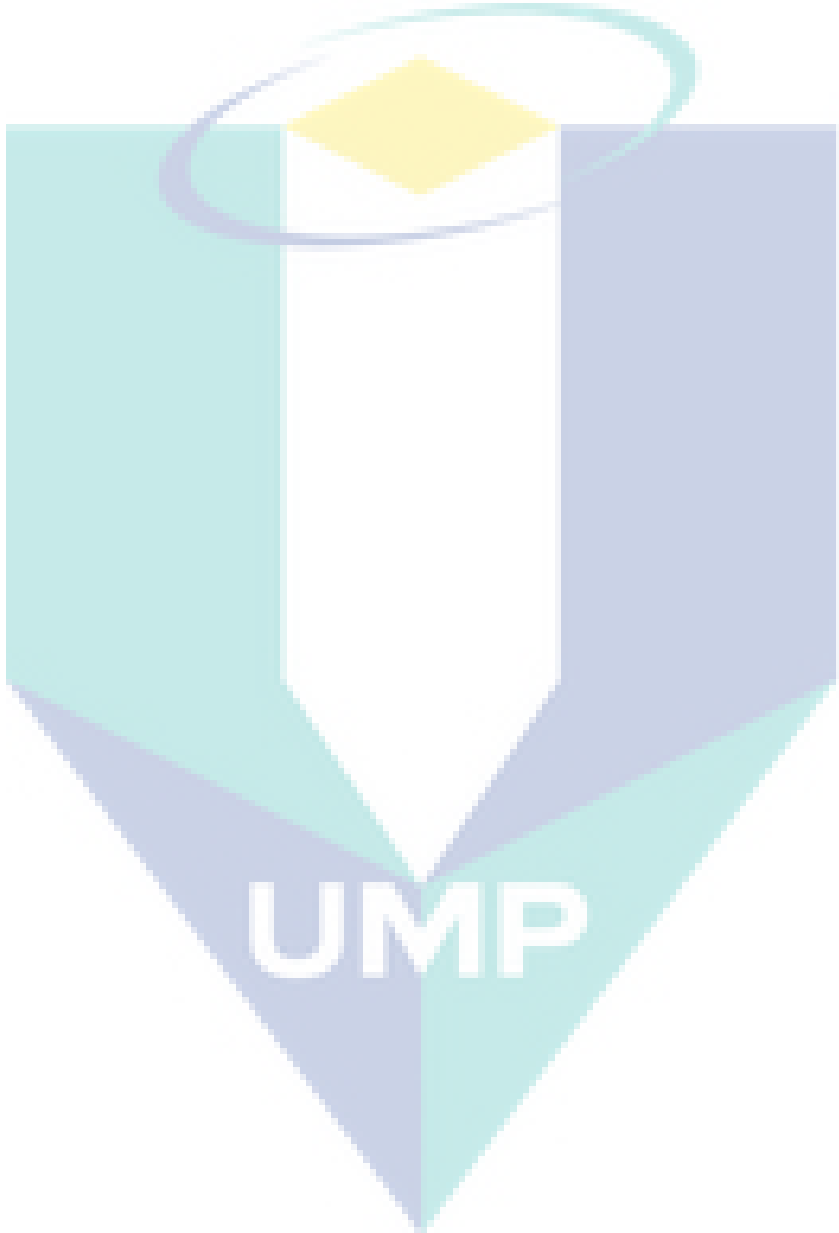
maximum bending. From the observation, there was an indentation effect at the bottom layer, aluminium alloy. The perforation on the fibre metal laminate happened at the third stage of failure. The indenter travelled through the fibre metal laminate and produced a clean hole with the same diameter of the indenter. The perforation of fibre metal laminate involved a local ductility of the aluminium alloy.

The higher crosshead speed resulted delamination in fibre metal laminate and increased impact resistance. In addition, there was a number of transverse cracks, due to delamination of the laminate especially at the middle area of the specimen. The delamination was conducted by a matrix cracking. When the testing was carried out with crosshead speed 100 mm/min it showed that an excess of the fibre delamination at the middle part and bottom ply. Furthermore, when the crosshead speed increased, the deformation of composite fibres would happen at the same time. The impact loading and connection between matrix–fibre could cause matrix damage and degradation. The thermoset epoxy characterised as brittle and has low resistance in a crack propagation. The crack would happen at a high transverse shearing stress, which was connected to the contact force. The bending crack was usually due to the volume of the matrix higher than the volume of the fibre.

The delamination fibre damage, plastic deformation and cracking of the metal layer had involved from the range of crosshead speed 1-100 mm/min during the experimental works. The lost energy would constitute the energy to rebound the impactor (Bieniaś et al., 2015). Other than that, the energy also used as to avoid the friction on the indenter and during the impact, a sound could produce. The sound produced was a mark where the failure like cracking and fibre breakage happened in the fibre metal laminate. The deformation behaviours on the bottom surface are shown in Figure 4.4, respectively. The increase of indentation crosshead speed caused the impact energy localised around the impacted area which led to fracture and penetration of the fibre metal laminate damage cross section with plain weave glass fibre.

In Figure 4.4, the surface area of damaged fibre metal laminates was due to the crosshead speed of quasi-static indentation. The composite structure was examined by the damage cross section. A delamination between a sheet metal and fibre layer normally found after cracking of the matrix and fibres. The damage cross section on the fibre metal laminates was analysed and followed by increasing the crosshead speed of the indentation. The values of the damage cross section were determined through an experimental. The values were

compared based on the crosshead speeds and a layup of the laminate. The shape of damage for all specimens is same, which is known called as petal pattern.



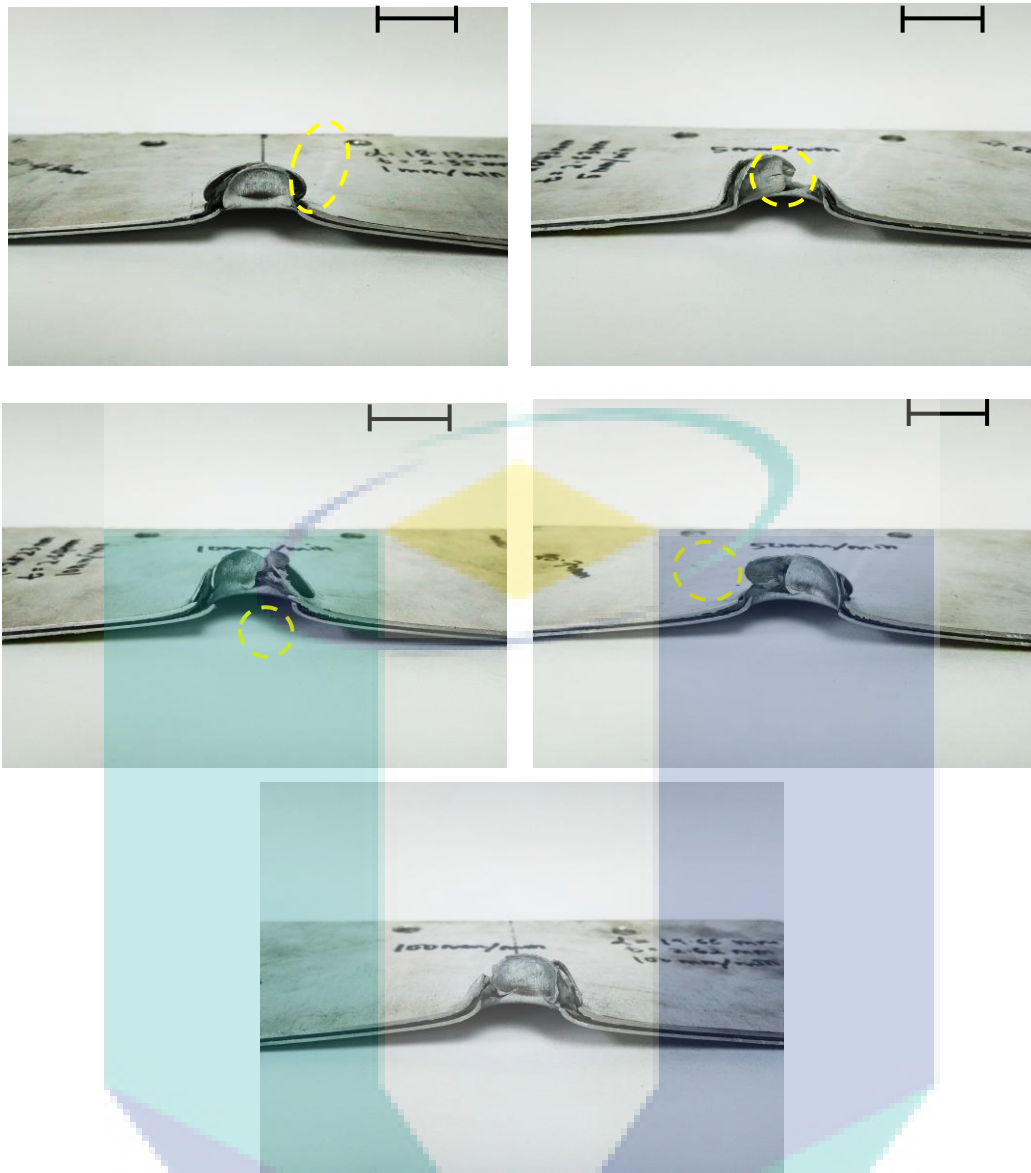


Figure 4.4 Typical damage of fibre metal laminate based on different crosshead speeds.
(a) 1 mm/min (b) 5 mm/min (c) 10 mm/min (d) 50 mm/min (e) 100 mm/min.

4.3.3 Aluminium/Unidirectional Carbon Fibre Laminate

The performance of the aluminium/unidirectional carbon fibre laminate was evaluated through a quasi-static indentation test by using various crosshead speed. The data of load-central deflection was recorded. The post impact damage of the fibre metal laminate was evaluated by measuring the depth deflection and compared with other specimens. Figure 4.5 showed that load against central deflection was recorded based on various crosshead speed 1, 5, 10, 50 and 100 mm/min. The indentation failure was depended on a crosshead speed. The crosshead speed and the constituent materials the aluminium 2024-0 series and unidirectional carbon fibre prepreg was tested in this testing.

The unidirectional prepreg fibre differs than a plain weave carbon fibre. The plain weave carbon fibre was laminated with the sheet metal by using the thermoset epoxy while this prepreg fibre already contained with resin. The fibre metal laminate was pressed by using a hot press machine at 125°C with 4 bar of pressure. The fibre metal laminate was pressed for two hours. As usual, to improve the bonding at the interlayer, the sheet metal was sanded with 100 grit sandpaper. Based on the graph load against central deflection, the performance of the aluminium/unidirectional carbon fibre with crosshead speed 50 mm/min has higher loading compared to another crosshead speed 1, 5 and 10 mm/min, whose value was 4.92 kN. While the performance of the fibre metal laminate with crosshead speed 50 and 100 mm/min have higher loading than 5 and 10 mm/min. So the value of 5 and 10 mm/min were stated as 4.78 kN and 4.80 kN.

Besides that, the length of deflection from the specimens with crosshead speed 1 to 100 mm/min were increased. From the observation of the graph, the failures because of the condition of the fibre. The fibre was exposed to the same curing temperature. The crack propagation on the fibre metal laminate was due to maximum loading at the indentation zone. Furthermore, another reason was the stacking technique. The fibre metal laminate contained with three plies of unidirectional carbon fibre. They were stacked by following the fibre orientation. This could also effect on the stiffness of the material. When the crosshead speed increased, it would reflect on the fibre metal laminate structure degradation.

The structure degradation continued with a few levels of fibre failures such as delamination, matrix cracking and fibre breakage. A symptom of cracking at bottom layer happened when the laminate hit by the impactor until reached maximum load. Based on

Figure 4.6, the length of deflection was increased. It showed that, the failure of the laminate based on the stiffness of the laminate. In addition, the specimen with 100 mm/min has a higher load than 1, 5, 10 and 50 mm/min. From these results, the specimen that has lower deflection because the crosshead speed was slower and the crack propagation would not rapidly due to starter defect. The laminate has the lower compressive strength and the load easily bent which due to plastic and elastic behaviour of the sheet metal. When the kinetic energy was hitting on the fibre metal laminate, an internal damage could happen. The perforation and penetration depended on the thickness of the laminate.

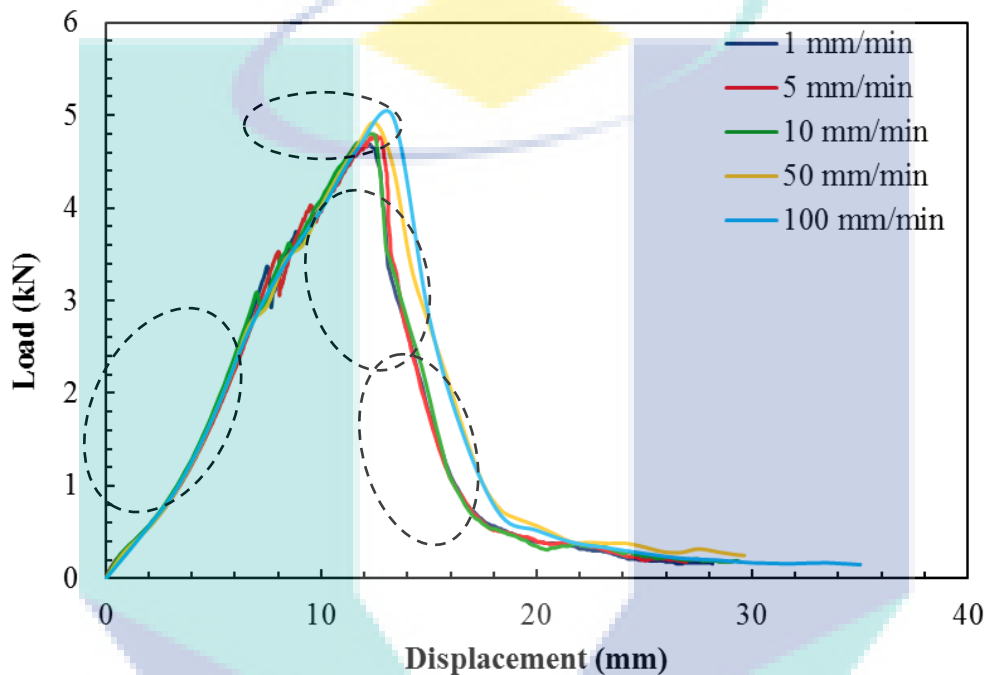


Figure 4.5 Graph of load against central deflection in Aluminium/Unidirectional Carbon Fibre Reinforced Polymer (UD CFRP) fibre metal laminate

The failure process during the quasi-static indentation was recorded. The damaged samples were investigated by measuring the length of deflection and examined through a load-central deflection curve. There was an initial fracture onto the 2/1 fibre metal laminate by 1 mm/min crosshead speed. The testing was done by using a compression machine, whereby, the compression plate was replaced with an indenter. The damage cross section has been taken through an indentation stage by the impactor at a first ply of the aluminium alloy. Based on the graph above, specimen 1 and 5 mm/min almost have same graph pattern. At the first stage, a load was acted on the fibre metal laminate until reached to the maximum load.

The load was caused the matrix started to appear and the sound of cracking could listen. When the continued load reached second stage, the fibre started to delaminate. From the continued load, it was caused a sheet metal of first ply started to crack. The indenter started to perforate the metal alloy at first ply and the maximum bending happened. The maximum bending caused the fibre to break. This happened at the third stage. After the load reached to ultimate value, the indenter started to penetrate the fibre metal laminate and happened at the fourth stage. At this stage, the penetration of a sheet metal also depended on its ductility.

The higher crosshead speed resulted in an increase of composite structure degradation. Besides that, there was a number of transverse cracks which increased the delamination of the laminate especially at the middle area of the specimen. The matrix crack also caused delamination of the laminate. When the testing was carried out with the highest crosshead speed of quasi-static loading it resulted in an extensive delamination at the middle part and bottom ply. When the crosshead speed increased, the deformation on the fibre metal laminate happened at the same time. The matrix of the laminate damaged caused by impact and the connection between matrix-fibre became degradation. The epoxy resin is brittle and has low resistance to the crack propagation. The crack happened at a high transverse shearing stress, which was connected with the contact force. The bending crack occurred easily if the volume of the matrix is higher than volume of the fibre

In the experimental works, the crosshead speed range, 1-100 mm/min had involved delamination layer, failure of the fibre, plastic deformation and cracking of the aluminium layer. The energy lost would be decreased when the impact crosshead speed was increased. The loss of energy would constituent the energy, which used to pick up the impactor. Besides that, the energy also used as to control the friction from the indenter and during the impact, a sound would be produced. The sound signed for the failure of the fibre and cracking of the aluminium alloy. The deformation behaviour of the top surface has been shown in Figure 4 respectively. The increasing of impact crosshead speed caused the impact energy confined around the impacted area, which led to fracture and penetration of that area for fibre metal laminate panels with plain weave composite fibre.

Figure 4.6 showed the damaged cross section in aluminium/unidirectional carbon fibre laminate by various crosshead speed of the indentation loading. The delamination between a sheet metal layer and a fibre layer was found after a cracking process in the matrix. These fibre metal laminates were tested by increasing the crosshead speeds. The measurement of the

damage cross section had been taken and recorded. The results were compared and analysed. The pattern of failure looked like as a petal.

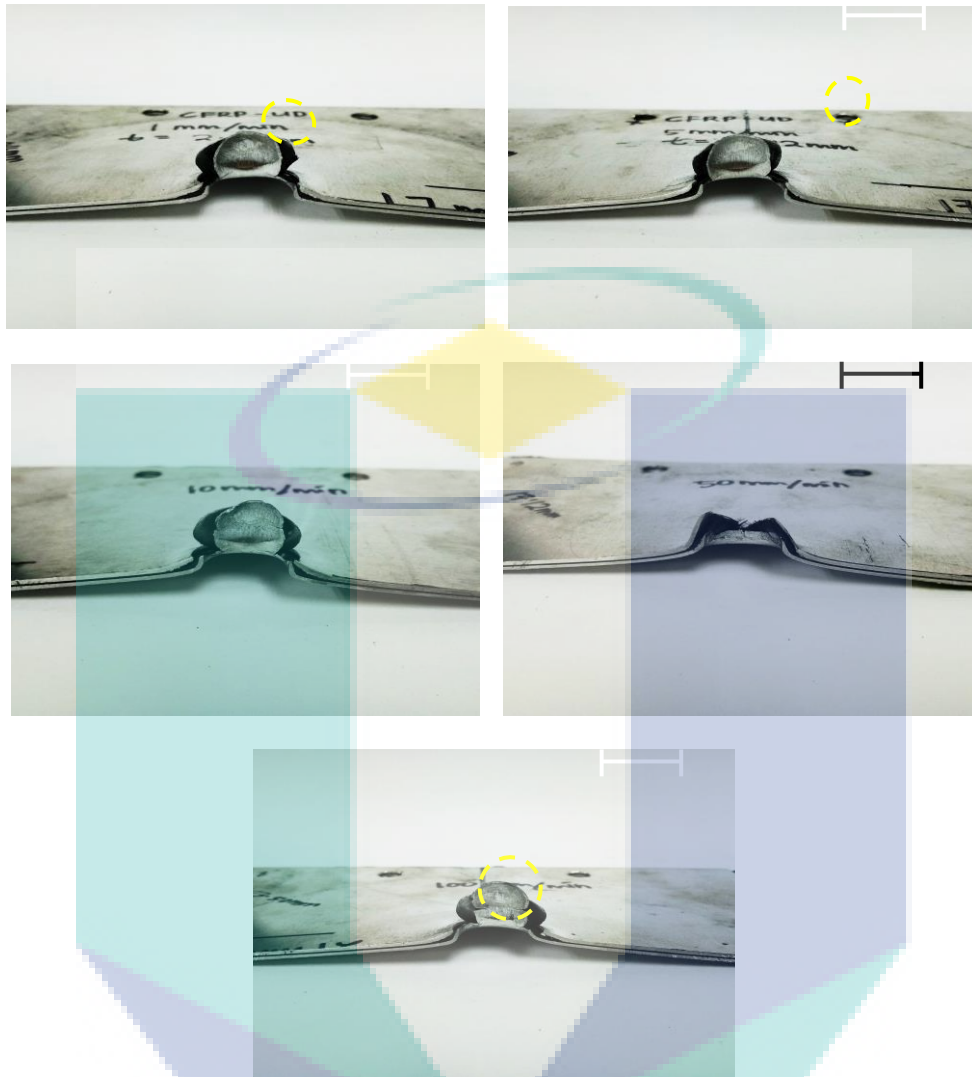


Figure 4.6 Typical damage of fibre metal laminate based on different crosshead speeds. (a) 1 mm/min (b) 5 mm/min (c) 10 mm/min (d) 50 mm/min (e) 100 mm/min.

4.3.4 Aluminium/self-Reinforced Polypropylene Polymer

A fibre metal laminate was fabricated by using the hot press machine. The type of configuration layup was decided which 2/1. The layup consisted with self-reinforced polypropylene polymer (SRPP). Then, the SRPP was covered with aluminium alloy 2024-0 sheet at the top and bottom layer. A thin film of polypropylene (PP) was used as an adhesive film at the interlayer and to attach the SRPP with the sheet metal.

The sheet metal surfaces have been roughening by using 100 grit grind disc. The surface roughness has the same value with a sand blasting effect. The fibre metal laminate was pressed at 165°C under a pressure of 30 bars. Based on the load-displacement curve, Figure 4.7, a quasi-static indentation was tested on the fibre metal laminate with difference crosshead speed.

An initial load has been traced in the graph, which meant the fibre metal laminate had responded by the maximum loading of the indentation. The maximum load is a point where the material started for a crack propagation (Abdullah et al., 2015). The top surface of the specimen started to form a U shape once got indentation form the indenter. The depth of indentation would get deeper once the displacement and loading were increased. From the graph information, the performance of FML at 100 mm/min has greater loading than 1, 5, 10, and 50 mm/min. The continued loading of the fibre metal laminate caused in propagation in the crack which it was occurring in a stable manner. While the failure of those specimens was 1, 5, 10, and 50 mm/min, respectively. At this condition, the crack would growth rapidly from a point where the defect started. When the cracks started to propagate, the crack growth would increase in a steady state until it reached a plateau. A small displacement of residual would appear when a residual stress was presented.

A 100 mm/min specimen had higher force than 10 and 50 mm/min. This was because the interfacial toughness was associated with the fibre bridging during the crack propagation. Besides that, the melted of polypropylene film was fully covered the SRPP and had good contact or bonding between PP film interlayer/SRPP and the sheet metal. In addition, the interlaminar properties of a fibre metal laminar depended on the adhesive layer. The adhesive film also acted as the peeling resistance. At the beginning of loading, the SRPP had permanent deformation until it reached maximum force. This was because of the characteristic of the SRPP had higher elasticity value. The line was smoothly increased even there was no matrix cracking. Once the fibre metal laminate hit with a maximum force, the laminate would had maximum deflection then caused a delamination. From the graph in Figure 4.7, the delamination happened layer by layer. If the FML would completely peel off if without the adhesive layer. The peeling at the interface, metal/prepreg fibre would result in a delamination and damage on the prepreg fibre.

Depth of indentation in 1 mm/min sample was 24.62 mm and longer than 5 mm/min specimen, while the length was 20.50 mm. When the crosshead speed increased, it would cause a failure of the material, SRPP became bigger. Mostly, the failure of SRPP examined through its elastic and plastic behaviour and the adhesive effect on the FML. Based on the graph, the performance of 100 mm/min specimen better than 1, 5, 10, and 50 mm/min, respectively, because it had good toughness than other specimens. There were three stages of failure were found in the SRPP. At the first stage, there was a material deformation in 100 mm/min specimen from the start until the maximum load, 7.20 kN. The deformation occurred because a maximum load was acted on the specimen. The second failure, the onset of fibre breakage started from a load of 5.36 kN. Finally, at the third stage, the perforation was reached. There were four stages of failure in the fibre metal laminate. At the first stage defined as permanent deformation. The types of failures were identified at three stages such as first and second cracking, onset fibre breakage and perforation. These were explained in failure behaviour of SRPP. These failures started from load value of 0.58 until 1.07 kN. Once a load acted on the fibre metal laminate, the fibre metal laminate would respond elastically. For example, in 1 mm/min specimen, the specimen acts elastically at a load of 0 to 0.57 kN. Then, the continued load made the fibre metal laminate behaviour change to plasticity which also known as a permanent deformation.

The permanent deformation responded at load 0.73 kN and ended at 6.72 kN. The deformation ended with an onset fibre breakage. When the load impacted on a sheet metal, at the impacted area the fibres were sheared by the crack lips (Múgica et al., 2014). Once the maximum load has reached the limit, the cracks at the bottom layer started to generate at 6.53 kN. A semi-circular path was traced in the non-impacted area cracks, which it was due to the shape of the indenter. The cracks would continue generated when increasing the crosshead speed and caused a shear crack. Lastly, least, the laminate was fully perforated at a load of 4.56 kN.

The behaviour at the interlayer, the melted adhesive film would keep the sheet metal bonded to the SRPP. A force from the impactor would cause failure in some regions. However, cohesion at the interlayer would occur if the bonding between substrates were failed. The increase of crosshead speed would result in the composite structure degradation. There was a number of transverse cracks that have been found and caused delamination between metal and SRPP layer (Bieniaś et al., 2015). The degradation of the structure

happened at the middle area where the indenter acted perpendicular to the fibre metal laminate top surface.

A quasi-static indentation was carried out by using highest crosshead speed, 100 mm/min, and found that an extensive delamination at the deflection length was bigger than 1, 5, 10 and 50 mm/min, respectively. The reason of this failure is that the localised crack rapidly grow once there is continuous class. The crack would propagate at high transverse shearing stress, which related to a contact force. Then, the bending crack normally would occur if the volume the adhesive more than an optimum amount. The deformation on a fibre metal laminate would follow once a load acted on it. The connection between metal and SRPP also became looser.

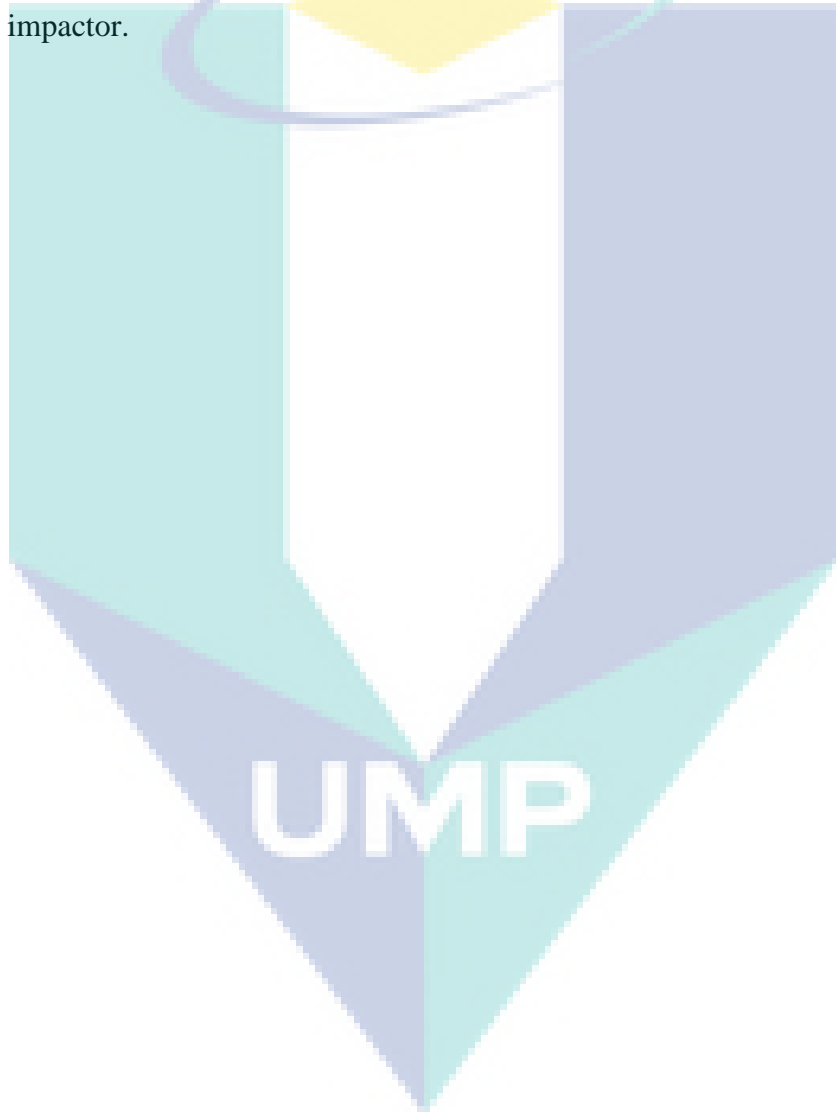
The failure process of the indentation test was done and examined by the front surface and rear surface of the impact damaged samples. The damaging effects on the 2/1 laminate samples were found by the crosshead speed, 1mm/min. The Instron 3369 series machine was used in this testing and collaborates with a BlueHills software. A top view of the 1 mm/min sample, a measurement on the damaged part was taken. The fibre metal laminate was impacted by an indenter until reached to a maximum load and found cracks on the interlayer. The laminate would start to bend because of the maximum load that acted on it and caused the laminate has maximum bending. After that, a process of fibre breakage would happen because of the maximum bending by the loading and stiffness of the SRPP. There was an effect of indentation at the bottom ply, aluminium alloy sheet metal. A perforation would happen at the third stage. The indenter travelled through fibre metal laminate at a constant speed and produce a clean hole. The Figure 4.8 shows the /length of deflection was different to each other because of the material ductility.

4.4 Low-Velocity Impact (LVI) Test

The low-velocity impact tests have been done by using the testing machine, Drop Tower Impact tester Instron CEAST 9350. The testing has been accomplished at UTM, Skudai. The samples were tested at room temperature and the machine was synchronised with a software, Ceast. The total low-velocity impact specimen is 32 and tested under difference velocities. 2.70, 3.33, 3.90, and 4.50 m/s. The material clamber has the same size to the material clamber of indentation test equipment. The outer diameter is 160 mm and the inner diameter is 127 mm. The results of testing were recorded through a load-displacement curve.

4.4.1 Aluminium/Plain Weave Carbon Fibre Laminate

Figure 4.9 illustrates the distinct curve of load against displacement of the laminates and depends on the impact velocities. The curve shown has an ascending of loading, attains to a maximum load value and has a descending section of unloading moment. The curve of load-displacement was not smooth and some alternation were recognised. The ascending of loading and caused failures in the laminates because the stiffness of the laminated structure decreased. This case could be illuminated as a generation of delamination in the composite laminate or aluminium-CFRP interface. A matrix cracking and failures of fibre occurred once a capability load convinced around it. The carbon fibre was characterised based on higher perceptibility to damage by an impactor.



The results of the maximum force were recorded during the impact test and increased linearly by increasing the impact of the velocity. Although the testing was carried with the same frequency, the damage cross section on each sample has its differences. The damage cross section of each sample was measured roughly and analysed the failures through the curve. The photos of damage area are shown in Figure 4.10. The damage cross section increased and accompanied by increasing of the impact velocities. From the figure shown, the inspection of failure behaviour especially a boundary delamination in the fibre metal laminate is by a plastic deformation. The delamination is one of a prevailing damage. The delamination occurred at diversified depths. Besides that, the elongation of delamination shape was accompanied by the fibre orientation in each layers (Pärnänen et al., 2015). There was some addition of delamination, which is a plastic deformation by the aluminium layers and delamination at the interface of Al/CFRP laminates.

The aluminium/CFRP laminate was subjected to a 12.70 mm impactor by the different velocities. When the laminates impacted by a 2.70 m/s, there was a few transverse cracks at a lower layer in an impactor area. A higher impact velocity of 4.50 m/s was used and degradation on a composite structure increased. The crack growth would cause more delamination at middle area when the loading was continued. A matrix crack appeared at a structure joint. A destruction of a lower layer of the laminates ensued at the impact area. The testing was carried in an average 2.70 – 4.50 m/s, and showed the result of a general delamination at the middle part of the laminates and pursued to a complete delamination.

In the fibre metal laminate, there were a few cracks on the matrix, which grow in a specific composite layer and analysed at the lowest impact velocity, 2.70 m/s. The impact velocity increased and led to an appearance of delamination at the middle area, and there was a laminate interface delaminate as well. Furthermore, the transverse cracks (Bieniaś et al., 2015) in the lower ply of the laminates have grown a lot once it is impacted at 4.50 m/s. Once the velocity increased, the deformation behaviour of the fibre metal laminates would also increase and at the same time, it effects on the impacted area. The laminate has a damage on the matrix, which caused by the impact and usually caused a crack and has some degradation at a connection of fibre-matrix interface. Unfortunately, the cracking did not affect the whole laminates structure. The crack acted as a beginning point for a delamination between ply of fibre. The laminate that has a high thickness would have a higher stiffness and lower fibre metal laminate deformation.

4.4.2 Aluminium/Glass Fibre Laminate

In the graph below, Figure 4.11 shows a load-displacement that was recorded for an impact test. The variable of the testing was decided by using the different velocity of impact. The results of experimental would be compared with numerical analysis, Abaqus 6.13. The curve of load – displacement was used to determine a behaviour of aluminium/glass fibre laminate with various velocity in a range as stated in the beginning of this chapter. Based on the graph, it showed a comparison of maximum force of the laminate in the different impact velocity. The graph has an ascending line during the loading until it reached to a maximum load value. In addition, the graph also has a descending line because the fibres were started to have failure such as fibre breakage. When the fibre metal laminate was loading by an impactor, there a few fluctuation on the laminates were found. The trend of this graph showed a probability failure of the material and a laminate structure. A failure of the laminate depended by its structure and decreased in a stiffness. The generation of delamination in the laminate occurred by a major effect, the maximum load. The delamination might occur at the area of the aluminium/glass fibre interface, a cracked matrix and the failure fibres.

The failure of the laminates could be synchronised with laminate thickness. The thickness of a laminate was also one of a factor to resist from a dynamic load. Based on the figure of the visual laminate failures, Figure 4.12 shows that the increase of laminate thickness would increase the force to resist the load acted on it. A maximum force of impact velocity, 3.33 m/s through a 10 kN load was about 4.10 kN. From the observation, the maximum force would increase when the impact velocity was increased to 3.90 m/s and the value was about 4.84 kN. A structure degradation accompanied with an initial crack in a matrix and reinforcing fibres. A progress of the delamination in the composite material and at the interface of metal-composite was associated with the structure degradation. In a 2/1 laminate, a sudden drop weight affected on a matrix and had a crack symptom.

A damage surface area of the fibre metal laminate was executed by the low-velocity impact test. The damage cross section was used to evaluate the failure behaviour, which resisted to the impact test. In the test, the fibre metal laminate found a few failures such as a delamination at the interface of metal – fibre, matrix cracks and fibre breakage. These are failure patterns that are easily identified in a fibre metal laminate. An analysis of damaged surface area was made by taking a measurement of the area. However, increasing the impact

velocity would increase damage on the laminate and surface area. The measurement of the surface area was taken and compared with the various velocity.

The damage shape depended by the impact velocities. The shape changed and started with a bent shape. The bent shape was produced by an impact velocity of 2.70 m/s. The impactor was not penetrated through the fibre metal laminate. Based on the visual results, Figure 4.12 shows that there was a small hole in the fibre metal laminate after being hit by an impact velocity of 3.33 m/s. Other than that, when an impactor hit the fibre metal laminate at 4.5 m/s, it was penetrated. Then, a petal shape was formed because higher impact could increase the damage of the surface area.

The specimens were cut into half (150 mm x 75 mm) by using a hand saw to see a cross-section of each specimen. The cross-section in each specimen was compared and analysed by synchronizing it with the load-graph curve. Based on the observation that has been made, damage contour in the sheet metal and composite fibre layers were mainly followed by the lower layer in a particularised composite interface. The diverse fibre orientation could cause bending stiffness that had happened in different phases. The differences in bending stiffness referred to the anisotropy of mechanical properties in composite laminates. These have been related to Young's modulus in the longitudinal and perpendicular direction of the fibre arrangement. (Greenhalgh et al., 1996) had made a conclusion that the delamination would happen in the area with higher bending stiffness.

4.4.3 Aluminium/Unidirectional Carbon Fibre Laminate

The performance of the aluminium/unidirectional carbon fibre laminate was valued through a low-velocity impact test by using various speeds. The data of load-central deflection was recorded. The post impact damage of the fibre metal laminate was evaluated by measuring the deflection area and compared with other specimens. Figure 4.13 shows that load against displacement was recorded based on the various speed range 2.70 – 4.50 m/s. The failure area was depended on the impact velocities. The speeds and the constituent materials; aluminium 2024-0 series and unidirectional carbon fibre prepreg was used to be tested in this testing.

The unidirectional prepreg fibre differs than a plain weave carbon fibre. The plain weave carbon fibre was laminated with the sheet metal by using the thermoset epoxy while this prepreg fibre already contained with resin. The fibre metal laminate has to be pressed by using a hot press machine at 125°C with four bar of pressure. The fibre metal laminate was pressed for one and half hour. As usual, to improve the bonding at the interlayer, the sheet metal was sanded with 100 grit sand paper. Based on the graph of the load against displacement, the performance of the aluminium/unidirectional carbon fibre with speed 4.50 m/s has higher loading compared to another crosshead speed 2.70, 3.33 and 3.90 m/s, whereby the value was 4.67 kN. The thickness of the specimen; 2.26 mm.

Meanwhile, the performance of the fibre metal laminate with speed 2.70 and 3.33 m/s, respectively have lower loading than 4.50 m/s. Therefore, the value of 2.70 and 3.33 m/s were 3.58 kN and 4.42 kN. Besides that, the size of the damage cross section of the specimens with speed increased 2.70 – 4.50 m/s, respectively. From the observation of the graph, the failures were because of the condition of the fibre. The fibre was exposed to the same curing temperature. The crack propagation on the fibre metal laminate was due to maximum loading at the indentation zone. Besides that, another reason was the stacking technique. The fibre metal laminate contained with three plies of unidirectional carbon fibre. They were stacked by following the fibre orientation. This could also effect on the stiffness of the material.

When velocity increased, it would reflect on the fibre metal laminate edifice and degraded. The cracks degradation continued with a few levels of fibre failures such as delamination, matrix cracking and fibre breakage. A symptom of cracking at bottom layer happened when the laminate knockout by the impactor until it reached a maximum load.

Based on Figure 4.13, the displacement was increased. It showed that the failure of the laminate based on the stiffness of the laminate.

In addition, the specimen with speed 2.70 m/s has a total energy and lower than 3.33 m/s. Therefore, the total energy under 2.70 m/s and 3.33 m/s were about 0.02 kJ and 0.03 kJ. From the results, the specimen that has lower deflection because of the velocity was slower and the crack propagation would simply form from beginning of the defect. The laminate that has lower compressive strength and load was easily bent which was due to plastic and elastic behaviour of the sheet metal. When the kinetic energy was a defeat on the fibre metal laminate, an internal damage could happen. The perforation and penetration depended on the thickness of the laminate. The specimen that has lower load, due to the continued loading that acted in disturbed position (Pärnänen et al., 2015).

The impact process during the low-velocity impact test was recorded. The damaged samples were investigated by assessing the depth of deflection and reviewed through a load-central deflection curve. There was an initial fracture onto the 2/1 fibre metal laminate by a speed of 2.70 m/s. The testing was done by using a diameter of a hemispherical impactor, 12.70 mm. The damage cross section was taken through the impact effect by the impactor at a first ply of the aluminium alloy. At the first stage, a load was acted on the fibre metal laminate until reached to the maximum load. The load was caused the matrix started to appear and the sound of cracking could listen. When the continued load reached the second stage, the fibre started to delaminate. From the continued load, a sheet metal of first ply started to crack. The indenter started to perforate the metal alloy at first ply and the maximum bending happened. The maximum bending caused the fibre to break. This happened at the third stage. After the load reached to ultimate value, the indenter started to penetrate the fibre metal laminate and happened at the fourth stage. At this stage, the penetration of a sheet metal also depended on its ductility.

The higher crosshead speed resulted in an increase of composite structure degradation. Besides that, there were a number of transverse cracks, which increased the delamination of the laminate especially at the middle area of the specimen. The matrix crack also caused delamination of the laminate. When the testing was carried out with the highest speed of the dynamic loading it resulted in a far-reaching delamination at the middle part. When the crosshead speed increased, the deformation on the fibre metal laminate happened at the same

time. The matrix of the laminate damaged caused by impact and the connection between matrix-fibre became degradation. The resin is brittle and has low resistance to the crack propagation. The crack happened at a high transverse shearing stress, which connected with the contact force. The bending crack would occur easily if the volume of the matrix is higher than volume of the fibre cessation (Bienias et al., 2015).

In the experimental works, the speed range, 2.70 – 4.50 m/s had involved delamination layer, failure of the fibre, plastic deformation and cracking of the aluminium layer. The energy lost would be decreasing when the impact velocity was increased. The absorbed of energy would tell how much the energy needed to have matrix cracking, fibre breakage, fibre delaminated, penetration of laminate and perforation of fibre metal laminate. Besides that, the energy also used as to control the friction from the indenter and during the impact (Pärnänen et al., 2015), a sound would be produced. The sound signed for the failure of the fibre and cracking of the aluminium alloy. The deformation behaviour of the top surface has been shown in Figure 4.14, respectively. The increasing impact of crosshead speed caused the impact energy to be confined around the impacted area, which led to fracture and penetration of that area for fibre metal laminate panels with prepreg composite fibre.

Figure 4.14 showed the damaged surface area in aluminium/unidirectional carbon fibre laminate by numerous velocity of the indentation loading. The evaluation of the damage fibre metal laminate depended on the surface area. The delamination between a sheet metal layer and a fibre layer was found after a cracking process in the matrix. These fibre metal laminates were tested by increasing the crosshead speeds. The measurement of damage cross section were taken and recorded. The results were compared and the reasons of failure analysed. The form of failure looked like petal.

4.4.4 Aluminium/self-Reinforced Polypropylene Laminate

A dynamic impact test with different velocities was carried out on a fibre metal laminate by using drop tower machine. The machine was equipped with a 10 kN load and calibrated with a software, Ceast. The 10 kN of a load cell attached to a 12.70 mm diameter of a hemispherical nose indenter which it measured a contact force history. The velocity range of the striker varied from 2.70 to 4.50 m/s. The SRPP could have a permanent deformation because the SRPP is consisted with full polypropylene then formed within a family of self-reinforced composites. The fibre metal laminate Al/SRPP and matrix are in the same family of polymer. For example, polypropylene, polyethylene and so on. The main advantage of this

fibre is recyclable. The SRPP is highly oriented to produce higher strength and stiffness than a bulk of polymer material. The self-reinforced composite has been introduced in a transportation sector which for impact resistance and capability in thermoformed (Múgica et al., 2014). Circular plates hold the fibre metal laminate samples. So, the sample gripped by an inner and outer diameter of 160 mm and 127 mm respectively. The sample was held by a pneumatic fixing device, which has the same diameter for supporting the sample.

According to the load-displacement curve, Figure 4.15, shows an initial load that has been traced in the graph, which meant the fibre metal laminate had responded by the maximum force during the loading. The material reached up to the maximum force. The maximum force is a point where the material started form a crack propagation. From the graph information, the performance of fibre metal laminate at 4.5 m/s has a greater loading than 2.70, 3.33, and 3.90 m/s, respectively. The continued force on the fibre metal laminate caused a growth of crack, which occurred in a stable manner. The crack propagation happened in an unstable manner. At this condition, the crack would grow rapidly from a point where the defect started. When the cracks started to propagate, the crack growth would increase in a steady state until it reached a plateau. A small displacement of residual would appear when a residual stress was presented. A sample of 3.90 m/s has higher loading than 2.70 and 3.33 m/s, because the interfacial toughness was associated with the fibre bridging during the crack propagation. Besides that, the melted PP film fully covered the SRPP and has good contact or bonding between PP interlayer/SRPP and the sheet metal. The results of 2.70 and 3.33 m/s have a lower volume of polypropylene and contained a few amount of composite fragments that remained on the substrate. The factor of the adhesive amount would lead to the formation of a crack on the interlayer and the crack continued to grow within the SRPP. In addition, the interlaminar possessions of a fibre metal laminar depended on the adhesive layer. The adhesive film also acted as the flaking resistance. If the fibre metal laminate would completely peel off if without the adhesive layer. The flaking at the interface, metal/prepreg fibre would result in a delamination and damage on the prepreg fibre.

The size of the damage cross section for a sample of 2.70 m/s was 9.75 mm and smaller than a sample of 3.33 m/s, whereby the length was recorded as 11.60 mm. When the impact velocity increased, it would cause a failure of the material, and SRPP became bigger. Mostly, the failure of SRPP examined through its elastic and plastic behaviour. Based on the graph, the performance of the 4.50 m/s sample has a virtuous toughness than the other

specimens. There were two stages of failure found in the SRPP. At the first stage, there was a material deformation in this specimen from the start until the maximum force, 5.65 kN. The deformation happened since a maximum loading was performed on the specimen. The second failure happened when the fibre breakage started from a load of 5.45 kN until dropped to 5.07 kN.

The stage of failures in the fibre metal laminate were defined as above. At the first stage was defined as permanent deformation. These are explained in failure behaviour of SRPP. These failures started from load value of 0.34 kN until 0.5 kN. Once a load acted on the fibre metal laminate, the fibre metal laminate would respond elastically. For example, in 2.70 m/s sample, the sample acted elastically at a load of 0 to 0.21 kN. Then, the load was continued and made the fibre metal laminate behaviour change to plasticity which also known as a permanent deformation. The permanent deformation responded at load 0.73 kN and ended at 3.58 kN. The deformation ended fibre breakage. At the impacted area, the crack lips sheared the fibres. Once the maximum load has reached the limit, the cracks at the bottom layer started to generate at 2.27 kN. A semi-circular path was traced cracks at the bottom layer, which caused the shape of the indenter. The cracks would continue and generate when the speed increased and caused a shear crack. Lastly, the laminate was not perforated. The behaviour at the interlayer, the melted adhesive film would keep the sheet metal bonded to the SRPP. A force from the impactor would cause failure in some regions. However, cohesion at the interlayer would occur if the bonding between substrates were failed.

The increasing of crosshead speed would result in the composite structure degradation and showed in Figure 4.16. There was a number of transverse cracks that have been found and caused delamination between metal and SRPP layer (Bieniaś et al., 2015). The degradation of the structure happened at the middle area where the indenter acted perpendicular to the fibre metal laminate top surface. An impact test was carried out by using the highest speed, 4.50 m/s and found that an extensive delamination at the deflection length was bigger than 2.70, 3.33 and 3.90 m/s.

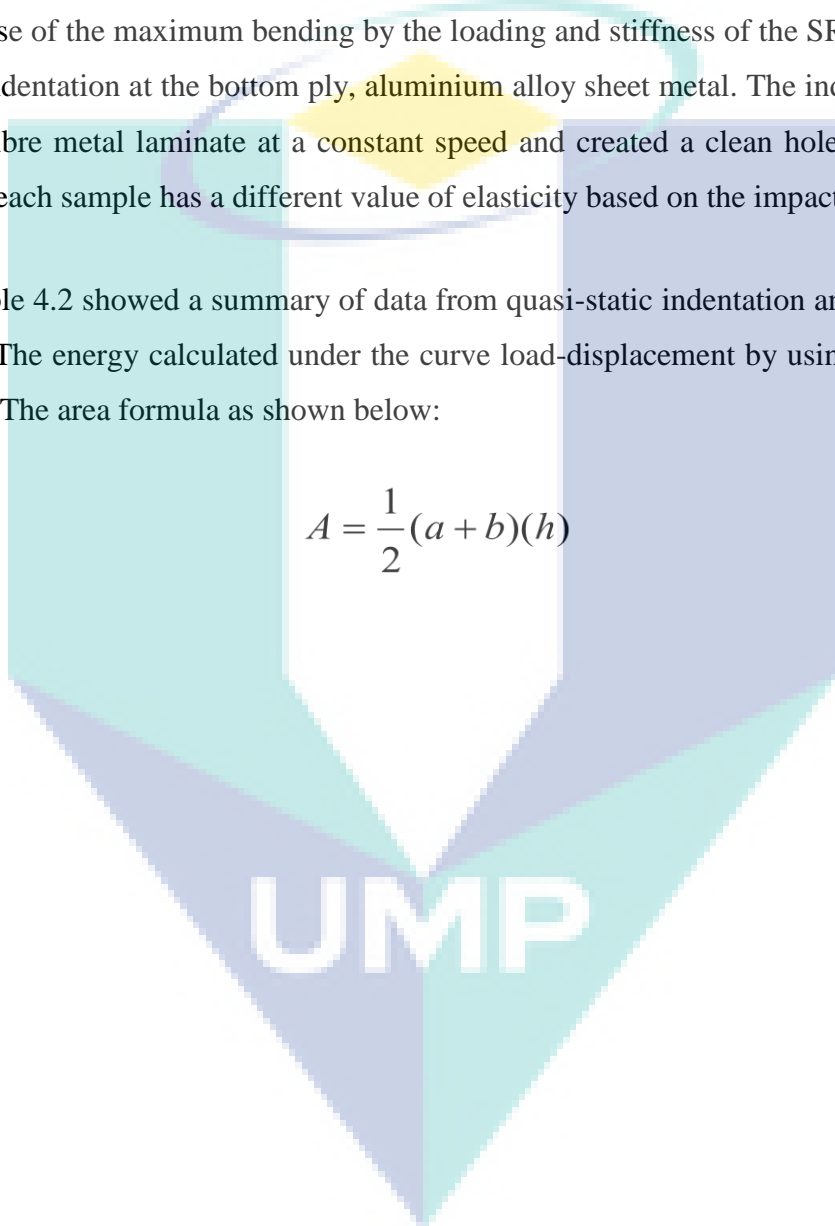
The reason of this failure which the localised crack rapidly growth once there was a continue loading. The crack would propagate at high transverse shearing stress, which related to a contact force. Then, the bending crack normally would occur if the volume the adhesive more than an optimum amount. The deformation on a fibre metal laminate would follow once a load acted on it. The connection between metal and SRPP became unattached. The failure

process of the impact test was inspected on the front surface and rear-surface by taking a measurement.

The damaging effects on the 2/1 laminate samples were found at a speed of 2.70 m/s. A top view of the 2.70 m/s sample, a measurement on the damaged part was taken. An indenter dented until reached to a maximum load and found cracks at the interlayer impacted the fibre metal laminate. The laminate bent because of the maximum load that acted on it and caused the laminate has a maximum bending. After that, a process of fibre breakage would happen because of the maximum bending by the loading and stiffness of the SRPP. There was an effect of indentation at the bottom ply, aluminium alloy sheet metal. The indenter travelled through the fibre metal laminate at a constant speed and created a clean hole. Based on the graph above, each sample has a different value of elasticity based on the impact velocity.

In Table 4.2 showed a summary of data from quasi-static indentation and low-velocity impact tests. The energy calculated under the curve load-displacement by using area formula of trapezium. The area formula as shown below:

$$A = \frac{1}{2}(a + b)(h) \tag{4.1}$$



UMP

Table 4.2 Summary of experimental data

Low-velocity impact test					
Specimen	Velocity (m/s)	F_{max} (kN)	Stiffness (mm/mm)	Energy (J)	Remarks
AL/CFRP	2.70	3.66	0.26	19.96	Not penetrate
	3.33	4.02	0.25	28.09	Not penetrate
	3.9	4.10	0.18	39.26	Not penetrate
	4.5	4.14	0.13	46.56	Penetrate
AL/GFRP	2.70	3.80	0.28	19.95	Not penetrate
	3.33	4.10	0.26	28.08	Not penetrate
	3.9	4.84	0.25	39.17	Not penetrate
	4.5	4.91	0.16	52.21	Penetrate
AL/SRPP	2.70	3.58	0.23	20.12	Not penetrate
	3.33	4.42	0.25	28.30	Not penetrate
	3.9	5.38	0.26	39.24	Not penetrate
	4.5	5.65	0.24	52.20	Penetrate
AL/UD CFRP	2.70	3.70	0.26	19.70	Not penetrate
	3.33	4.38	0.27	28.26	Not penetrate
	3.9	4.57	0.23	39.21	Not penetrate
	4.5	4.67	0.07	50.24	Penetrate
Quasi-static indentation test					
Specimen	Crosshead displacement (mm/min)	F_{max} (kN)	Stiffness (mm/mm)	Energy (J)	Remarks
AL/CFRP	1	4.11	0.49	1356.74	Penetrate
	5	4.14	0.46	1366.64	Penetrate
	10	4.34	0.46	1432.67	Penetrate
	50	4.35	0.51	1435.97	Penetrate
	100	4.44	0.47	1465.43	Penetrate
AL/GFRP	1	4.52	0.53	1492.09	Penetrate
	5	4.55	0.52	1501.99	Penetrate
	10	4.91	0.49	1620.83	Penetrate
	50	5.25	0.49	1733.06	Penetrate
	100	5.61	0.50	1851.90	Penetrate
AL/SRPP	1	6.72	0.52	2281.32	Penetrate
	5	6.80	0.53	2244.73	Penetrate
	10	6.82	0.51	2251.33	Penetrate
	50	6.89	0.49	2274.44	Penetrate
	100	7.2	0.53	2376.77	Penetrate
AL/UD CFRP	1	4.69	0.58	1548.20	Penetrate
	5	4.78	0.57	1577.91	Penetrate
	10	4.80	0.55	1564.52	Penetrate
	50	4.92	0.53	1624.13	Penetrate
	100	4.98	0.56	1643.94	Penetrate

4.5 Comparison between QSI and LVI

The final stage of both experiments would be compared as in Figure 4.17. The tolerant damage in the quasi-static loading has a similar pattern to the low-velocity impact. Besides that, the radius of fracture area was not similar. Both the responses have a similar pattern. From the graph, it could be concluded that the LVI specimen was almost identically to the response of QSI specimen. The load-displacement curve was plotted as in Figure 4.17. The QSI specimens with crosshead speed 100 mm/min was correlated with velocity 4.50 m/s of LVI specimens.

The capability of the QSI test to act out the low-velocity impact test data and the results showed the failure, behaviour of the fibre metal laminate depended on a material and impact parameter, velocity, and crosshead speed. Since, the failure behaviours of the fibre metal laminate were different, a specimen, which has been tested with this impact velocity, 4.50 m/s, would be compared with a specimen of 100 mm/min. The comparing also depended on these materials; AL/CFRP, AL/GFRP, AL/SRPP and AL/UD CFRP. The impact velocity of the aluminium/self-reinforced polypropylene and aluminium/unidirectional carbon fibre were not well simulated and from the experimental work of QSI provided a higher value of the acted force. The other laminates; aluminium/carbon fibre, and aluminium/glass fibre were punctured well between the two tests. For the aluminium/unidirectional carbon fibre, the central deflection in the QSI test has far exceeded than a LVI test. In the aluminium/glass fibre laminate, a central deflection in the LVI test was higher than the QSI test even the deflection of the both tests were not similar. The value of central deflection in the unidirectional carbon fibre laminates was higher than a carbon/epoxy laminate. The carbon/epoxy is brittle and it does not need much force for the matrix cracking and fibre breakage.

Graph in Figures 4.18, 4.19, 4.20 and 4.21 showed the ability of quasi-static indentation test, whereby the results depended on the material and crosshead speed. All those materials in QSI test were well simulated by low-velocity impact test. A contact force from QSI test increased linearly and almost exactly same trend line to LVI test. The graph has a liner line due to a drop impact and indentation of the indenter on the fibre metal laminate and. The impactor and indenter caused a failure at an initial stage, the top surface of aluminium sheet has bending effect. The bending effect happened due to a contact of maximum force.

The first effect at a first layer continued and there was a cracked of matrix. The crack developed which due to a constant rate of a loading. Once the force has reached to the maximum value, the fibre metal laminate would have fibre breakage and delamination between the fibre and metal layer. Delamination happened when a layer of the fibre metal laminate has a maximum deflection. The deflection of a structure due to a material stiffness when a load acted on the specimen.

The total of energy absorbed in the QSI test to reach a plateau force for each material was different. A total energy of aluminium/CFRP, aluminium/GFRP, aluminium/CFRP UD and aluminium/SRPP to reach the plateau force was noticed as these following values; 1.47 kJ, 1.62 kJ, 1.64 kJ and 2.38 kJ. After passing these values, the indenter was able to perforate the fibre metal laminate under a constant crosshead speed. Meanwhile, the motion of LVI assumed as a free fall motion. The impactor will start with a small velocity. The impactor travelled in every time interval and increased as a sign that the impactor is speeding up as it falls downward. In every second, the speed of the impactor will speed up. Therefore, the total energy absorbed for aluminium/CFRP, aluminium/GFRP, aluminium/CFRP UD and aluminium/SRPP to perforate the fibre metal laminated were recorded as these values; 0.047 kJ, 0.052 kJ, 0.050 kJ and 0.0522 kJ.

4.5 Validation of Result between Experimental and Finite Analysis

The 2/1 FML model based on aluminium and carbon fibre was predicted through a finite element method; Abaqus. The numerical analysis was done as to predict the failure behaviour of the FML model under the dynamic impact loading. The model was analysed by different velocities. The failure mechanism of the model was recorded. The FE model became successful perforated and penetrated through the FML. The failure area of the FML increased because the impact velocity has been applied increasingly. The FML exhibited and appeared with little plastic deformation at the impact location. The plastic deformation was in aluminium and there was a fracture on the composite ply.

The results clearly showed that the different impact velocity resulted in the flexural stiffness. The number of elements for indenter is 288 while for the FML consisted with 2220 elements of aluminium and 4440 elements of the composite material. The 3D FML panel consists of the aluminium alloy and composite layer, which both of them were layered and separating as two parts. The aluminium alloy was modelled by using continuum, have an

eight-node linear brick element, 3D elements (C3D8R). While the composite material modelled by using eight-node of a quadrilateral, the model created as a shell and reduced integration (SC8R).

The boundary condition play an important element for the impact response. The boundary condition was applied to circumstance and centre of the FML model because at that area where the FML was clamped during the testing. The indenter was modelled through a method of 360 revolutions. A rigid body constraint was used to model an impactor and its motion led by a reference point. An algorithm was applied for a definition of contact between the aluminium layer and composite material layer. The Abaqus conducted the general algorithm.

Figure 4.22 showed a comparison of the initial part in low-velocity impact and quasi-static indentation test for aluminium/CFRP with the failure prediction by using finite element analysis. In FE prediction, it should be noticed that the failure based on the velocity. The model was modelling as 2/1 layup configuration. The failure depended on the material properties; elasticity, plasticity, density and other advance elements for each material. The Figure 4.22 compared to a curve of load-displacement from FE and experimental data. The prediction over-estimated force from the experimental result. The predicted value of maximum force was well agreed with the experimental value. From the graph, it clearly showed that the displacement increased so that the maximum force was able to perforate the fibre metal laminate.

Besides that, a comparison of visual failure between FE and experimental has been done for both test, LVI and QSI. The experimental figures showed that the fibre metal laminate exhibited like a petal on the rear surface around the impacted area. Those were affected by a plastic behaviour from both materials. From the figures, delamination between composite fibre and aluminium could be seen at a point of impact. Delamination caused by the force, which increased with a diameter of the rear surface. Other than that, based on the visual failure figures, the aluminium at bottom ply had higher deflection than the composite fibre. The aluminium characteristics differ than the composite fibre. The elasticity and plasticity value of the aluminium higher than the composite fibre. The stiffness of the FML plate decreased with increasing area of the rear surface. Once the indenter or impactor had a small hole (penetration), the maximum force would drop and used lower force to go through the fibre metal laminate. The whole diameter would become larger.

The validation between finite element analysis and experimental results were compared then illustrated as in Figure 4.23. The comparison has been made for Al/CFRP at speed 4.50 m/s. In FE has reached to higher load than experimental load. Based on the result, it could be assumed that the FE model is a perfect model and some technical errors in fabrication process might affect to the data of specimen. The percentage error was 1.43 %.

Figure 4.24 demonstrates a validation results between numerical analysis and experimental for quasi-static indentation which a specific crosshead speed has been subjected to the indenter; 100 mm/min. The numerical analysis result was not same as experimental result because has some errors in fabrication process. Therefore, the percentage of errors was 2 %.

4.6 Summary

The experimental results were presented in this chapter for the plain weave and prepreg CFRP, plain weave GFRP and SRPP fibre metal laminates materials. The mechanism of failure was identified and examined the impacted area by taking a measurement of length deflection. The fundamental theories to support each of the tests were explained. A numerical method, Abaqus was used to predict the failure behaviour of the fibre metal laminate. The data of quasi-static indentation test correlate with low-velocity impact test results. The data of load against central deflection was presented in this chapter.

CHAPTER 5

CONCLUSION

5.1 Introduction

The purpose of this research was to fabricate and investigate the failure behaviour of fibre metal laminate under quasi-static indentation and low-velocity impact test. The fibre metal laminate made from aluminium 2024-0 and layered with composite materials. The quasi-static indentation test was conducted in a variant crosshead speed; 1, 5, 10, 50 and 100 mm/min. Meanwhile, in low-velocity impact test the specimens were tested under four different velocities; 2.70, 3.33, 3.90 and 4.50 m/s. The tests were conducted to understand the mechanical failure modes and energy absorption of the specimen by different crosshead speed. A finite element model has been used to predict the failure behaviour for the both tests. Based on the findings, the research can be concluded as follows:

5.2 Conclusion Research

To compare behaviour of fibre metal laminate materials for automotive applications subjected to static and dynamic impacts:

The failure of fibre metal laminate in the both tests was recorded. The performance was evaluated through a curve of load against displacement. The failure based on the stiffness of material. Besides that, the tests also depended on crosshead speed and velocity. These factors might effect on the fibre metal laminate performance.

In quasi-static and low-velocity loading, the strength of the laminate was controlled by the loading condition. In the metal material, after initial loading, plastic deformation would occur progressively in exhibit at the end of the loading. In addition, the composite material failed due to fibre fracture and matrix cracking. Delamination was found once the laminate had maximum deflection by the maximum loading.

Increasing the force would cause perforation and penetration of the laminate. At the bottom surface of laminate would produce a failure shape which is known as petal.

Different types of composite materials (plain weave of GFRP and CFRP, SRPP and CFRP UD prepreg) have a significant influence on the failure behaviour of the fibre metal laminate. The strength of the fibre metal laminate increased when the crosshead and velocity also increased. The strength of SRPP compared to GFRP, CFRP and CFRP UD. The SRPP has high plasticity value that those materials. Besides that, the higher thickness of laminate would has lower deflection. The strength of CFRP UD is higher than plain weave CFRP. The strength of Al/CFRP UD controlled by the fibre content and did not have excess resin. While Al/CFRP consisted an excess of epoxy. Epoxy has a brittle characteristics and easily to crack once hit by an indenter. The numerical prediction by the model agreed well with the experimental performance.

To model the structural behaviour, then predict the failure pattern and mechanism of fibre metal laminate structures for quasi-static indentation and low-velocity impact:

The results of numerical analysis were validated with experimental data. Based on the validation graphs, there have shown the good agreements comparing in load-displacement traces and failure displacement with percentage error as 1.43% and 2%, respectively.

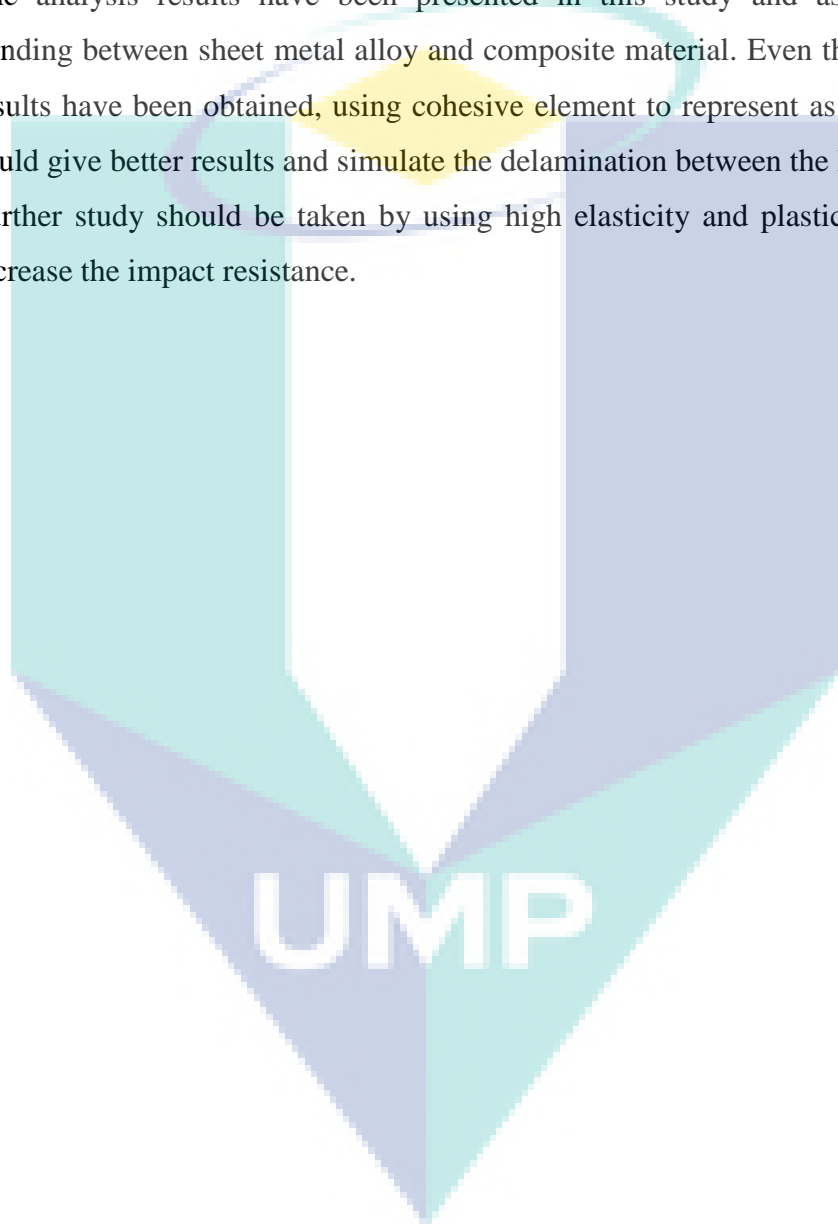
To investigate the correlation between two types of behaviours under quasi-static indentation and low-velocity affect tests:

The experimental data from quasi-static indentation test was correlated with low-velocity impact test data. The pattern of both graphs were similar. The QSI result has higher force; 7.20 kN than the LVI result; 5.65 kN. The one of reason which QSI specimen was fully perforated while LVI specimen was not fully perforate even has penetration mark on the specimen.

5.3 Future Recommendation

This research study has been shown the performance of the fibre metal laminate was compared with different materials and velocities. Here are some recommendations for future work as be.

- (i) Fibre metal laminates increasingly used in aerospace industry. This study can be interesting to study the mechanical properties of fibre metal laminate for automotive industry.
- (ii) Further testing should be carried out to analyse the failure behaviour of the fibre metal laminate under high-velocity and ballistic test.
- (iii) The fibre metal laminate should be optimised to achieve as lightweight material by using other materials such as prepreg glass fibre and carbon fibre.
- (iv) The analysis results have been presented in this study and assumed perfect bonding between sheet metal alloy and composite material. Even though the good results have been obtained, using cohesive element to represent as adhesive layer could give better results and simulate the delamination between the layers.
- (v) Further study should be taken by using high elasticity and plasticity material to increase the impact resistance.



REFERENCES

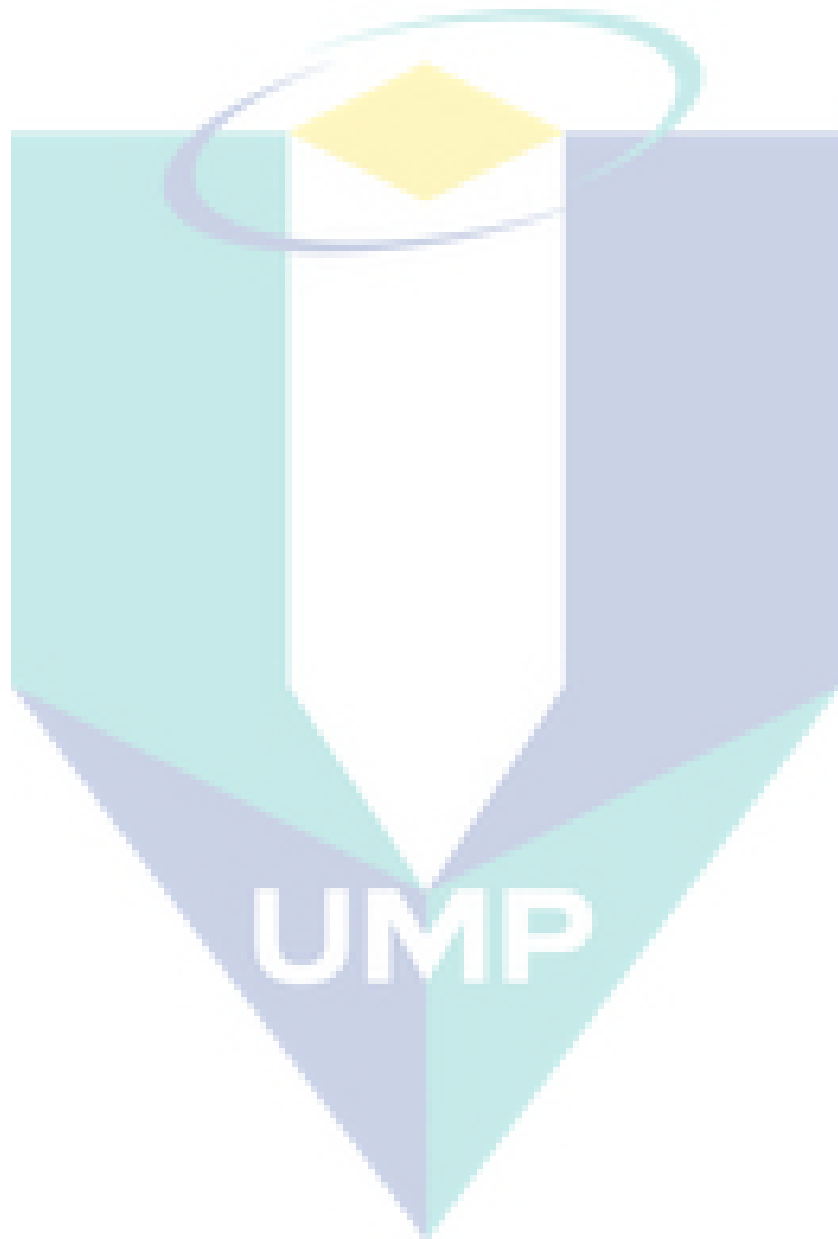
- Abdullah, M. R., & Cantwell, W. J. (2006). The impact resistance of polypropylene-based fibre–metal laminates. *Composites Science and Technology*, *66*(11–12), 1682-1693. doi: <http://dx.doi.org/10.1016/j.compscitech.2005.11.008>
- Abdullah, M. R., Prawoto, Y., & Cantwell, W. J. (2015). Interfacial fracture of the fibre-metal laminates based on fibre reinforced thermoplastics. *Materials & Design*, *66, Part B*, 446-452. doi: <http://dx.doi.org/10.1016/j.matdes.2014.03.058>
- Aboudi, J., & Paley, M. (1992). Plastic buckling of ARALL plates. *Composite Structures*, *22*(4), 217-221. doi: [http://dx.doi.org/10.1016/0263-8223\(92\)90058-K](http://dx.doi.org/10.1016/0263-8223(92)90058-K)
- Abouhamzeh, M., Sinke, J., & Benedictus, R. (2015). Investigation of curing effects on distortion of fibre metal laminates. *Composite Structures*, *122*, 546-552. doi: <http://dx.doi.org/10.1016/j.compstruct.2014.12.019>
- Asundi, A., & Choi, A. Y. N. (1997). Fiber metal laminates: An advanced material for future aircraft. *Journal of Materials Processing Technology*, *63*(1–3), 384-394. doi: [http://dx.doi.org/10.1016/S0924-0136\(96\)02652-0](http://dx.doi.org/10.1016/S0924-0136(96)02652-0)
- Beumler, T., Pellenkoft, F., Tillich, A., Wohlers, W., & Smart, C. (2006). Airbus costumer benefit from fiber metal laminates. *Airbus Deutschland GmbH*, *1*, 1-18.
- Bieniaś, J., Jakubczak, P., Surowska, B., & Dragan, K. (2015). Low-energy impact behaviour and damage characterization of carbon fibre reinforced polymer and aluminium hybrid laminates. *Archives of Civil and Mechanical Engineering*, *15*(4), 925-932. doi: <http://dx.doi.org/10.1016/j.acme.2014.09.007>
- Botelho, E. C., Pardini, L. C., & Rezende, M. C. (2007). Evaluation of hygrothermal effects on the shear properties of Carall composites. *Materials Science and Engineering: A*, *452-453*, 292-301. doi: <https://doi.org/10.1016/j.msea.2006.10.127>
- Botelho, E. C., Silva, R. A., Pardini, L. C., & Rezende, M. C. (2006). A review on the development and properties of continuous fiber/epoxy/aluminum hybrid composites for aircraft structures. *Materials Research*, *9*(3), 247-256.
- Bucci, R. J., Mueller, L. N., Vogelesang, L. B., & Gunnink, J. W. (1989). 10 - ARALL® Laminates. In A. K. Vasudevan & R. D. Doherty (Eds.), *Treatise on Materials Science & Technology* (Vol. 31, pp. 295-322): Elsevier.
- Chen, J.-F., Morozov, E. V., & Shankar, K. (2014). Progressive failure analysis of perforated aluminium/CFRP fibre metal laminates using a combined elastoplastic damage model and including delamination effects. *Composite Structures*, *114*, 64-79. doi: <http://dx.doi.org/10.1016/j.compstruct.2014.03.046>
- Dadej, K., Surowska, B., & Bieniaś, J. (2018). Isostrain elastoplastic model for prediction of static strength and fatigue life of fiber metal laminates. *International Journal of Fatigue*, *110*, 31-41. doi: <https://doi.org/10.1016/j.ijfatigue.2018.01.009>

- Dhaliwal, G. S., & Newaz, G. M. (2017). Compression after impact characteristics of carbon fiber reinforced aluminum laminates. *Composite Structures*, *160*, 1212-1224. doi: <https://doi.org/10.1016/j.compstruct.2016.11.015>
- Duarte, A. P. C., Díaz Sáez, A., & Silvestre, N. (2017). Comparative study between XFEM and Hashin damage criterion applied to failure of composites. *Thin-Walled Structures*, *115*, 277-288. doi: <http://dx.doi.org/10.1016/j.tws.2017.02.020>
- Fan, J., Guan, Z. W., & Cantwell, W. J. (2011). Numerical modelling of perforation failure in fibre metal laminates subjected to low velocity impact loading. *Composite Structures*, *93*(9), 2430-2436. doi: <http://dx.doi.org/10.1016/j.compstruct.2011.04.008>
- Frizzell, R. M., McCarthy, C. T., & McCarthy, M. A. (2008). An experimental investigation into the progression of damage in pin-loaded fibre metal laminates. *Composites Part B: Engineering*, *39*(6), 907-925. doi: <http://dx.doi.org/10.1016/j.compositesb.2008.01.007>
- Frizzell, R. M., McCarthy, C. T., & McCarthy, M. A. (2011). Predicting the effects of geometry on the behaviour of fibre metal laminate joints. *Composite Structures*, *93*(7), 1877-1889. doi: <http://dx.doi.org/10.1016/j.compstruct.2011.01.018>
- Giasin, K., Ayvar-Soberanis, S., & Hodzic, A. (2016). Evaluation of cryogenic cooling and minimum quantity lubrication effects on machining GLARE laminates using design of experiments. *Journal of Cleaner Production*, *135*, 533-548. doi: <http://dx.doi.org/10.1016/j.jclepro.2016.06.098>
- Greenhalgh, E., Bishop, S. M., Bray, D., Hughes, D., Lahiff, S., & Millson, B. (1996). Characterisation of impact damage in skin-stringer composite structures. *Composite Structures*, *36*(3), 187-207. doi: [http://dx.doi.org/10.1016/S0263-8223\(96\)00077-3](http://dx.doi.org/10.1016/S0263-8223(96)00077-3)
- Gunnink, J. W. (1988). Damage tolerance and supportability aspects of ARALL laminate aircraft structures. *Composite Structures*, *10*(1), 83-104. doi: [http://dx.doi.org/10.1016/0263-8223\(88\)90062-1](http://dx.doi.org/10.1016/0263-8223(88)90062-1)
- Hai, Y., Rongzhen, R., Chunhu, T., & Hongyun, L. (1996). Study on arall failure behaviour under tensile loading. *Scripta Materialia*, *35*(12), 1379-1384. doi: [https://doi.org/10.1016/S1359-6462\(96\)00322-3](https://doi.org/10.1016/S1359-6462(96)00322-3)
- Hashin, Z. (1980). Failure criteria for unidirectional fiber composites. *Journal of applied mechanics*, *47*(2), 329-334.
- Hashin, Z., & Rotem, A. (1973). A fatigue failure criterion for fiber reinforced materials. *Journal of Composite Materials*, *7*(4), 448-464.
- Hu, D., Zhang, C., Ma, X., & Song, B. (2016). Effect of fiber orientation on energy absorption characteristics of glass cloth/epoxy composite tubes under axial quasi-static and impact crushing condition. *Composites Part A: Applied Science and Manufacturing*, *90*, 489-501. doi: <http://dx.doi.org/10.1016/j.compositesa.2016.08.017>

- Hu, Y., Zheng, X., Wang, D., Zhang, Z., Xie, Y., & Yao, Z. (2015). Application of laser peen forming to bend fibre metal laminates by high dynamic loading. *Journal of Materials Processing Technology*, 226, 32-39. doi: <http://dx.doi.org/10.1016/j.jmatprotec.2015.07.003>
- Huaguan, Hu, Y., Fu, X., Zheng, X., Liu, H., & Tao, J. (2016). Effect of adhesive quantity on failure behavior and mechanical properties of fiber metal laminates based on the aluminum–lithium alloy. *Composite Structures*, 152, 687-692. doi: <http://dx.doi.org/10.1016/j.compstruct.2016.05.098>
- Jefferson Andrew, J., Arumugam, V., & Santulli, C. (2016). Effect of post-cure temperature and different reinforcements in adhesive bonded repair for damaged glass/epoxy composites under multiple quasi-static indentation loading. *Composite Structures*, 143, 63-74. doi: <http://dx.doi.org/10.1016/j.compstruct.2015.10.037>
- Jones, N. (2017). Note on the impact behaviour of fibre-metal laminates. *International Journal of Impact Engineering*, 108, 147-152. doi: <https://doi.org/10.1016/j.ijimpeng.2017.04.004>
- Kumar, M. A., Prasad, A. M. K., Ravishankar, D. V., Sateesh, N., & Ravi, D. (2015). Effect of Indenter Displacement On angle Plied Composite Plates Subjected to Quasi-Static Loading. *Materials Today: Proceedings*, 2(4-5), 2938-2943. doi: <http://dx.doi.org/10.1016/j.matpr.2015.07.258>
- Li, X., Zhang, X., Guo, Y., Shim, V. P. W., Yang, J., & Chai, G. B. (2018). Influence of fiber type on the impact response of titanium-based fiber-metal laminates. *International Journal of Impact Engineering*, 114, 32-42. doi: <https://doi.org/10.1016/j.ijimpeng.2017.12.011>
- Lin, C. T., & Kao, P. W. (1995). Effect of fiber bridging on the fatigue crack propagation in carbon fiber-reinforced aluminum laminates. *Materials Science and Engineering: A*, 190(1), 65-73. doi: [https://doi.org/10.1016/0921-5093\(94\)09613-2](https://doi.org/10.1016/0921-5093(94)09613-2)
- Lin, C. T., Kao, P. W., & Jen, M. H. R. (1994). Thermal residual strains in carbon fibre-reinforced aluminium laminates. *Composites*, 25(4), 303-307. doi: [https://doi.org/10.1016/0010-4361\(94\)90223-2](https://doi.org/10.1016/0010-4361(94)90223-2)
- Liu, D., Tang, Y., & Cong, W. (2012). A review of mechanical drilling for composite laminates. *Composite Structures*, 94(4), 1265-1279.
- Liu, G., Li, Q., Msekh, M. A., & Zuo, Z. (2016). Abaqus implementation of monolithic and staggered schemes for quasi-static and dynamic fracture phase-field model. *Computational Materials Science*, 121, 35-47. doi: <http://dx.doi.org/10.1016/j.commatsci.2016.04.009>
- Majerski, K., Surowska, B., & Bienias, J. (2018). The comparison of effects of hygrothermal conditioning on mechanical properties of fibre metal laminates and fibre reinforced polymers. *Composites Part B: Engineering*, 142, 108-116. doi: <https://doi.org/10.1016/j.compositesb.2018.01.002>

- Marissen, R. (1984). Flight simulation behaviour of aramid reinforced aluminium laminates (ARALL). *Engineering Fracture Mechanics*, 19(2), 261-277. doi: [https://doi.org/10.1016/0013-7944\(84\)90021-3](https://doi.org/10.1016/0013-7944(84)90021-3)
- McGregor, C., Vaziri, R., Poursartip, A., & Xiao, X. (2016). Axial crushing of triaxially braided composite tubes at quasi-static and dynamic rates. *Composite Structures*, 157, 197-206. doi: <http://dx.doi.org/10.1016/j.compstruct.2016.08.035>
- Morinière, F. D., Alderliesten, R. C., & Benedictus, R. (2014). Modelling of impact damage and dynamics in fibre-metal laminates – A review. *International Journal of Impact Engineering*, 67, 27-38. doi: <http://dx.doi.org/10.1016/j.ijimpeng.2014.01.004>
- Múgica, J. I., Aretxabaleta, L., Ulacia, I., & Aurrekoetxea, J. (2014). Impact characterization of thermoformable fibre metal laminates of 2024-T3 aluminium and AZ31B-H24 magnesium based on self-reinforced polypropylene. *Composites Part A: Applied Science and Manufacturing*, 61, 67-75. doi: <http://dx.doi.org/10.1016/j.compositesa.2014.02.011>
- Nowak, T. (2018). Elastic-plastic behavior and failure analysis of selected Fiber Metal Laminates. *Composite Structures*, 183, 450-456. doi: <https://doi.org/10.1016/j.compstruct.2017.05.007>
- Pärnänen, T., Kanerva, M., Sarlin, E., & Saarela, O. (2015). Debonding and impact damage in stainless steel fibre metal laminates prior to metal fracture. *Composite Structures*, 119, 777-786. doi: <http://dx.doi.org/10.1016/j.compstruct.2014.09.056>
- Rao, H. J., Perumalla Janaki, R., Vardhan, M. V., & Chandramouli, C. H. (2016). Failure Prediction in Fiber Metal Laminates for Next Generation Aero Materials. *IOP Conference Series: Materials Science and Engineering*, 149(1), 012102.
- Rejab, M., & Cantwell, W. (2013). The mechanical behaviour of corrugated-core sandwich panels. *Composites Part B: Engineering*, 47, 267-277.
- Ritchie, R. O., Yu, W., & Bucci, R. J. (1989). Fatigue crack propagation in ARALL® LAMINATES: Measurement of the effect of crack-tip shielding from crack bridging. *Engineering Fracture Mechanics*, 32(3), 361-377. doi: [http://dx.doi.org/10.1016/0013-7944\(89\)90309-3](http://dx.doi.org/10.1016/0013-7944(89)90309-3)
- Santhanakrishnan Balakrishnan, V., & Seidlitz, H. (2018). Potential repair techniques for automotive composites: A review. *Composites Part B: Engineering*, 145, 28-38. doi: <https://doi.org/10.1016/j.compositesb.2018.03.016>
- Santiago, R. C., Cantwell, W. J., Jones, N., & Alves, M. (2018). The modelling of impact loading on thermoplastic fibre-metal laminates. *Composite Structures*, 189, 228-238. doi: <https://doi.org/10.1016/j.compstruct.2018.01.052>
- Schijve, J. (1990). Crack stoppers and arall laminates. *Engineering Fracture Mechanics*, 37(2), 405-421. doi: [https://doi.org/10.1016/0013-7944\(90\)90050-Q](https://doi.org/10.1016/0013-7944(90)90050-Q)

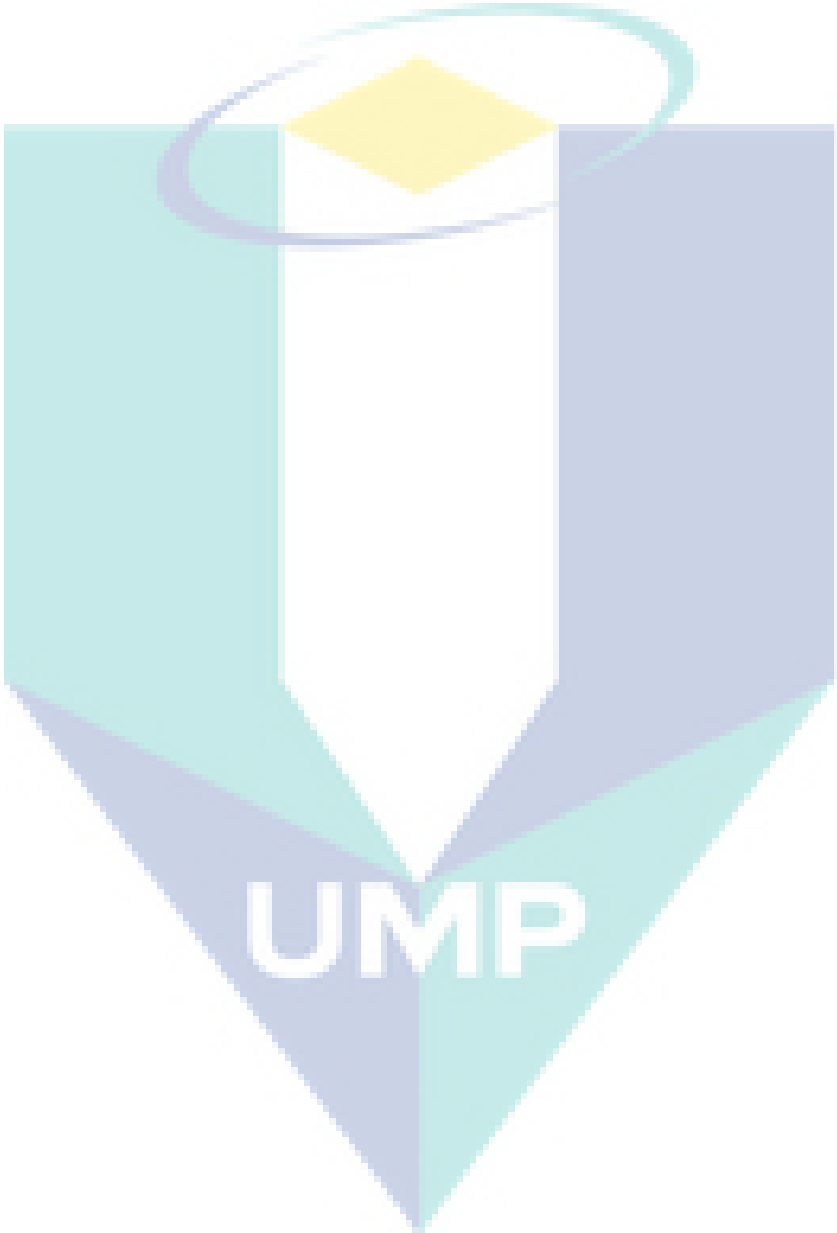
- Şen, I., Alderliesten, R. C., & Benedictus, R. (2015a). Design optimisation procedure for fibre metal laminates based on fatigue crack initiation. *Composite Structures*, *120*, 275-284. doi: <http://dx.doi.org/10.1016/j.compstruct.2014.10.010>
- Şen, I., Alderliesten, R. C., & Benedictus, R. (2015b). Lay-up optimisation of fibre metal laminates based on fatigue crack propagation and residual strength. *Composite Structures*, *124*, 77-87. doi: <http://dx.doi.org/10.1016/j.compstruct.2014.12.060>
- Simas Filho, E. F., Silva Jr, M. M., Farias, P. C. M. A., Albuquerque, M. C. S., Silva, I. C., & Farias, C. T. T. (2016). Flexible decision support system for ultrasound evaluation of fiber-metal laminates implemented in a DSP. *NDT & E International*, *79*, 38-45. doi: <http://dx.doi.org/10.1016/j.ndteint.2015.12.001>
- Sinmazçelik, T., Avcu, E., Bora, M. Ö., & Çoban, O. (2011). A review: Fibre metal laminates, background, bonding types and applied test methods. *Materials & Design*, *32*(7), 3671-3685. doi: <https://doi.org/10.1016/j.matdes.2011.03.011>
- Sun, C. T., Dicken, A., & Wu, H. F. (1993). Characterization of impact damage in ARALL laminates. *Composites Science and Technology*, *49*(2), 139-144. doi: [http://dx.doi.org/10.1016/0266-3538\(93\)90053-J](http://dx.doi.org/10.1016/0266-3538(93)90053-J)
- Tsai, S. W. (1965). Strength Characteristics of Composite Materials: DTIC Document.
- Tsai, S. W., & Wu, E. M. (1971). A general theory of strength for anisotropic materials. *Journal of Composite Materials*, *5*(1), 58-80.
- Vermeeren, C. A. J. R. (2003). An Historic Overview of the Development of Fibre Metal Laminates. *Applied Composite Materials*, *10*(4), 189-205. doi: [10.1023/a:1025533701806](https://doi.org/10.1023/a:1025533701806)
- Vogelgesang, L. B., & Vlot, A. (2000). Development of fibre metal laminates for advanced aerospace structures. *Journal of Materials Processing Technology*, *103*(1), 1-5. doi: [http://dx.doi.org/10.1016/S0924-0136\(00\)00411-8](http://dx.doi.org/10.1016/S0924-0136(00)00411-8)
- Xue, J., Wang, W.-X., Takao, Y., & Matsubara, T. (2011). Reduction of thermal residual stress in carbon fiber aluminum laminates using a thermal expansion clamp. *Composites Part A: Applied Science and Manufacturing*, *42*(8), 986-992. doi: <https://doi.org/10.1016/j.compositesa.2011.04.001>
- Yu, G.-C., Wu, L.-Z., Ma, L., & Xiong, J. (2015). Low velocity impact of carbon fiber aluminum laminates. *Composite Structures*, *119*, 757-766. doi: <https://doi.org/10.1016/j.compstruct.2014.09.054>
- Zamani Zakaria, A., Shelesh-nezhad, K., Navid Chakherlou, T., & Olad, A. (2017). Effects of aluminum surface treatments on the interfacial fracture toughness of carbon-fiber aluminum laminates. *Engineering Fracture Mechanics*, *172*, 139-151. doi: <https://doi.org/10.1016/j.engfracmech.2017.01.004>



/

Figure AD: Data sheet of Aluminium alloy

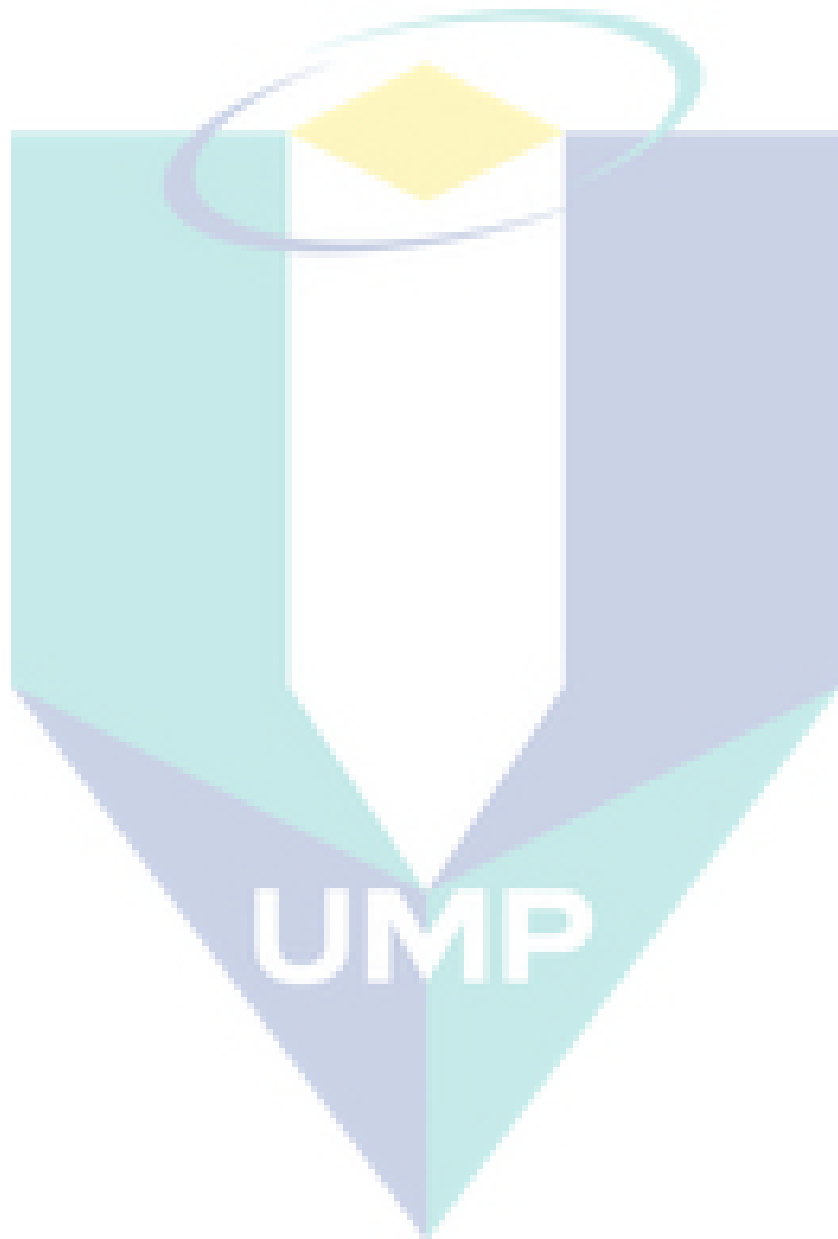
(Source: <http://www.matweb.com/>)



/

Figure AE: Data sheet of SRPP

(Source: <https://www.curvonline.com/>)

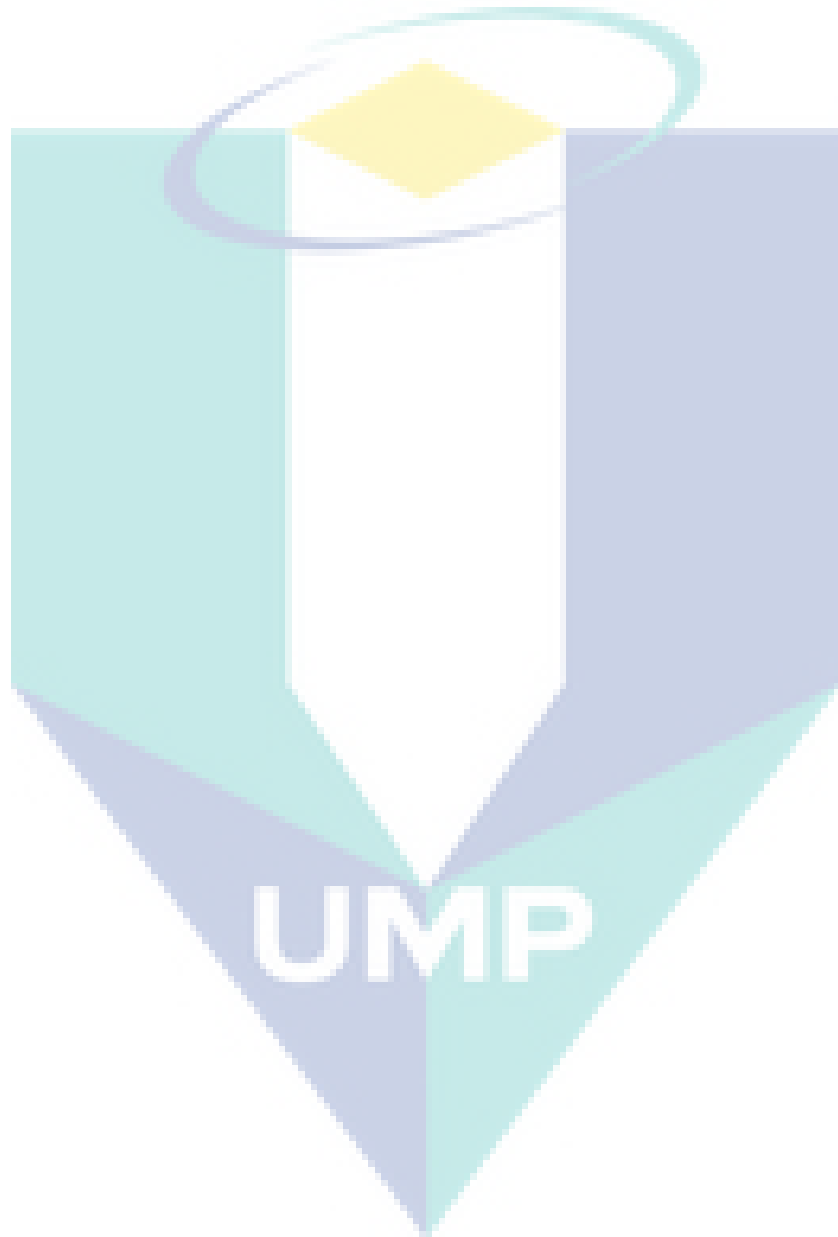


APPENDIX F: Data Sheet of Polypropylene Film

//

Figure AF: Data sheet of polypropylene film

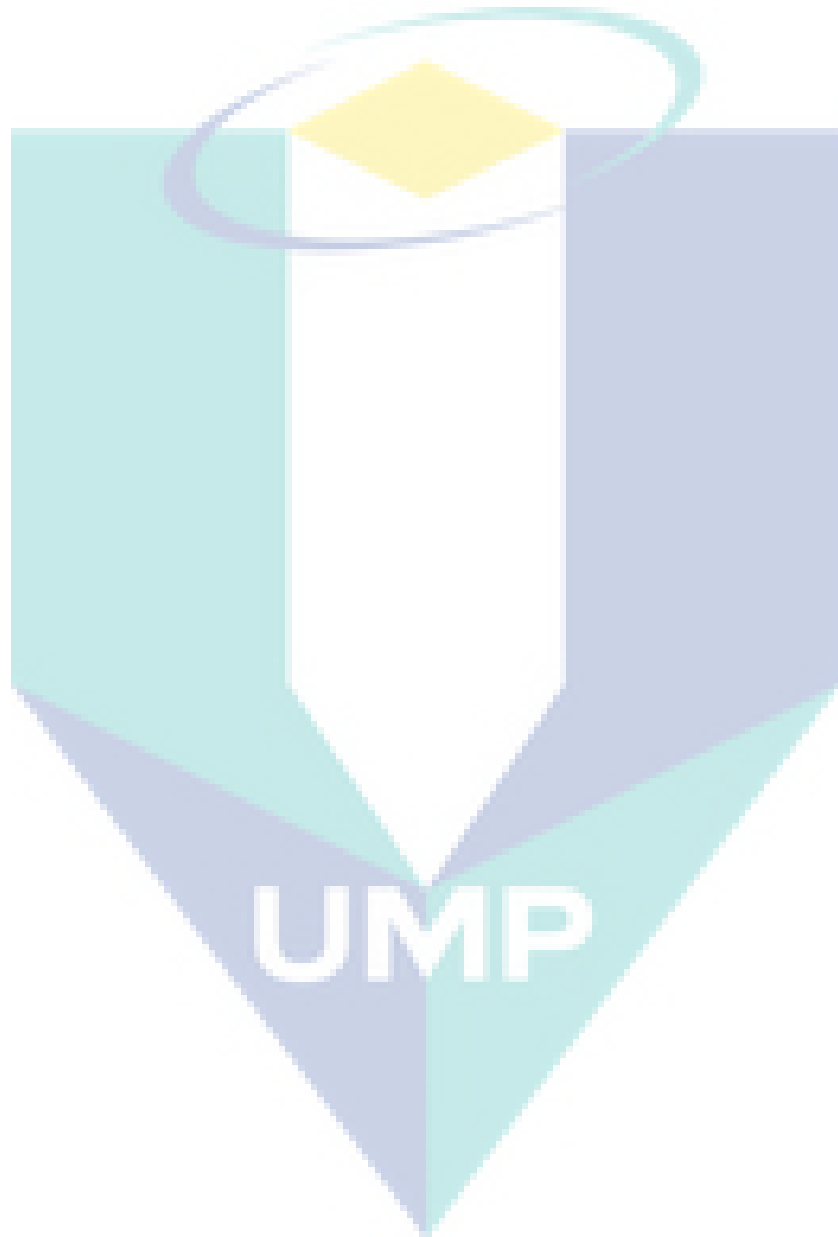
(Source: <https://www.collano.com/>)



/

Figure AG Data sheet of carbon fibre reinforced polymer

(Source: <https://www.facebook.com/ZAComposites-566137303396792/>)



APPENDIX H: Conference

1. The Effect of Variant Unit Cell and Thickness of Trapezoidal carbon/Epoxy Composite Sandwich Panel. 2nd Composite Materials and Manufacturing Symposium by Centre of Composite, UTM KL. Date: 11-12 November 2016.
2. The Behavior of Aluminium Carbon/Epoxy Fibre Metal Laminate Under Quasi-Static Loading. 2nd International Conference of Mechanical Engineering 2017 by Faculty of Mechanical Engineering, UMP. Date: 1-2 August 2017.
3. Finite Element Simulation of Aluminium/GFRP Fibre Metal Laminate under Tensile Loading. Malaysia Technical Universities Conference on Engineering and Technology by MUCET, UNIMAP. Date: 5-6 December 2017.
4. Failure Behaviour of Aluminium/CFRP with Varying Fibre Orientation in Quasi-Static Indentation. 4th Asia Pacific Conference on Manufacturing System & 3rd International Manufacturing Engineering Conference (iMEC) by Bandung Institute of Technology (ITB), Yogyakarta. Date: 7-8 December 2017.



APPENDIX I: Journal

1. N.K. Romli, M.R.M.Rejab, D. Bachtiar, J.Siregar, M.F.Rani, W.S.W.Harun, Salwani Mohd Salleh, M.N.M.Merzuki. (2017). The Behavior of Aluminium Carbon/Epoxy Fibre Metal Laminate Under Quasi-Static Loading. IOP Conference Series: Material and Science. **257**, 1-13.
2. M N M Merzuki, M R M Rejab, N K Romli, D Bachtiar, J Siregar, M F Rani, Salwani Mohd Salleh. (2018). Finite Element Simulation of Aluminium/GFRP Fibre Metal Laminate under Tensile Loading. Accepted to be published in MATEC.
3. N.K. Romli, M.R.M.Rejab, D. Bachtiar, J.Siregar, M.F.Rani, Salwani Mohd Salleh, M.N.M.Merzuki. Failure Behavior of Aluminium/CFRP with Varying Fibre Orientation in Quasi-static Indentation. Accepted to be published in IOP Conference Series: Material and Science.
4. N.K.Romli, M.R.M.Rejab, A.F.Jusoh, M.F.M.Noor, J.P.Siregar. The Effect of Variant Unit Cell and Thickness of Trapezoidal carbon/Epoxy Composite Sandwich Panel. Accepted to be published in Facta Universitatis Series Mechanical Engineering.



UMP

APPENDIX J: Exhibition

1. Creation, Innovation, Technology & Research Exposition (CITREx) 2018

Tilte: Fibre Metal Laminate for Quasi-Static Damage Resistance

Award: Silver medal

Date: 7-8 February 2018

